

## AN ABSTRACT OF THE DISSERTATION OF

Adrian Carlos Gallo for the degree of Doctor of Philosophy in Sustainable Forest Management presented on 12 October 2022.

Title: Tracing Sources of Soil Organic Matter Through Time, Across Ecosystems, and Down Soil Profiles

Abstract approved: \_\_\_\_\_

Jeffery A. Hatten

Soils contain the largest pool of carbon that is actively cycling on human timescales, leading many to view soils as a natural climate solution with multiple co-benefits. The field of soil science is rapidly evolving, but without a unified understanding of soil carbon dynamics. This dissertation leverages two distinct long-term monitoring projects that were sampled in their infancy. First, a biomass manipulation experiment in an Oregon Cascade timber farm that contains treatments with a ten-fold difference in residual tree biomass left on site. Standard soil collection methods would otherwise obscure the dynamism occurring in this forest. We observed losses in native soil carbon, buffered by a replacement of newly senesced root-carbon, and the participation of a previously thought ‘stable’ carbon pool. We find that soils are both incredibly resilient, but potentially vulnerable if they are not given enough time to rebuild after perturbations. The second project began during the installation of

the National Ecological Observatory Network with 40 sites representing nearly every biome in North America. To the author's knowledge, this is the most broad systematic organic matter inventory and deepest soil horizon assessment that have ever been investigated with the copper oxidation method. Despite the inclusion of desert, grassland, forest and permafrost ecosystems, we find a striking similarity in lignin contributions and soil organic matter composition across sites and down soil profiles. Taken together, this work emphasizes the broad resilience of soils is likely due to a universal ecosystem inertia that transforms diverse plant inputs into homogenized soil organic matter signatures. There were, however, many exceptions which emphasizes that site-specificity will always preclude any potential land management recommendation.

© Copyright by Adrian Carlos Gallo  
12 October 2022  
All Rights Reserved

Tracing Sources of Soil Organic Matter Through Time, Across  
Ecosystems, and Down Soil Profiles

by

Adrian Carlos Gallo

A DISSERTATION

submitted to

Oregon State University

in partial fulfillment of  
the requirements for the  
degree of

Doctor of Philosophy

Presented 12 October 2022  
Commencement June 2023

Doctor of Philosophy dissertation of Adrian Carlos Gallo presented on  
12 October 2022.

APPROVED:

---

Major Professor, representing Sustainable Forest Management

---

Head of the Department of Forest Engineering, Resources, and Management

---

Dean of the Graduate School

I understand that my dissertation will become part of the permanent collection of Oregon State University libraries. My signature below authorizes release of my dissertation to any reader upon request.

---

Adrian Carlos Gallo, Author

## ACKNOWLEDGEMENTS

I would like to acknowledge all of the graduate students who I've met over my years at Oregon State. You have taught me more about the world around me than the contents of this dissertation can provide, and for that I am forever grateful. My time with the Inspiration Dissemination radio team nurtured my insatiable curiosity, and has shaped my future goals more than you can imagine. The folks at KBVR - the many student workers and especially Steven Sandberg - made recording shows in the radio booth a true joy. I am sad to leave the ID team, but I know it's in truly capable hands and I'm excited to see how the show continue to progress.

I would like to thank my advisor Dr. Jeff Hatten for his support and guidance in my graduate studies. When given the option to continue my graduate career with Jeff after my Masters I thought I hit the gold mine because of how knowledgeable and considerate he was as my advisor. That proved to be the case and my success as a student, researcher, teacher, and as a person is in large part to him and his diligent support in the lab and in life.

I'd like to thank my committee Dr. Miguel Goñi, Dr. Katherine Heckman, Dr. Kate Lajtha, Dr. Ron Reuter, and Dr. Kimberly Halsey for their help, encouragement, and understanding (especially this last year!).

I was lucky enough to be surrounded by a number of thoughtful and productive co-authors on both of my projects. They include: Yvan Alleau, Maggie Bowman, Scott Holub, Kate Lajtha, Kate Heckman, Kim Littke, Lauren Matosziuk, Brett Morissette, Luke Nave, Angela Possinger, Mike SanClements, Brian Strahm and

Tyler Weiglein. They are all incredible scientists, and people, and I'm lucky to consider them collaborators.

A special academic thanks to: Si Gao, Franco Guerrero-Bolano, Lauren Matosziuk, Katherine McCool, Brett Morrissette, Karla Jarecke, and Matt Konkler. Some of the undergraduate workers that did everything from sample labeling to liquid nitrogen fun include: Chantal Jorgenson, Hayden Myles, Raven Chavez, and Maylita Broughter. Rommel Zulueta remains instrumental in the current operation of NEON sites, but without his attention to detail early in project life the soil cores that most of my dissertation is based upon might not have existed.

The College of Forestry is filled with wonderful people, many were essential to my success in graduate school. Without Yvan Alleau none of the carbon/nitrogen, GCMS, or CuO biomarker data would have been possible. Ariel Muldoon taught me more about stats and coding than I ever imagined, without her guidance I would probably still be using ANOVA's incorrectly. In the final stretch of my degree, Sukhyun Joo was instrumental in keeping my statistics cohesive. The College of Forestry Computer Help Desk is an amazing resource. I cannot count the number of times I needed help troubleshooting with the printer, connecting an external monitor, classroom setup for teaching, software glitches, etc... Their knowledge of all things computer and tech helped me focus on my *actual* job of teaching and research. The administrative support staff in the FERM Department, in particular Madison Dudley and Chelsey Durling, were equally knowledgeable about all contract and class curriculum and credit enrollment and other weird bureaucratic shenanigans that I never would have figured out without them.

Thank you to Stephany Chacon for all the writing group time, and helping me figure out this dissertation formatting nonsense. I could not have completed my Ph.D without the camaraderie of the soils graduate students these past years, their knowledge about all things soils continues to amaze me. A few of them include: Stephany Chacon, Vance Almquist, Kris Osterloh, Burl Carpenter, Martina Gonzalez, and Clara Weidman (+Roan and Riff and EV), Pedro Martinez, Amy Mayedo, Erin Rooney, Trang Nguyen and many many more!

The faculty and staff in the Cal Poly Earth and Soil Science Department were instrumental in my success as a graduate student. I felt incredibly prepared as a result of my undergraduate education, which allowed me to jump with two feet into the field of biogeochemistry with relative ease. Just a few that come to mind include: Lisa Wallraven, Tony Garcia, Scott Johnston, Elizabeth Will, Lynn Moody, Karen Vaughan, Tom Rice, Chip Appel, and Craig Stubler. Craig Stubler taught a number of undergraduate students how to really understand the Carbon:Nitrogen analyzer, those skills made learning an even more complicated machine less daunting.

My sanity through graduate school could not have been maintained without the many joyous adventure buddies I've had along the way. Thank you to Aili, June, Joanie, Ian, Jason, KK, Jordan, Keiki, Paul, and [I'm sorry I know I forgot people]. To the beach volleyball folks, I'm glad you let me run around like a drunken flamingo and invited me back. To the lunchtime soccer crew, I don't care what my ankle surgeon says, all the injuries are still worth the fun. An extra special adventure appreciation for Taylor Lucey and Lauren Matosziuk who made suffering through big miles in the mountains fun (well, Type II fun) that I will continue to sign up for.

Even though we usually run in circles, the conversations and deep thinking we do while adventuring always helps me feel like I learn more about myself, and for that I am eternally grateful.

Finally, to my loving extended and immediate family who might finally figure out what I've been studying in school this whole time, only to discover I'm changing careers. Words cannot convey my appreciation and love to you all, but especially to Eli, Carlos, Christina, and Delta.

## CONTRIBUTION OF AUTHORS

Yvan Alleau, Maggie Bowman, Scott Holub, Kate Lajtha, Kate Heckman, Kim Littke, Lauren Matosziuk, Brett Morissette, Luke Nave, Angela Possinger, Mike SanClements, Brian Strahm and Tyler Weiglein.

## PREFACE

Fossil fuel extraction and unregulated emissions have altered the planet's climate at a rate never before seen in Earth's recorded history. Under the auspices of then-President Ronald Reagan, the Environmental Protection Agency released their Global Warming Greenhouse study (EPA, 1983). They warned a 2°C increase in global temperature was possible by 2050, they also write in the executive summary:

*“Temperature increases are likely to be accompanied by dramatic changes in precipitation and storm patterns and a rise in global average sea level. As a result, agricultural conditions will be significantly altered, environmental and economic systems potentially disrupted, and political institutions stressed.”*

Approximately five years prior to that EPA report, Exxon contracted scientists to build climate models and create a mini-ocean acidification experiment to examine their own impact on the climate. Senior researchers concluded “mankind is influencing the global climate [...] through carbon dioxide release from the burning of fossil fuels.” (Hall, 2015 Scientific American). Exxon withheld that knowledge and instead began setting a culture of climate misinformation that has hindered any meaningful climate action until August of this year (Mulvey and Shulman, 2015). The year the I was born, the IPCC released their first report whose predictions have not meaningfully changed in their 5th or 6th IPCC iterations released in 2013 and 2019 respectively (IPCC 1990, IPCC 2013, IPCC 2019). As reported by Mufson et al. (2019) – and earning the Pulitzer Prize in the process for explanatory journal-

ism – the 2°C rise in average temperature has already arrived in some places in the United States, thirty years earlier than predicted by the 1983 EPA report.

The passage of the Inflation Reduction Act in August of 2022, without a single Republican Senator voting in favor, allows for many more positive futures (Yarmuth, 2022). Those alternative futures largely depend on the moral clarity and political will of citizens and elected politicians. While the solution to a rapidly warming climate is abundantly obvious, it remains economically and politically inconvenient. Nonetheless, scientists are tasked with identifying as many potential climate solutions that are technically feasible. Political ecologists, water policy analysts, economists and local communities can better translate those technical recommendations to the practical world and whether they are plausible, an efficient use of resources, and justice oriented. Although this author believes academic researchers should more meaningfully engage with other fields to understand the practical limitations of our land/soil/water management prescriptions (van Groenigen, 2018; van Groenigen et al., 2017; Janzen et al., 2022; Schlesinger and Amundson, 2019; Poulton et al., 2018; McGill et al., 2018; Powlson et al., 2011; Sultana and Loftus, 2020; Cha and Pastor, 2022), especially in the current political context that limits idealized science-based decision making (Lajtha et al., 2017), these concerns are not the purpose of this dissertation. My purpose in directing readers towards decades of inaction to address the climate crisis is that we should be wary of over promising how much soils can serve as an effective natural climate solution while our emissions continue nearly unabated.

# TABLE OF CONTENTS

	<u>Page</u>
1 Introduction . . . . .	1
1.1 Soil Science History . . . . .	1
1.2 Overview of Manuscripts . . . . .	6
2 Root carbon from harvested trees replaces native mineral carbon within two years following biomass removal treatments in a Western Oregon Douglas-fir forest . . . . .	8
2.1 Abstract . . . . .	9
2.2 Introduction . . . . .	11
2.3 Materials and Methods . . . . .	15
2.3.1 Site description . . . . .	15
2.3.2 Experimental design and sampling . . . . .	16
2.3.3 Density fractionation . . . . .	18
2.3.4 CN and stable isotopes . . . . .	20
2.3.5 Cupric oxidation (CuO) procedures . . . . .	20
2.3.6 Statistics . . . . .	22
2.4 Results . . . . .	23
2.4.1 Soil carbon and nitrogen . . . . .	23
2.4.2 Stable isotopes (bulk soils) . . . . .	26
2.4.3 Cupric oxidation (bulk soils) . . . . .	28
2.4.4 Density fraction C and N characteristics . . . . .	31
2.4.5 Stable isotopes (density fractions) . . . . .	35
2.5 Discussion . . . . .	37
2.5.1 Bulk soil responses . . . . .	37
2.5.2 Density fraction responses . . . . .	42
2.5.3 Pacific Northwest forest organic matter cycling . . . . .	46
2.5.4 Soil organic matter response to perturbations, and management	47
2.6 Conclusions . . . . .	49
2.7 References . . . . .	51
2.8 Supplemental Materials for Chapter 2 . . . . .	62

## TABLE OF CONTENTS (Continued)

	<u>Page</u>
3 Continental patterns in plant sources of soil organic matter across the National Ecological Observatory Network (NEON) and down soil profiles . . . . .	63
3.1 Abstract . . . . .	64
3.2 Introduction . . . . .	65
3.3 Materials and Methods . . . . .	69
3.3.1 Site description and soil sampling . . . . .	69
3.3.2 Cupric oxidation procedures . . . . .	75
3.3.3 Statistics . . . . .	78
3.4 Results . . . . .	79
3.4.1 Lignin contributions . . . . .	81
3.4.2 Lignin degradation . . . . .	86
3.4.3 Substituted fatty acids (SFA) . . . . .	89
3.4.4 Alternative biomarkers for sourcing techniques . . . . .	91
3.5 Discussion . . . . .	91
3.5.1 Vegetation endmembers and surface soil lignin contributions . . . . .	93
3.5.2 Deep soil lignin and SFA patterns . . . . .	95
3.5.3 Density fractions . . . . .	98
3.5.4 Cupric oxidation (CuO) as a tool . . . . .	99
3.5.5 Implications for SOM patterns across ecosystems . . . . .	102
3.6 Conclusion . . . . .	104
3.6.1 Acknowledgements . . . . .	106
3.7 Supplemental Materials . . . . .	107
3.8 References . . . . .	112
4 Assessing the biochemical relationships between litter endmembers, surface horizons, and the ability to predict deep soil characteristics across the National Ecological Observatory Network (NEON) . . . . .	125
4.1 Abstract . . . . .	126
4.2 Introduction . . . . .	127
4.3 Methods . . . . .	129
4.3.1 Site description, design, and sampling . . . . .	129
4.3.2 Cupric oxidation (CuO) procedures . . . . .	130
4.3.3 Bray-Curtis Statistics . . . . .	131

## TABLE OF CONTENTS (Continued)

	<u>Page</u>
4.4 Results . . . . .	132
4.4.1 Endmember organic matter composition . . . . .	132
4.4.2 Soil organic matter composition . . . . .	135
4.4.3 Average Bray-Curtis dissimilarity index . . . . .	137
4.4.4 Unique within-site Bray-Curtis dissimilarity index . . . . .	138
4.4.5 Bray-Curtis relationship with climatic factors . . . . .	139
4.5 Discussion . . . . .	144
4.5.1 A-horizon SOM signature relative to endmembers . . . . .	145
4.5.2 Soil horizon SOM dissimilarity patterns . . . . .	145
4.5.3 Potential CuO method limitations . . . . .	146
4.6 Conclusions . . . . .	148
4.6.1 Acknowledgements . . . . .	150
4.7 Supplemental Materials . . . . .	151
4.8 References . . . . .	153
5 Conclusion . . . . .	162
5.1 Bibliography For Preface, Introduction, and Conclusion . . . . .	165

## LIST OF FIGURES

<u>Figure</u>		<u>Page</u>
2.1	Soil organic carbon stocks and CN data for three periods of sample collection and both depths across all treatments at the NARA-LTSP site near Springfield, OR. Treatments include bole only (BO), whole tree (WT), and whole tree plus forest floor removals with compaction (WTFFC). (*) denotes significant difference ( $p < 0.1$ ) from pre-treatment value. Box and whisker plots with open circles indicating outliers. . . . .	25
2.2	Carbon and nitrogen stable isotope data for three periods of sample collection and both depths across all treatments at the NARA-LTSP site near Springfield, OR. Treatments include bole only (BO), whole tree (WT), and whole tree plus forest floor removals with compaction (WTFFC). (*) denotes significant difference ( $p < 0.1$ ) from pre-treatment value. Box and whisker plots with open circles indicating outliers. . . . .	28
2.3	Soil biomarker data derived from the cupric oxidation method for two periods of sample collection and both depths across all treatments at the NARA-LTSP site near Springfield, OR. Treatments include bole only (BO), whole tree (WT), and whole tree plus forest floor removals with compaction (WTFFC). The P:V ratio includes para-hydroxybenzene (P) to vanillyl (V) phenols with higher values indicating greater microbial lignin decomposition. Cutin and suberin are leaf and root waxes respectively. (*) denotes significant difference ( $p < 0.1$ ) from pre-treatment value. Box and whisker plots with open circles indicating outliers. . . . .	30
2.4	Soil C/N data and soil carbon pools derived from density fractionation (light fraction $> 1.8$ g/cm <sup>3</sup> ; intermediate fraction 1.8-2.5 g/cm <sup>3</sup> ; heavy fraction $> 2.5$ g/cm <sup>3</sup> ) for two periods of sample collection and both depths across all treatments at the NARA-LTSP site near Springfield, OR. Treatments include bole only (BO), whole tree (WT), and whole tree plus forest floor removals with compaction (WTFFC). (*) denotes significant difference ( $p < 0.1$ ) from pre-treatment value. Box and whisker plots with open circles indicating outliers. . . . .	34

## LIST OF FIGURES (Continued)

<u>Figure</u>		<u>Page</u>
2.5	Carbon and nitrogen stable isotope data derived from density fractionation (light fraction >1.8 g/cm <sup>3</sup> ; intermediate fraction 1.8-2.5 g/cm <sup>3</sup> ; heavy fraction >2.5 g/cm <sup>3</sup> ) for two periods of sample collection and both depths across all treatments at the NARA-LTSP site near Springfield, OR. Treatments include bole only (BO), whole tree (WT), and whole tree plus forest floor removals with compaction (WTFFC). (*) denotes significant difference (p<0.1) from pre-treatment value. Box and whisker plots with open circles indicating outliers. . . . .	36
2.6	Figure 6. Carbon and nitrogen stable isotope data derived from bulk soils and density fractionation (light fraction >1.8 g/cm <sup>3</sup> ; intermediate fraction 1.8-2.5 g/cm <sup>3</sup> ; heavy fraction >2.5 g/cm <sup>3</sup> ) for two periods of sample collection and both depths across all treatments at the NARA-LTSP site near Springfield, OR. We also present representative root and needle isotopic signatures from similarly situated forests. Needle litter from three-year old seedlings at this NARA-LTSP site (Littke, K. personal communication), and root data from two National Ecological Observatory Network sites that include the Wind River Experimental Forest (WREF) and Abby Road (ABBY) both in southern Washington containing an old-growth mixed conifer forest and Douglas-fir plantation forest respectively (NEON, 2022). . . . .	41
3.1	Hydroclimatic patterns across a subset (n=39) of the National Ecological Observatory Network (NEON). Whittaker Biomes were used to increase the number of sites with each ecosystem category rather than the ecoclimatic domains used by NEON which only contain 1-3 sites per domain. See Table 1 for a full site description corresponding to the four-letter codes. . . . .	74
3.2	Carbon normalized lignin contributions to bulk soils (A, upper and lower B-horizons) relative to a hydroclimatic moisture index for a subset (n=39) of the National Ecological Observatory Network (NEON) sites. . . . .	83

## LIST OF FIGURES (Continued)

<u>Figure</u>		<u>Page</u>
3.3	Carbon normalized lignin contributions to bulk soils (A, upper and lower B-horizon) and density fractions (FLF: free light, OCC: occluded; HF: heavy fraction) for a subset (n=31) of the National Ecological Observatory Network (NEON) sites. Due to logistical constraints, not all bulk soils yielded enough occluded fraction mass to be both analyzed for elemental carbon and cupric oxidation. We opportunistically included a subset of upper B and lower B-horizons but they are not meant to be representative sample sets. . . . .	85
3.4	Lignin and non-lignin cupric oxidation product yields for all sample types, horizons, and density fractions available from the National Ecological Observatory Network (NEON). We present four panels that include (A) lignin degradation index with higher values indicating greater lignin degradation, (B) microbial to plant biomarker index with higher values indicating higher microbial processing of lignin, and (C, D) the acid to aldehyde ratios of two lignin phenols with higher values indicating greater lignin oxidation. Due to unequal recovery of internal standards, the observed occluded and heavy fraction data may be underestimating the amount of acid phenols relative to aldehyde phenols, and these data should be viewed with caution. . . . .	87
3.5	Plant wax yields (substituted fatty acids) from the cupric oxidation procedure for all sample types, horizons, and density fractions available from the National Ecological Observatory Network (NEON). Due to unequal recovery of internal standards, the observed occluded and heavy fraction data may be underestimating the amount of acid phenols relative to aldehyde phenols, and these data should be viewed with caution. . . . .	90
3.6	Plant wax yields (substituted fatty acids) from the cupric oxidation procedure for all sample types, horizons, and density fractions available from the National Ecological Observatory Network (NEON). Due to unequal recovery of internal standards, the observed occluded and heavy fraction data may be underestimating the amount of acid phenols relative to aldehyde phenols, and these data should be viewed with caution. . . . .	108

## LIST OF FIGURES (Continued)

<u>Figure</u>		<u>Page</u>
3.7	Comparing two lignin phenol categories from bulk soils of the National Ecological Observatory Network (NEON). Higher values indicate a non-woody source of lignin, and lower values indicate a woody source. The C:V ratio correctly identifies the biomes that dominate in grasses/shrubs vs trees in the A horizon, but the aboveground biomarker signal diminishes with increasing depth. See Table 2 for estimated midpoint depths for all three horizons meant to capture representative horizons for each site with the widest pedogenic influence down soil profiles . . . . .	109
3.8	Comparing two lignin phenol categories from bulk soils of the National Ecological Observatory Network (NEON). Higher values indicate an angiosperm (flowers, grasses) source of lignin, and lower values indicate a gymnosperm (tree) source. The S:V ratio correctly identifies the biomes that dominate in grasses/shrubs vs trees in the A horizon, but the aboveground biomarker signal quickly diminishes with increasing depth. See Table 2 for estimated midpoint depths for all three horizons meant to capture representative horizons for each site with the widest pedogenic influence down soil profiles . . . . .	110
3.9	Comparing acid to aldehyde ratios of two lignin phenol categories from all three bulk soil types from the National Ecological Observatory Network (NEON). As depth of soils increase, research shows the organic matter is generally more decomposed (characterized by more -OH functional groups substituted onto SOM). Higher acid:aldehyde ratios indicate greater oxidation of those lignin phenols. Vanillyl phenols may persist longer, or are less vulnerable to oxidation, compared to syringyl phenols which observe expected patterns of increased degree of oxidation as depth of soil increases. . . . .	111
4.1	Proportion of cupric oxidation (CuO) extracted compound classes in available vegetation and root samples across the National Ecological Observatory Network. Individual CuO products (n=72) are normalized to the total extracted material within each sample, and are grouped according to broad compound class. Abbreviations: P Phenols - para-hydroxybenzoic acid phenols; BDA - benzenedicarboxylic acids, BTA - benzenetricarboxylic acids. . . . .	134

## LIST OF FIGURES (Continued)

<u>Figure</u>		<u>Page</u>
4.2	Proportion of cupric oxidation (CuO) extracted compound classes in available A-horizon, upper B-horizon, and lower B-horizons across the National Ecological Observatory Network. Individual CuO products (n=72) are normalized to the total extracted material within each sample, and are grouped according to broad compound class. Abbreviations: P Phenols - para-hydroxybenzoic acid phenols; BDA - benzenedicarboxylic acids, BTA - benzenetricarboxylic acids. . . . .	136
4.3	Unique Bray-Curtis ecological dissimilarity values for all available organic matter endmembers and A-horizon soils from the National Ecological Observatory Network. Smaller values (closer to 0) indicate samples have less dissimilarity and share more organic matter composition abundances with each other, larger values (closer to 1) indicate samples have greater dissimilarity. Only sites with all three sample types are presented. A-horizon similarity preference is determined by comparing the Bray-Curtis index of A vs Root and A vs Vegetation samples within each site. . . . .	142
4.4	Unique Bray-Curtis ecological dissimilarity values for all available A, Upper, and Lower B-horizon soils from the National Ecological Observatory Network. Smaller values (closer to 0) indicate samples have less dissimilarity and share more organic matter composition abundances with each other, larger values (closer to 1) indicate samples have greater dissimilarity. Only sites with all three sample types are presented. A-horizon and B-horizon similarity preferences are determined by comparing the Bray-Curtis index of each endmember and soil sample type. . . . .	143

## LIST OF TABLES

<u>Table</u>		<u>Page</u>
2.1	Summary data for three periods of sample collection and both depths across all treatments at the NARA-LTSP site near Springfield, OR. Treatments include bole only (BO), whole tree (WT), and whole tree plus forest floor removals with compaction (WTFFC). Bold indicates significant differences ( $p < 0.1$ ) compared to pre-treatment values with a family-wise Bonferroni adjustment for multiple comparisons. . . . .	26
2.2	Density fraction mass, carbon, and nitrogen contributions for two periods of sample collection and both depths across all treatments at the NARA-LTSP site near Springfield, OR. Treatments include bole only (BO), whole tree (WT), and whole tree plus forest floor removals with compaction (WTFFC). Bold indicates significant difference ( $p < 0.1$ ) from the pre-treatment values. . . . .	33
3.1	Site information for a subset ( $n=39$ ) of the National Ecological Observatory Network (NEON). Soil horizon depths were calculated from cores collected at the five soil plots within the flux tower footprint, and represent three distinct pedogenic horizons. . . . .	73
3.2	Summary of cupric oxidation products for all sample types, bulk soil horizons, and A-horizon density fractions. Bulk soil horizons were meant to encapsulate representative horizons for each site with the widest pedogenic influence down soil profiles. Letters indicate significant differences ( $p < 0.1$ ) between bulk soil horizons. Due to logistical constraints, organic samples were not analyzed for elemental carbon or nitrogen analysis and thus could not be carbon normalized. . . . .	80
4.1	Average Bray-Curtis ecological dissimilarity values for grouped organic matter endmembers and A-horizon soils from the National Ecological Observatory Network. Smaller values (closer to 0) indicate samples have less dissimilarity and share more organic matter composition abundances with each other, larger values (closer to 1) indicate samples have greater dissimilarity. Diagonals represent the dissimilarity <i>within</i> each sample class. . . . .	137

## LIST OF TABLES (Continued)

<u>Table</u>		<u>Page</u>
4.2	Average Bray-Curtis ecological dissimilarity values for grouped A-horizon, upper B-horizon, and lower B-horizon soils from the National Ecological Observatory Network. Smaller values (closer to 0) indicate samples have less dissimilarity and share more organic matter composition abundances with each other, larger values (closer to 1) indicate samples have greater dissimilarity. Diagonals represent the dissimilarity <i>within</i> each sample class. . . . .	138
4.3	Unique Bray-Curtis ecological dissimilarity values for all available organic matter endmembers and A-horizon soils from the National Ecological Observatory Network. Smaller values (closer to 0) indicate samples have less dissimilarity and share more organic matter composition abundances with each other, larger values (closer to 1) indicate samples have greater dissimilarity. Only sites with all three sample types are presented. . . . .	139
4.4	Unique Bray-Curtis ecological dissimilarity values for all available A-horizon, upper B-horizon, and lower B-horizon soils from the National Ecological Observatory Network. Smaller values (closer to 0) indicate samples have less dissimilarity and share more organic matter composition abundances with each other, larger values (closer to 1) indicate samples have greater dissimilarity. Only sites with at least two sample types are presented. . . . .	141
4.5	Site information for a subset (n=39) of the National Ecological Observatory Network (NEON). Soil horizon depths were calculated from cores collected at the five soil plots within the flux tower footprint, and represent three distinct pedogenic horizons. . . . .	152

## Chapter 1: Introduction

### 1.1 Soil Science History

Soils are integrators of past and present climates, geologies, plant and human communities (Jenny, 1941). As one of my first soil science professors said, “in addition to the sun shining and the rain raining, we humans would be cold and hungry and – worst of all – sober without soil.” Dr. Lynn Moody is indeed correct, and it’s a testament to how many ecosystem services soils provide. But in addition to relying on soils for food and clothing and clean water, many are now hoping soils can absorb our excess fossil fuel emissions (Wozniacka, 2020).

Due to human’s large land footprint, we have the opportunity to alter our agriculture and wildland management practices that could theoretically result in globally-meaningful reductions in atmospheric greenhouse gasses (Minasny et al., 2017; Lal, 2018; Nave et al., 2018; Sanderman et al., 2017; Bernhardt and Schlesinger, 2013). Even with a better understanding of soil organic matter (SOM) dynamics, we may not be able to translate that technical knowledge into actionable policy because of the many additional hurdles in between (Poulton et al., 2018; Setzer and Vanhala, 2019; Fleischman et al., 2021; Schlesinger, 2022). For example, increasing agriculture SOM would also require a large addition of nitrogen, phosphorus, and potassium fertilizers to maintain stoichiometric constraints (van Groenigen et al., 2006; van Groenigen et al., 2017; Schlesinger and Amundson, 2019; Amundson et al., 2022). Since the

1950's, the excess application of these fertilizers, in addition to warming oceans and nitrogen pollution from nearby emitting facilities, has resulted in a large dead zone in the Gulf of Mexico negatively affecting wildlife and the communities who depend on oceans for jobs and sustenance (Rabalais et al., 2002).

Tree plantings have also begun to emerge as another natural climate solution. To combat deforestation across the world and increase the land carbon sink, tree planting schemes have quickly accelerated as a win-win scenario. It is relatively easy to count how many trees were planted and create the illusion of ecosystems benefits (Fleischman et al., 2021b), but it is exceedingly difficult to keep young trees alive when local communities responsible for seedling maintenance are excluded from consideration (Fleischman et al., 2020; Fleischman et al., 2022). Even within intensively managed forests in the western Oregon cascades, wildfires have caused considerable losses in aboveground timber and belowground soil carbon stocks (In Review, McCool et al., 2022). Independent of a warming climate, these large wildfires are consistent with dendro-ecological records (Reilley et al., 2022). With the advent of forest carbon markets, relying on a 100-year permanent time horizon, we must recognize that they may fail to practically sequester any meaningful amount of carbon because of how quickly ecosystems are changing (Badgley, et al., 2022). Taken holistically, we should be careful not to over-promise how much carbon we can add to soils especially as a carbon crediting mechanism.

Despite the general understanding that more soil organic matter (SOM) is beneficial for a host of ecosystem services (e.g. increased water holding capacity, reduced fertilizer usage, stronger bioremediation effects), soil scientists have yet to develop a

unifying predictive theory of why some SOM can persist for millenia, or return to the atmosphere within hours of being photosynthetically captured by plants. It is noteworthy that soil scientists rarely dig past the surface horizon (Yost and Hartemink, 2020), we barely have a standardized way to collect bulk density (Wendt and Hauser, 2013), and sample storage practices can significantly alter certain soil nutrient status (Rhymes et al., 2020). These are all rather simple process issues that limit the scope of our research; but having a large-scale systematic study design will begin to help us validate past work, and allow us to engage in more mechanistic questions.

Modern soil science research has pushed out the old humic-substances view of organic matter that had been ubiquitous since the 1800's (Lehman and Kleber, 2015). We now understand SOM to be a continuum of plant debris and microbially altered organic matter that is in various stages of decomposition with a number of different protection mechanisms (e.g. physical occlusion, extreme temperature or moisture controls), that likely requires some microbial processing of plant organic matter before it can attach onto soil particles (Cotrufo, et al., 2013; Liang et al., 2017; Kopittke et al., 2020). Despite our advancements, there remain many unknowns (Stockmann et al., 2013). Despite its awareness in popular press (Wozniacka, 2020), organic matter represents only  $\approx 5\%$  of the total soil volume, minerals occupy  $\approx 50\%$  and is also an evolving field of research.

The original 1900's concept of Gouy and Chapman's Double Diffuse Layer (DDL) theory attempted to describe sorption behavior between ions and a charged surface (Sparks, 2003 and references therein). The theory had many limitations, but has undergone improvements by Stern (1924) to account for ion size as opposed to diffuse

ion clouds, and later iterations by van Raji and Peech (1972) rectified the observations showing surface charge density decreasing as a function of greater distance from the particle. We now appreciate sorption phenomenon to include many processes (e.g., mineral edges, weathered pits) that interact with organic molecules in highly complex ways leading to a proliferation of sorption models to describe the narrower window of mineral-ion interactions (Goldberg, 1992; Sparks, 2003; Possinger et al., 2020). These nano- to micro-scale interactions between minerals and organic matter continue to be explored today with modern spectroscopic techniques (Kogel-Knabner, et al., 2008; Masoom et al., 2016). Despite the increasing complexity of these mathematical models, they generally rely on the basic assumption that as the distance of ions to mineral surfaces decreases, stronger sorption phenomena occur. For example, outer-sphere complexation (mineral-water molecule(s)-ion association) is thought to be rapid and reversible, but inner-sphere complexation (mineral-ion association, in the absence of an ion-hydration sphere) is slower and irreversible. The kinetics of these mineral-organic attachments and soil solution continue to be refined, but the assumption generally remains the same: direct mineral-ion associations are more permanent and potentially irreversible (Bailey et al., 2019).

Unlike the humic-substances paradigm that has been thrown out, modern research emphasizes that the stability of SOM is linked to their physicochemical proximity to mineral surfaces. As we expect land-uses to shift considerably in the near future (Lambin and Meyfroidy, 2011), the types of OM that build up and have been stabilized by soils over the Holocene period are likely to shift in the quality and total quantity of plant-derived inputs (Six et al., 2002). Therefore it is essential that we

understand the current sources of SOM, and how they may be susceptible to losses, or gains, in response to environmental changes if we are to consider soils a natural climate solution.

Globally, soils down to 1 m hold more carbon ( $\approx 1,500$  Pg) than the atmospheric ( $\approx 867$  Pg) and terrestrial vegetation pools ( $\approx 560$  Pg) combined (Batjes, 1994). About half of these carbon (C) stocks are in subsoils (Batjes, 2014; Lal, 2018). If accounting for permafrost soils and deeper profiles (3 m), the estimated soil C pool is  $\approx 3,000$  Pg (Scharlemann et al., 2014). Plant and soil respiration returns CO<sub>2</sub> to the atmosphere at almost the same rate as photosynthetic carbon enters the soil; on an annual basis soils are only a net sink of carbon by  $< 5$  Gt C/yr (IPCC 2013; Minasny, et al., 2017). Furthermore, despite the importance of deep soil C pools (Gross and Harrison, 2019; Button et al., 2022), the average maximum depth of studies from four prominent soil science journals is only 24 cm (Yost and Hartemink, 2020). This lack of sampling deep soils, and dearth of soil data where there is the most C limits our ability to develop a holistic understanding of global scale C dynamics. The purpose of this general field of research is to try and fill that knowledge gap because the co-benefits of global increases in SOM are vast and undervalued. But the purpose of this specific dissertation is simply an attempt to push those larger aims forward, in any small way possible.

## 1.2 Overview of Manuscripts

The first manuscript presented in this dissertation focuses exclusively on a highly productive, andic-influenced, forest soil supporting industrial timber production. Leveraging a standardized biomass manipulation study design replicated across the world, we examine how SOM changed as a result of experimental biomass removal treatments. This manuscript exemplifies the strength of the cupric oxidation (CuO) method in identifying and tracking sources of plant-derived OM. We used soil density separation techniques to identify more sensitive indices of SOM losses that are not apparent when examining only bulk soil samples. Using stable isotopes, we show that ‘stable’ carbon on mineral soils, are not always stable. Using a variety of methods we explain how this unique forest soil is resilient to major disturbances, likely due to the root biomass stores that have developed over millennia. But we also caution that not all soils are as productive, and if only examining surface bulk soil samples the signal of disturbance is still present, but heavily obscured.

The second and third manuscripts use an observational study that incorporates nearly every major biome type present in North America. As part of the construction and installation of the National Ecological Observatory Network (NEON), we received soil cores that regularly exceeded 100 cm in depth. We identified three representative soil horizons, in a continuum of soil pedologic processes, and examined patterns in SOM using the CuO method. Through a collaboration with the USDA Forest Service, we also separated these soils based on density to better understand how different pools of SOM are shaped by climatic conditions and local plant communities. The second manuscript focuses on characterizing how certain

classes of plant-derived biomarkers change across ecosystems. We find a surprising consistency in the lignin contributions to SOM stores across ecosystems, and suggest these ecosystems - and their microbial counterparts - push the diverse range of plant OM inputs towards a more homogenized SOM composition. The third manuscript uses the full suite of CuO extracted organic compounds to compare the OM signature of plant endmembers (aboveground vegetation and roots) to the A-horizons, upper-most illuvial B-horizons, and the deepest B-horizons. We find exactly half of A-horizons studied reflect a more root-derived signature, with the other half resembling a more aboveground vegetation signature. While the proportion of organic compounds between vegetation endmembers and mineral soils vary, mineral soil horizon OM compositions were somewhat uniform down soil profiles, with some notable exceptions. This reinforces the view that despite a wide range in the quantity and quality of plant inputs there is a homogenizing effect on SOM composition, but that site-specificity is still an integral part in the observed soil organic matter composition across sites and down soil profiles.

Chapter 2: Root carbon from harvested trees replaces native mineral  
carbon within two years following biomass removal treatments in a  
Western Oregon Douglas-fir forest

Adrian C. Gallo

Co-Authors: Yvan Alleau, Scott M. Holub, Kate Lajtha, Kim Littke, Brett  
Morissette, Jeff A. Hatten

Expected Submission: Soil Science Society of America Journal

## 2.1 Abstract

Global forest carbon studies have shown mineral soil carbon stocks to be largely resilient from harvesting yet no robust mechanism for this resilience has been shown. We examine the immediate effects of forest harvesting and surface biomass removals on belowground carbon and nutrient stores to identify the mechanisms responsible for the apparent resilience in forest mineral-soil organic matter. We used a Douglas-fir dominated plantation in the Oregon Cascades with three levels of harvest and experimental biomass treatments representing a 10-fold range in surface biomass retention (190 to 20 Mg-C/ha). Six-months following all treatments the surface and subsurface soils increased soil organic carbon (SOC) stocks by 8-42%. Two years later surface soil SOC returned to pre-treatment values but subsoils lost 8-17% of their original stocks. Surface and subsurface enrichment of  $\delta^{13}\text{C}$  began immediately post harvest, but  $\delta^{15}\text{N}$  enrichment required two years to manifest suggesting a time-dependent decoupling in carbon and nitrogen cycling rates. Biomarker analysis indicates the remaining soil carbon after two years shifted towards a more root-derived signature with a stronger microbial imprint. Separating the soil using density fractionation, representing particulate and mineral-associated organic matter fractions, we find significant losses in carbon and nitrogen pools from the free light and intermediate fractions. Heavy fraction carbon pools appeared not to change, however all heavy fraction depths and treatments exhibited strong  $\delta^{13}\text{C}$  enrichment suggesting this 'stable' carbon is dynamic. The apparent resilience of forest soil C is likely due to root-carbon pools rapidly decomposing and replacing native organic matter. If forest harvest rotations shorten before root-carbon pools can be replenished, forests

may lose their resilience.

## 2.2 Introduction

Forests contain a large proportion of the carbon stores in terrestrial systems. Natural disasters (e.g. wildfires, pathogens) (Nave et al., 2011) and decreased time of tree harvest rotations are shifting how terrestrial systems are cycling organic matter (Nave et al., 2010; James and Harrison, 2018). Increasing demand for wood products in high income countries places market pressures on lower-income countries to increase timber production (Zhang et al., 2020), often at unsustainable levels. In the Pacific Northwest, which accounts for 12% of the total US forest sector carbon sink (Nave et al., 2022), high timber demand puts pressure on increasingly smaller areas of intensively managed forested lands to provide a disproportionate amount of wood products (Food and Agriculture Organization, 2006). The expected higher intensity of timber harvesting occurring on smaller land areas that increase organic matter removals and decrease time for ecosystems to recover will require site-specific knowledge to sustainably manage (Fox, 2000). Therefore, we need a better understanding of soil organic matter (SOM) dynamics immediately following different timber harvest regimes to predict the long-term sustainability of our current forest practices.

Long-term forest soil productivity studies on compaction and surface biomass removal effects have shown that soil carbon (C) is surprisingly resilient to these perturbations (Powers et al., 2005). Although forests that are already dry or contain low nutrient holding capacity remain at risk of site degradation (Fox, 2000; Paz 2001; Evans 1992). Deep soils are understudied compared to surface soil horizons, but they tend to show larger SOC losses (James and Harrison, 2018; Gross and

Harrison, 2019). The mechanism underlying the resilience – or lack thereof – to extreme biomass removals require long-term studies (e.g. detrital input and removal treatments – DIRT; long-term soil productivity – LTSP), but it is less common to examine the site’s immediate resistance to change following these biomass removals. Identifying changes in bulk soil C stocks is both difficult to find statistically significant differences due to large pool sizes relative to small shifts in stocks (Holub and Hatten, 2019). They may also be too slow to identify responses given shortened rotations of intensively managed plantations (Fox, 2000). For example, afforested lands require at least 20 years to see consistent changes to SOC (Nave et al., 2013). To address this knowledge gap, we examined the immediate effects of intense biomass removal treatments using more sensitive indices of SOM cycling using operationally defined pools of SOM that can provide a mechanistic understanding of SOM cycling to infer how other forests are responding to shorter forest harvest rotations and their long-term sustainability.

Separating SOM based on density is thought to represent a more effective distinction between rapidly cycling and more stable forms of organic matter that cannot be obtained from bulk soils alone (von Lutzow et al., 2007 and references therein). The free light fraction (FLF) is generally composed of particulate organic matter (POM) and has a relatively lower density compared to the heavy fraction (HF) which generally consists of mineral associated organic matter (MAOM). The FLF is often composed of less decomposed plant and animal fragments (Lavelle et al., 2019; Lehmann and Kleber, 2015), with short turnover times on the scale of years to decades (von Lutzow et al., 2007; Sollins et al., 2009). The MAOM has a much lower

carbon density, usually 0.1-1.0% C, and longer turnover times (hundreds to thousands of years (Heckman et al., 2022 GCB). The greater turnover times of MAOM compared to POM is thought to be due to physical protection due to the majority of the mass fraction being mineral material allowing organic matter to be directly sorbed to mineral surfaces by stronger sorption phenomenon such as inner-sphere complexation rather than weaker outer-sphere ionic exchange. Furthermore, the rates of MAOM stabilization are generally slower than the rates of destabilization (Bailey et al., 2019). Thus, the partitioning of organic matter into the FLF vs MAOM fractions may be able to capture both near term responses to changes in organic matter inputs and long-term SOM dynamics.

The LTSP experimental design has been replicated globally that includes three levels of biomass harvesting treatments crossed with compaction. The three biomass treatments include bole only (BO) that removes only the merchantable wood, whole tree (WT) that removes the merchantable wood and branches, needles, tree tops and any legacy wood; and whole tree plus forest floor (WTFF) that removes the whole tree and any forest floor, but leaving stumps, resulting in bare exposed mineral soil. After a decade of LTSP research, Powers et al. (2005) observed mineral soil carbon concentrations were mostly unaffected by BO or WT removals, but decreases in carbon concentration following WTFF. Mineral soil carbon resilience following forest biomass removals has many possible mechanisms, one of which is the root biomass pool rapidly decomposing and contributing to the mineral soil carbon pool thus buffering any losses from aboveground removals that we explore below. Based on previous research conducted on this site, we showed that the average and max-

imum daily soil temperature increased as a function of increased biomass removals with limited evidence of any moisture limitations on any treatment even through the summer seasons (Gallo et al., 2022). However, we also found soil respiration rates on these sites were not statistically different across the three biomass removal treatments, even when accounting for different sources of respiration (Gallo, 2016). We posit the physical disturbance of harvesting on all plots masked the microbial respiration response in the ensuing two years, but that other metrics of SOM cycling should be more sensitive to these soil biophysical shifts. Furthermore, research at this site (Little et al. 2021) reported strong 0-3 year seedling growth responses compared to other PNW LTSP sites, and that the warmest plots with the least amount of residual organic matter (WTFF) had the highest foliar N content of any other treatment. This is despite a decade of findings from the LTSP network showing that WTFF removals were the only treatment to consistently reduce soil C and N concentrations as well as reduce mineralizable N (Powers et al., 2005).

In this study, we used a combination of soil separation techniques and biomarker analysis to better understand the biochemical dynamics of a newly installed LTSP-affiliate site. We hypothesized that bulk SOC pool sizes would remain stable on BO and WT treatments, but that WTFF removal treatments would see a decrease in both soil C and N stocks due to losses from the FLF fraction. We expected the CN ratio to decrease in BO treatments due to increased high-N inputs from needle litter. We also expected bulk soil  $\delta^{15}\text{N}$  and  $\delta^{13}\text{C}$  would become depleted in BO treatments as a result of new fresh C and N inputs and become enriched in WT and WTFF treatments due to a lack of aboveground inputs, and that these bulk soil responses

would be mirrored in FLF but the intermediate and heavy fractions would remain stable. Finally, we expected the composition of SOM to shift towards an overall root-derived signature that would be greater as more residual biomass was removed.

Based on our emerging understanding of forest response to differing harvest regimes the objectives of this study were to (1) quantify changes to SOM pool sizes immediately following harvests and two years post-biomass removal treatments, and (2) assess whether the SOM composition shifted within individual SOM pools. By examining the stock sizes and the composition of soil organic matter we hope to identify the mechanisms that contribute to a site's apparent resistance and/or resilience to perturbations in biomass inputs or removals.

## 2.3 Materials and Methods

### 2.3.1 Site description

A complete site description and study design are provided in Gallo et al. (2022). Briefly, the study site is along the western side of the Cascades east of Springfield, OR on a uniform 15-25% south facing slope. This was installed as an affiliate site of Long-term Soil Productivity (LTSP) Experiment (Powers et al., 1990), with funds provided by the Northwest Renewables Alliance (NARA). In accordance with other research on this area, this site is described herein as the "NARA LTSP Springfield" site (Gallo et al., 2022; Littke et al., 2021). The soils are best represented by the Kinney series described as Fine-loamy, isotic, mesic Andic Humudepts with clay and clay loam textural classes to 100 cm depth and an average surface soil pH of 5.2

(Soil Survey Staff, 2015). The andic influence of this site likely results in higher than average extractable Fe and Al compared to other forest soils (Wada, 1980; Strahm et al., 2006). During the two years of observation, the mean annual temperature was 10°C with a mean annual precipitation of 135 cm falling as rain mostly from October to May. The area had an original harvest in  $\approx$ 1950, presumably an old mature stand, that used a broadcast burn and natural regeneration to re-seed the site entirely with Douglas-fir (*Pseudotsuga menziesii*) and with a mid-rotation thinning. The second harvest, occurring in 2013, recorded a King’s site index of 37 m (121 ft) at 50 years (King, 1966).

### 2.3.2 Experimental design and sampling

As an LTSP affiliate site, only five of the original nine treatments were established that manipulated residual surface biomass and the bulk density of mineral horizons (Powers 1990, 2005). The three biomass removal treatments include: bole only (BO) harvests that removed the merchantable stem but retained the branches, tops, and other needle litter on site. Whole tree (WT) biomass harvests removed all above-ground tree biomass and legacy wood, but retained stumps and an intact O-horizon. The whole tree plus forest floor (WTFF) treatments removed all merchantable and non-merchantable tree biomass, the O-horizon, and legacy wood but retained all stumps. Compaction was measured using bulk density hammer cores for 0-15 and 15-30 cm depths prior to treatments and immediately post-treatments. Moderate compaction (denoted with a “C”) was fully crossed in the bole only and whole tree

removals, resulting in BOC and WTC treatments. Due to practical limitations of removing the forest floor, likely inducing compaction, we only have WTFFC treatments and lack a non-compacted pairing. Each plot ( $n = 20$ ) is 0.4 ha in area, with an internal measurement area 0.2 ha (1-acre), with all five treatments assigned to four blocks based on 0-100 cm soil nitrogen stores. Treatment installation (harvesting, compaction, and/or forest floor removal if necessary) concluded during the summer of 2013.

Compared to pre-harvest values, moderate compaction increased the bulk density of the surface mineral soil by 16, 17, and 23% for the BOC, WTC, and WTFFC treatments respectively (Gallo et al., 2022). However, the andic mineralogy of this site is apparent from the average pre-treatment mineral soil bulk density values of  $\approx 0.60$  and  $\approx 0.70$  g/cm<sup>3</sup> for the 0-15 and 15-30 cm depths respectively. The residual surface biomass post-treatment retained approximately 190, 80, and 20 Mg/ha for the BO/C, WT/C and WTFFC treatments respectively. The WTFFC treatments were never conceived as a forest management practice for industrial or public land management agencies and they should only be viewed as a purely experimental product (Powers, 1990). Additional details of compaction application can be found in Gallo et al. (2022).

Soil sampling occurred during three time-points: pre-harvest in 2012, immediate post harvest in late 2013, and two years post-harvest in 2015. During pre- and immediate-post harvest sampling, plots were sampled from 25-unique locations collecting forest floor biomass, 0-15, 15-30, and 30-100 cm bulk density samples. These 25 points were then composited (herein described as ‘bulk soils’) for final analysis,

with the bulk density data used to calculate pre and post bulk soil C and N stocks. The 2015 sampling effort only collected forest floor, 0-15, and 15-30 cm samples at 25 unique locations to form the composite sample for final analysis. We assumed bulk density did not change from immediate-post to two-year post sampling.

### 2.3.3 Density fractionation

We performed sequential density separations on the 0-15 and 15-30 cm soil samples pre- and two-year post treatment following the standard procedures outlined in Sollins et al. (2009). Briefly, 7 g of 60°C dried soils were mixed with a total of 70 mL ultra-pure sodium polytungstate (SPT-0, GeoLiquids, Prospect Heights, Illinois) to collect the light fraction ( $>1.8$  g/cm<sup>3</sup>), the intermediate fraction (1.8-2.5 g/cm<sup>3</sup>), and the heavy fraction ( $>2.5$  g/cm<sup>3</sup>). Each fraction was extracted twice with the same density of liquid by mixing for 2 hours, centrifugation for 1 hr, aspiration of the supernatant, followed by vortexing the remaining pellet to resuspend the remaining material for the next round of SPT addition. The supernatant was then rinsed with 1,000 mL of DDI water on a combusted GF/F filter attached to a vacuum buchner funnel to efficiently remove any remaining polytungstate salt and collect the remaining fraction on the filter. The fraction remaining on the filter was quantitatively transferred with DDI water to an acid-washed and pre-weighed dish, oven dried overnight at 40°C, then scraped off into a scintillation vial for final analysis. The acid-washed dish was re-weighed to calculate masses of individual fractions. Aliquots of the SPT solution were periodically collected throughout individual steps

to ensure the density of the SPT solution remained consistent.

Each density fraction is thought to represent a unique pool of soil organic matter. The selection of 1.8 g/cm<sup>3</sup> for the light fraction and 2.5 g/cm<sup>3</sup> for the heavy fraction was based on analysis conducted by Sollins et al. (2006) which also used andic-influenced soils from Oregon. The light fraction is generally characterized by a high organic matter content ( $\approx 30\%$  organic carbon) composed primarily of plant debris, and is considered sensitive to changes in management (Dalal and Mater, 1986; Compton and Boone, 2000). The heavy fraction is dominated by mineral material with low organic carbon content ( $\approx 1\%$  or less) that tends to have lower  $^{14}\text{C}$  values than bulk soil or light fractions implying some level of carbon persistence (Swanston 2005; Sollins et al., 2006, 2009). The intermediate fraction for this study (1.8-2.5 g/cm<sup>3</sup>) is likely to contain some plant fragments sorbed to mineral particles and microaggregates, but still dominated by a mineral matrix with an approximate organic C concentration of 3-5 %. For ease of comparing across other density fractionation studies, our FLF is generally consistent with particulate organic matter (POM) category; the mineral associated organic matter (MAOM) fraction from other studies is representative of the combination of our intermediate and heavy fractions (Sollins et al., 2009; Lavallee et al., 2019; Heckman et al., 2022)

Using ultra-pure sodium polytungstate (SPT-0) ensures the individual fractions can then be analyzed for carbon and nitrogen stable isotopes without C or N contamination issues (Sollins et al., 2009). While there is substantial rinsing of the density fractions with DDI water, there is little carbon lost in the dissolved fraction (Helbling et al., 2021), and if the sum of the three density separated masses were less

than 90% of the parent sample mass, the sequential density separation was repeated.

### 2.3.4 CN and stable isotopes

Bulk soil samples were air dried at 60°C then passed through a 2 mm sieve. All samples were then pulverized with a KLECO ball-mill grinder to fully homogenize the samples for further analysis. Depending on the sample type, between 3-30 mg of sample were loaded in tin boats and combusted in a Flash EA112 Elemental Analyzer for carbon and nitrogen with a precision of replicate samples of  $\pm 5\%$  and reference materials  $\pm 2\%$  of measured values. We used isotope ratio mass spectrometry following high-temperature combustion to determine the  $\delta^{13}\text{C}$  and  $\delta^{15}\text{N}$  values.

### 2.3.5 Cupric oxidation (CuO) procedures

We used the Cupric Oxidation (CuO) procedure to identify biomarkers that allow us to trace the sources of soil organic matter, especially from unique plant-tissue components (Hedges and Mann 1979). The procedure was originally developed by Hedges and Ertel (1982), modified by Goñi and Hedges (1992), and finally refined into our current working method by Goñi and Montgomery (2000). Due to practical constraints, CuO analysis was conducted on both mineral soil depths for the pre- and two-year post sample periods.

Briefly, each 55 mL Teflon bomb vessel (MARS Xpress) contains approximately 5 mg of organic carbon combined with cupric oxide, ferrous ammonium sulfate, and N<sub>2</sub> degassed NaOH before microwave digestion (CEM Mars 6 Xpress) for 1.5 hours at

150°C. Following the microwave-induced oxidation, internal recovery standards are added (ethyl vanillin and cinnamic acid) before a quantitative transfer into centrifuge tubes with an additional NaOH rinse. The solution is then centrifuged (Thermo Scientific, Sorvall Legend XTR) with the supernatant transferred and acidified to pH 1. Two rounds of ethyl acetate (HPLC grade) additions are used to extract the organic matter, with the organic supernatant transferred to 12 mL vials for efficient evaporation under heat (50°C) and N<sub>2</sub> purging (LabConco RapidVac Vertex Evaporator). The dried solution is then re-dissolved with pyridine and stored in amber vials in a refrigerator until final analysis.

For more efficient sample behavior in the gas chromatograph, a 50 uL subsample was derivatized with 50 uL BSTFA (+ 1% TCMS), vortexed, and heated to 40°C for 30 minutes. We used a Hewlett Packard (6890 series) gas chromatograph fitted to a Agilent Technologies (5973 Network) mass spectrometer with a DB-5 column (Agilent Technologies, 30 m length, 0.25 mm internal diameter, 0.25 um film thickness) for all analysis. We employed a six point calibration curve with concentrations ranging from 1-50 ug standard / mL. The calibration contained 22 commercially available compounds that include all CuO oxidation products presented herein.

We present data for the following CuO oxidation products: lignin (the sum of the vanillyl, syringyl, and cinnamyl phenols) (Hedges and Mann 1979, Hatten et al., 2012), cutin (16-hydroxyhexadecanoic acid, 8,16-dihydroxydecanoic acid, 9,16-dihydroxydecanoic acid, 10,16-Dihydroxydecanoic acid, 7-hydroxyhexadecane-1,16-dioic acid, 8-hydroxyhexadecane-1,16-dioic acid, 18-hydroxyoctadec-9-enoic acid) (Hatten et al., 2012, Goñi and Hedges 1995; Goñi and Hedges, 1990; Crow et al., 2009a),

suberin (hexadecanedioic acid and  $\omega$ -hydroxyoctadecenoic acid) (Crow et al., 2009a), and non-lignin para-phenols that are designated with the letter P (the sum of p-hydroxybenzaldehyde, p-hydroxyacetophene, p-hydroxybenzoic acid) (Goñi et al., 2008). These P compounds are predominantly of microbial origin, with higher P:V ratios indicating more microbial processing of lignin products. Illustrations of these lignin structures can be found in Hedges et al (1988), and non-lignin structures can be found in Goñi and Thomas (2000) and Kogel-Knabner (2002). We normalized these CuO indices to organic carbon, and use the term “lignin/suberin content” to indicate the lignin contributions to the total soil organic carbon pool.

### 2.3.6 Statistics

All statistical comparisons were done relative to the pre-harvest values, positive effect sizes indicate an increase in the response variable compared to pre-harvest, and negative effect sizes indicating losses compared to the pre-harvest values. Linear mixed-effect models were used to fit all data and comparisons of means were done using paired two-sided t-tests in R statistical software (v.3.3) (Bates, 2005; Zurr et al., 2008; Pinheiro et al., 2014; R Core Team, 2021). All models included year (2012, 2013, 2015) and treatment (BO, BOC, WT, WTC, WTFFC) as fixed effects, and plots nested within blocks as random effects. The interaction term between organic matter removals and compaction were tested, but was removed due to a lack of significant effect for any response variable at any depth or density fraction result that is presented. To simplify the analysis, we show the average responses across both

compaction treatments (with and without compaction) and are represented simply as the three biomass removal treatments (BO, WT, WTFFC). A family-wise Bonferroni adjustment was used for multiple comparisons, with  $\alpha=0.10$  used to assess statistical significance for all tests.

## 2.4 Results

Soil carbon stocks increased immediately after treatment, but with a return to near baseline after two years. Bulk soil stable isotopes exhibited different trends, with a general enrichment over time that was more prominent in  $\delta^{15}\text{N}$ . The CuO biomarkers trended towards a more root-derived origin across all treatments, but with stronger effects in the surface horizon. Density fraction data show consistent losses of C from the intermediate fraction in the surface, and the light and intermediate fractions in the subsurface horizon. Stable isotopes of each density fraction show an enrichment of  $\delta^{13}\text{C}$  across heavy and intermediate fractions, but  $\delta^{15}\text{N}$  show depletions in the light fraction.

### 2.4.1 Soil carbon and nitrogen

There was a general trend of increasing SOC stocks and CN ratios in both soil depths immediately after treatment, but a variety of responses two years post-treatment (Figure 2.1). Surface horizons increased SOC stocks by 17-42% immediately post treatment. Subsurface horizon SOC stocks increased by 13-18%, although with few statistically significant differences in both depths (Table 2.1). Surface horizon in-

creases in SOC stocks immediately post-treatment were approximately 2-3 times the increases seen in subsurface horizons. Across all treatments and depths, only the 0-15cm WTFFC treatment had statistically significant increases in SOC stocks (+28 Mg C/ha) (Table 2.1).

Two years after treatment installation, there was a consistent but non-significant trend of SOC losses of -4.6 to -8.5 MgC/ha across all plots in the 15-30cm depth. However, we could not detect any statistically significant differences in SOC stocks of pre vs two year post-treatment in any treatment or either depth.

The CN ratios across all treatments and depths generally increased immediately after treatment, and remained elevated after two years (Figure 2.1), but with few statistically significant differences (Table 2.1). The two 0-15 cm significant differences are WTFFC pre vs post, and WT pre vs two year post. Only one significant difference in the 15-30 cm was detected in the BO pre vs post treatment comparisons (Table 2.1).

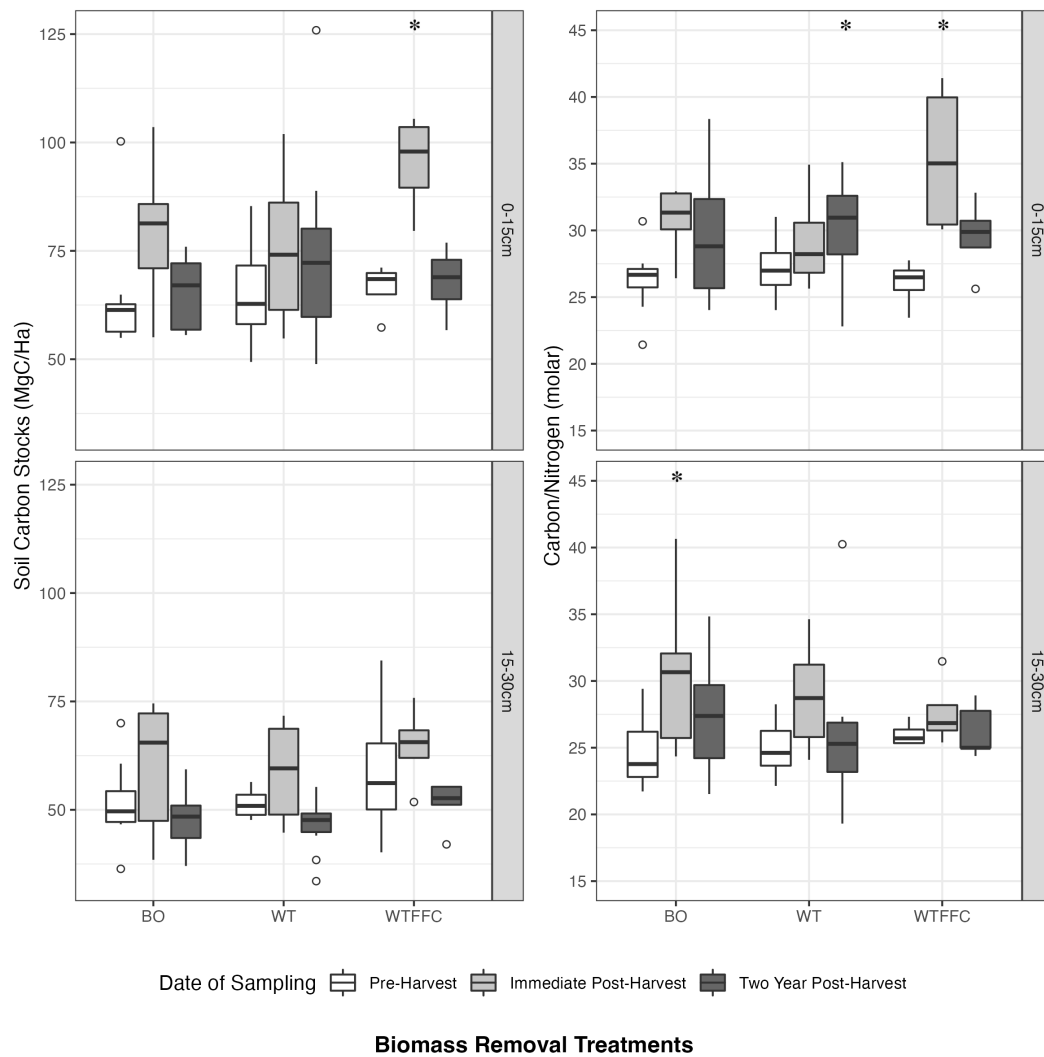


Figure 2.1: Soil organic carbon stocks and CN data for three periods of sample collection and both depths across all treatments at the NARA-LTSP site near Springfield, OR. Treatments include bole only (BO), whole tree (WT), and whole tree plus forest floor removals with compaction (WTFFC). (\*) denotes significant difference ( $p < 0.1$ ) from pre-treatment value. Box and whisker plots with open circles indicating outliers.

Sample Period	Variable	Units	0-15cm depth			15-30cm depth		
			BO	WT	WTFFC	BO	WT	WTFFC
Pre Treatment	SOC	(Mg C / ha)	64.7 (±5.2)	64.6 (±4.2)	66.4 (±3.1)	51.6 (±2.8)	51.5 (±1.2)	59.2 (±9.3)
	TN	(Kg N / ha)	2885.6 (±238.8)	2761.3 (±132.1)	2993.7 (±221)	2459.9 (±154.1)	2411.4 (±77.9)	2641.4 (±368.3)
	CN	unitless	26.31 (±0.94)	27.19 (±0.83)	26.04 (±0.92)	24.71 (±0.91)	25.04 (±0.79)	26 (±0.47)
	C13	(0/00)	-25.94 (±0.07)	-25.72 (±0.08)	-25.78 (±0.08)	-25.6 (±0.04)	-25.47 (±0.06)	-25.44 (±0.07)
	N15	(0/00)	3.79 (±0.18)	3.3 (±0.24)	3.61 (±0.29)	4.66 (±0.25)	4.4 (±0.23)	4.71 (±0.47)
Immediate-Post Treatment	SOC	(Mg C / ha)	78.86 (±5.63)	76.1 (±6.35)	<b>95.2 (±5.9)</b>	60.36 (±4.98)	58.94 (±4.07)	64.7 (±4.9)
	TN	(Kg N / ha)	2999.8 (±243)	3044.1 (±185.4)	3224.3 (±372.9)	2407.65 (±276.7)	2411.6 (±176.7)	2755.6 (±276.5)
	CN	unitless	30.92 (±0.78)	28.97 (±1.09)	<b>35.38 (±2.95)</b>	<b>30.28 (±1.89)</b>	28.86 (±1.4)	27.64 (±1.33)
	C13	(0/00)	-25.69 (±0.18)	-25.67 (±0.07)	-25.72 (±0.07)	<b>-25.53 (±0.09)</b>	-25.4 (±0.05)	-25.43 (±0.07)
	N15	(0/00)	3.99 (±0.28)	3.56 (±0.14)	3.61 (±0.29)	4.68 (±0.15)	4.82 (±0.2)	4.82 (±0.2)
Two-Year Post Treatment	SOC	(Mg C / ha)	65.5 (±2.92)	75.07 (±8.58)	67.9 (±4.3)	47.66 (±2.44)	46.56 (±2.08)	51.3 (±2.5)
	TN	(Kg N / ha)	2640.4 (±176)	2610.3 (±150.7)	2715.4 (±270.2)	<b>2062.6 (±162.9)</b>	2137.3 (±113.3)	2303 (±165.6)
	CN	unitless	29.55 (±1.76)	<b>33.93 (±4.1)</b>	29.55 (±1.48)	27.61 (±1.6)	25.97 (±1.77)	26.21 (±0.9)
	C13	(0/00)	-25.88 (±0.06)	-25.67 (±0.06)	-25.62 (±0.09)	-25.45 (±0.05)	-25.42 (±0.03)	-25.3 (±0.08)
	N15	(0/00)	4.26 (±0.14)	<b>4.26 (±0.11)</b>	<b>4.51 (±0.14)</b>	<b>5.5 (±0.12)</b>	<b>5.27 (±0.07)</b>	<b>5.44 (±0.24)</b>

Table 2.1: Summary data for three periods of sample collection and both depths across all treatments at the NARA-LTSP site near Springfield, OR. Treatments include bole only (BO), whole tree (WT), and whole tree plus forest floor removals with compaction (WTFFC). Bold indicates significant differences ( $p < 0.1$ ) compared to pre-treatment values with a family-wise Bonferroni adjustment for multiple comparisons.

## 2.4.2 Stable isotopes (bulk soils)

Across all treatments and depths there was a consistent overall enrichment of  $\delta^{13}\text{C}$  immediately after harvests, with the strongest effects of both  $\delta^{13}\text{C}$  and  $\delta^{15}\text{N}$  present two years after treatment installation (Figure 2.2). While there was a trend of enrichment of  $\delta^{13}\text{C}$  across both sampling periods, only the 15-30cm BO pre vs two year post was statistically significant (Table 2.1). In contrast,  $\delta^{15}\text{N}$  did not shift immediate-post treatment for any depth, but two years later nearly every comparison showed a statistically significant enrichment (Table 2.1). Across all treatments, the

average two year  $\delta^{15}\text{N}$  enrichment was +0.776 and +0.820 for the 0-15 and 15-30 cm depths respectively. The only pre vs two year comparison that was not statistically significant, was the BO 0-15cm treatment which showed an enrichment of +0.48 which was approximately half of the effect size of all other pre vs two year post comparisons (Table 2.1).

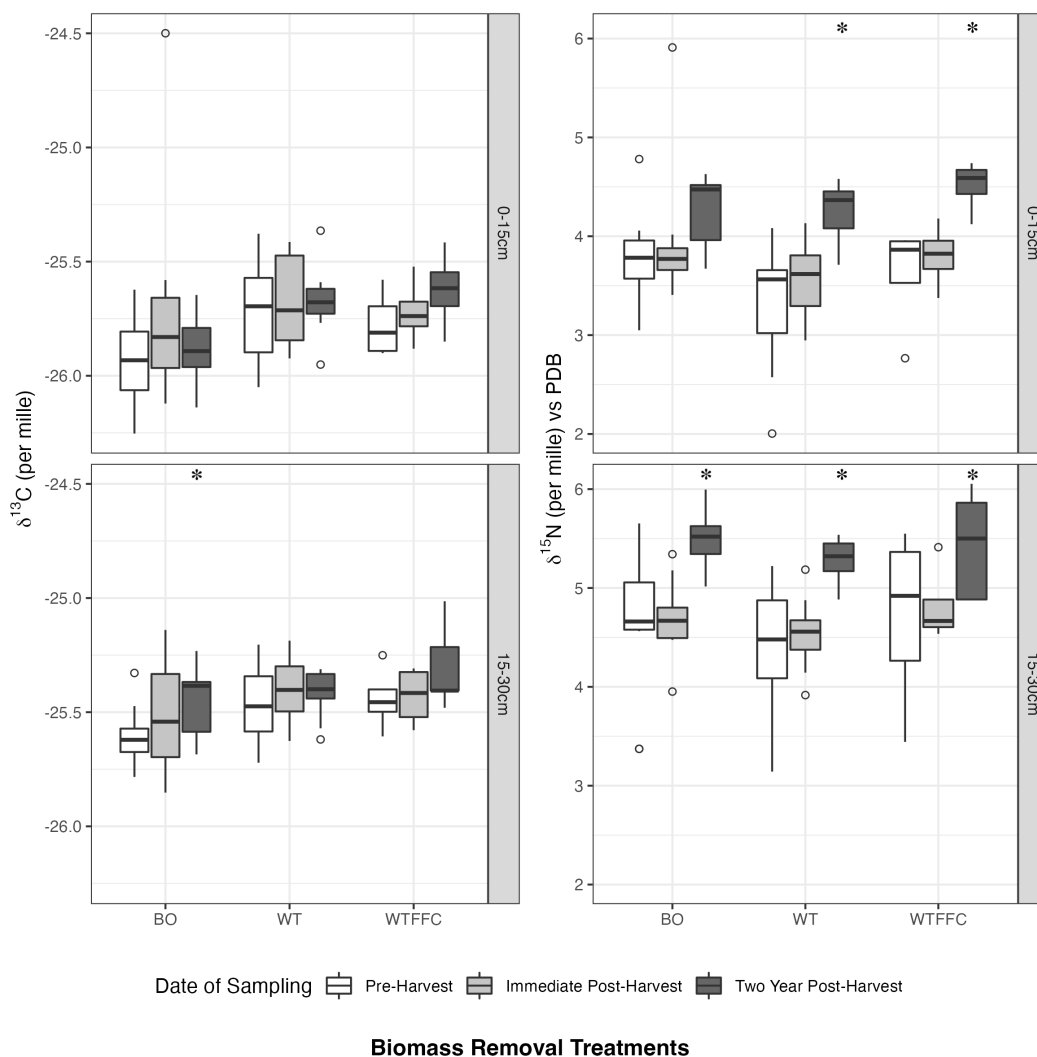


Figure 2.2: Carbon and nitrogen stable isotope data for three periods of sample collection and both depths across all treatments at the NARA-LTSP site near Springfield, OR. Treatments include bole only (BO), whole tree (WT), and whole tree plus forest floor removals with compaction (WTFFC). (\*) denotes significant difference ( $p < 0.1$ ) from pre-treatment value. Box and whisker plots with open circles indicating outliers.

### 2.4.3 Cupric oxidation (bulk soils)

Two years following treatment, there was a general trend of changes in biomarker composition across all treatments, although most statistically significant effects were only present in the surface soil horizons (Figure 2.3). Lignin and suberin content (both normalized to C) in the 0-15 cm tended to increase in all treatments, although with few

statistically significant differences. Both BO and WTFFC Cutin:Suberin values (an indication of plant vs root wax contributions) in surface soils decreased significantly and of similar magnitude (-9 and -10 units respectively). The P:V ratios (an indicator of microbial to plant derived organic matter) generally increased across all treatments and both depths, but only the WT saw statistically significant increases.

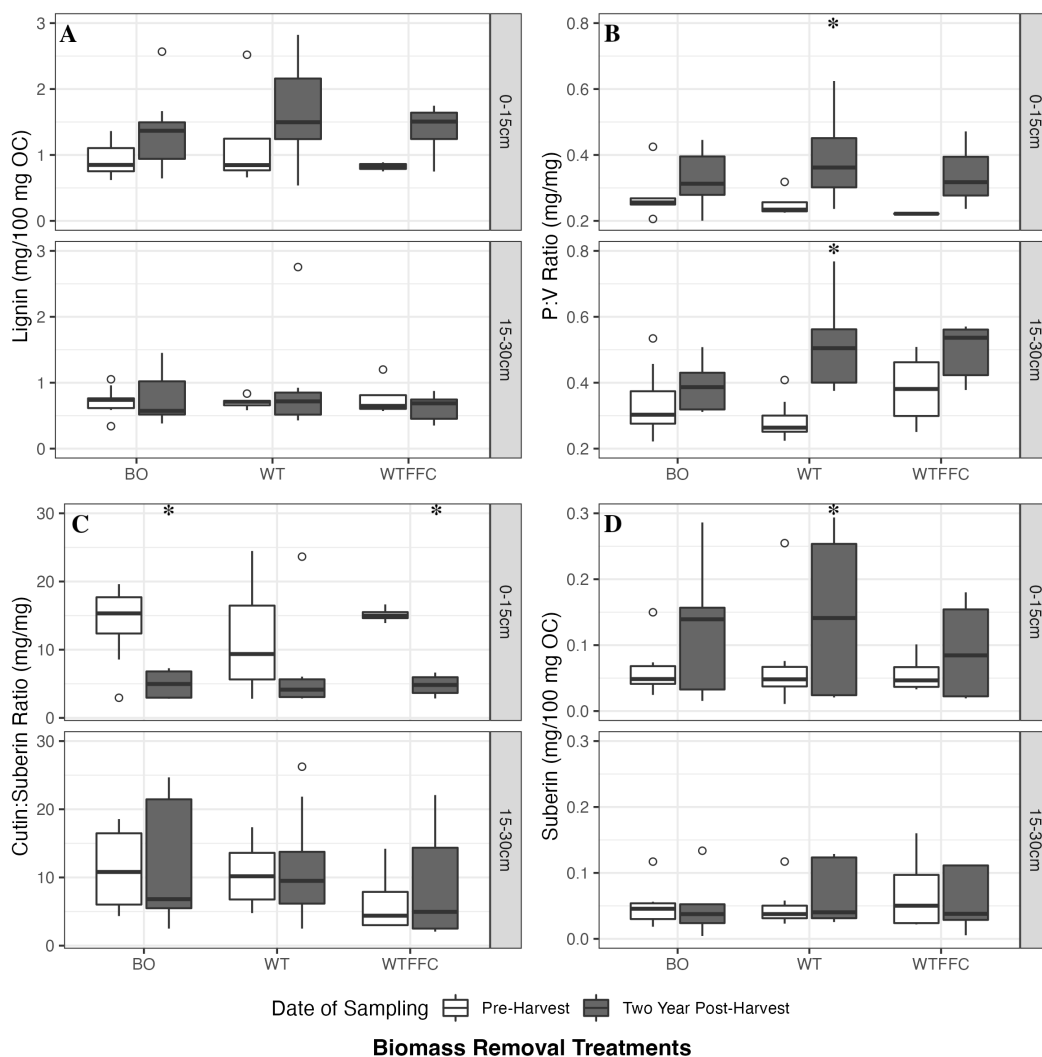


Figure 2.3: Soil biomarker data derived from the cupric oxidation method for two periods of sample collection and both depths across all treatments at the NARA-LTSP site near Springfield, OR. Treatments include bole only (BO), whole tree (WT), and whole tree plus forest floor removals with compaction (WTFFC). The P:V ratio includes para-hydroxybenzene (P) to vanillyl (V) phenols with higher values indicating greater microbial lignin decomposition. Cutin and suberin are leaf and root waxes respectively. (\*) denotes significant difference ( $p < 0.1$ ) from pre-treatment value. Box and whisker plots with open circles indicating outliers.

#### 2.4.4 Density fraction C and N characteristics

The relative carbon pools within each fraction were similar between pre and post biomass harvesting (Table 2.2), but the total carbon pool within each fraction tended to decrease in both light and intermediate fractions after treatment installation (Figure 2.4). For example, the surface soil light fraction accounted for 45 and 43% of the relative C recovered in pre and two year post samples, the intermediate fraction accounted for 44 and 49% respectively. The average heavy fraction (across all treatments, time points, and depths) accounted for 5-8% of the relative C pool. Total mass recovery across all treatments and both depths, were 97% of the original sample mass in both the pre and two year post time periods (Supplemental Materials). While the relative C pools and mass recoveries did not change across time periods, the total C pool from some density fractions decreased.

Two years after biomass removals, the intermediate fraction saw significantly lower total C pools that were consistent across all treatments and depths (Figure 2.4). The subsoil light fraction also saw consistent significant reductions in total C across all treatments, approximately -35 mg C/g soil (Table 2.2). The greatest subsoil C losses occurred in the intermediate fraction of the WTFFC treatments (-45 mg C/g soil). While the light fraction total C pool in the surface soil appeared to decrease after two years, they are not significantly lower than pre-treatment levels. However, the light fraction N pool was significantly lower across all treatments by approximately -1.6 and -1.1 mg N/g soil in the surface and subsurface horizons respectively (Supplementary Materials). These N pool losses in the light fraction increased as more surface biomass was removed (e.g. losses in WTFFC were -2.2

compared to 1.4 mg N/gsoil in BO). The magnitude of 0-15 cm N pool losses in the light and intermediate fractions were similar, even though the intermediate fraction N pool contains 3-4x more total N (Table 2.2).

The CN ratio in surface soil light fractions significantly increased across all treatments by 9.5, 8.5, and 11.5 units for the BO, WT, and WTFFC treatments respectively (Figure 2.4). Although the light fraction of the subsoil generally increased, only the WTFFC treatment saw a statistically significant increase of 12.4 units. The CN ratio of the intermediate and heavy fractions were similar, 16.6 and 14.5 respectively, with only the 0-15 cm WTFFC intermediate fraction showing a significant decrease of 1.5 units two years post-treatment.



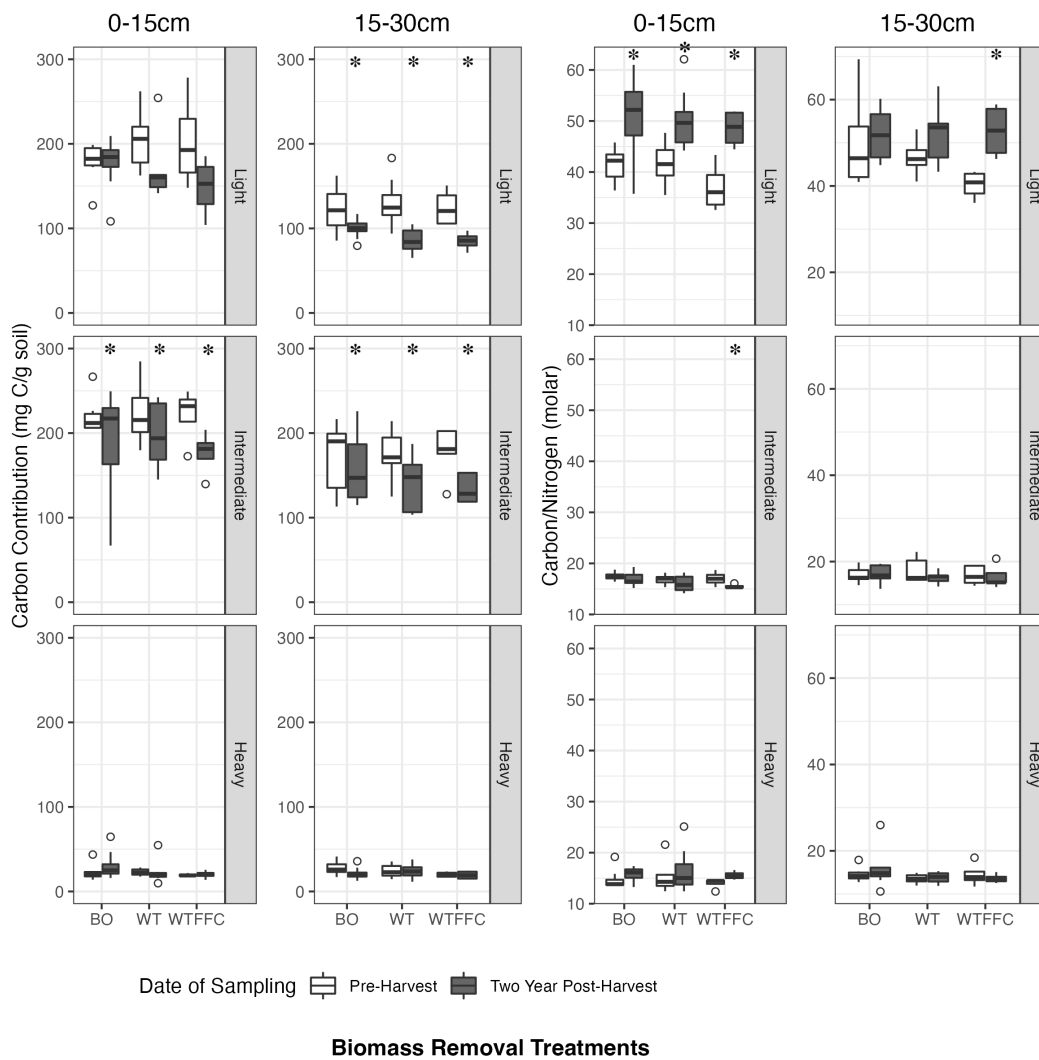


Figure 2.4: Soil C/N data and soil carbon pools derived from density fractionation (light fraction  $>1.8 \text{ g/cm}^3$ ; intermediate fraction  $1.8\text{-}2.5 \text{ g/cm}^3$ ; heavy fraction  $>2.5 \text{ g/cm}^3$ ) for two periods of sample collection and both depths across all treatments at the NARA-LTSP site near Springfield, OR. Treatments include bole only (BO), whole tree (WT), and whole tree plus forest floor removals with compaction (WTFFC). (\*) denotes significant difference ( $p < 0.1$ ) from pre-treatment value. Box and whisker plots with open circles indicating outliers.

### 2.4.5 Stable isotopes (density fractions)

Overall, intermediate and heavy fraction  $\delta^{13}\text{C}$  and  $\delta^{15}\text{N}$  enriched over time across all treatments, but light fraction stable isotope signatures were either unchanged or showed depletions after two years. The pre-treatment light fraction had a more depleted  $\delta^{13}\text{C}$  and  $\delta^{15}\text{N}$  signature compared to either the intermediate or heavy fractions. The heavy fractions tended to have the most enriched pre-treatment isotopic values. Unlike other metrics used to analyze the heavy fraction, the  $\delta^{13}\text{C}$  of all treatments and both depths significantly increased (became enriched in  $\delta^{13}\text{C}$ ) (Figure 2.5). This trend continued for the intermediate fraction of  $\delta^{13}\text{C}$ , as well as the intermediate fractions of  $\delta^{15}\text{N}$ . However, the light fraction  $\delta^{15}\text{N}$  signatures for BO in both depths significantly decreased (became depleted in  $\delta^{15}\text{N}$ ).

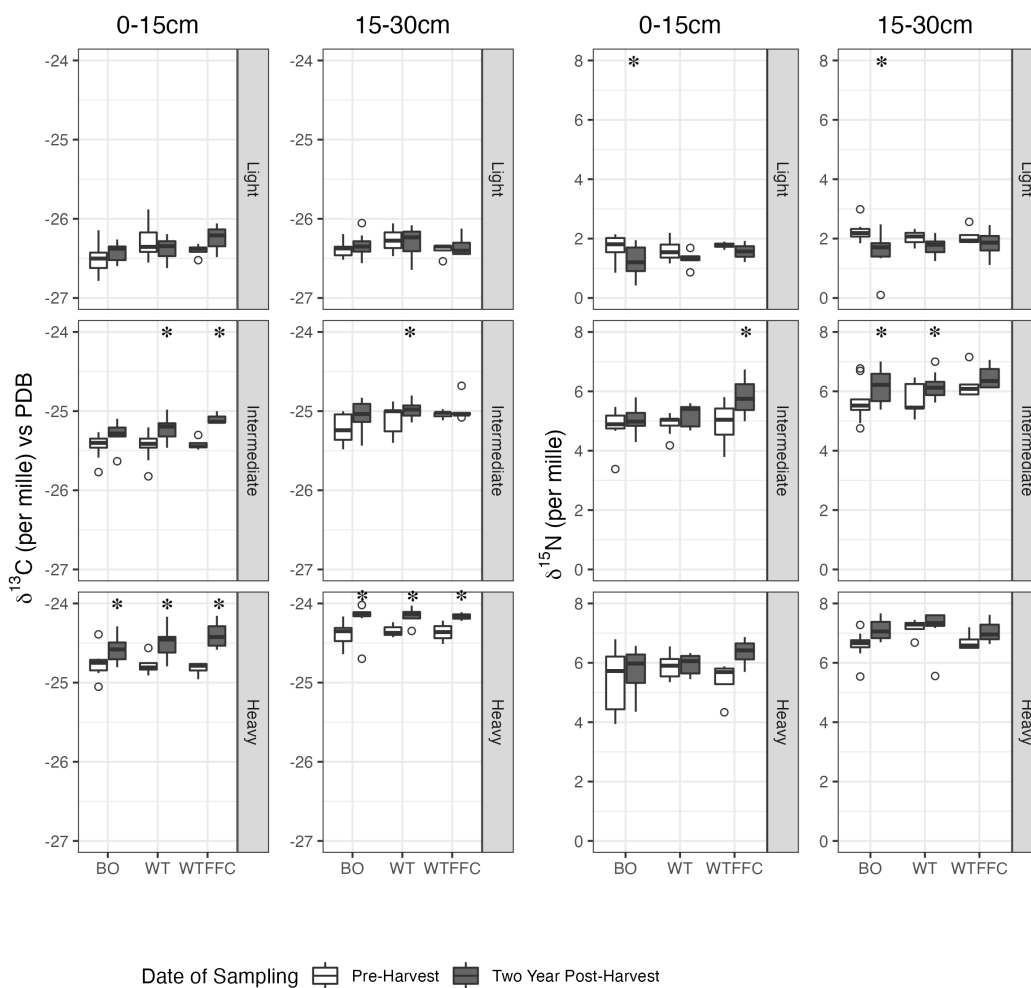


Figure 2.5: Carbon and nitrogen stable isotope data derived from density fractionation (light fraction  $>1.8 \text{ g/cm}^3$ ; intermediate fraction  $1.8\text{-}2.5 \text{ g/cm}^3$ ; heavy fraction  $>2.5 \text{ g/cm}^3$ ) for two periods of sample collection and both depths across all treatments at the NARA-LTSP site near Springfield, OR. Treatments include bole only (BO), whole tree (WT), and whole tree plus forest floor removals with compaction (WTFFC). (\*) denotes significant difference ( $p < 0.1$ ) from pre-treatment value. Box and whisker plots with open circles indicating outliers.

## 2.5 Discussion

### 2.5.1 Bulk soil responses

Contrary to our initial hypothesis, there is some evidence that bulk SOC stocks rapidly increased immediately after biomass removals (Figure 2.1), but these changes were only statistically significant for the 0-15 cm depth of the WTFFC treatment (Table 2.1). The magnitude of SOC increase is larger than measured pre-treatment fine-root biomass observations, suggesting that medium and coarse roots that were not quantified were rapidly fragmented and contributed to the bulk SOC pool immediately post-treatment. Two years after treatment, SOC stocks appear to return to pre-treatment levels in the surface soil and although there are no statistically significant differences in subsurface soils they tend to decrease (Table 2.1). One possible explanation is the recently senesced fine and medium sized roots were able to pass through the sieve during the immediate post-treatment sampling, and now the coarse-sized roots are providing an additional SOC buffer pool. There is additional strength in this explanation based on the biomarker analysis showing a strong shift in bulk soil carbon towards a root-derived signature that is replacing native mineral soil C.

Contrary to our second hypothesis, the CN ratio across all treatments generally increased despite BO receiving inputs from needle litter rich in N and WTFFC treatments receiving only belowground inputs from senesced roots. This is in spite of BO treatment receiving almost 10x more residual surface biomass compared to WTFFC (190 vs 20 Mg/ha respectively). Although there were few significant differences in

SOC and CN ratios, there is an apparent dynamism occurring in surface soils that resulted in an average across treatment SOC stock increase of  $\approx 28\%$  (+18 MgC/ha) immediately post-treatment that dissipates two years later to only a  $\approx 6\%$  increase compared to pre-treatment values (65 to 83 to 69 MgC/ha). We can conclude that, with regards to bulk SOC stocks, these soils appear to not be resistant to large biomass perturbations, but they are simultaneously highly resilient.

Stable isotopes may provide a more sensitive measure of SOM processing not otherwise recognized in bulk SOC and CN observations. We hypothesized treatments with less residual biomass left at the surface would become enriched in both  $\delta^{13}\text{C}$  and  $\delta^{15}\text{N}$ . We find weak evidence for bulk  $\delta^{13}\text{C}$  enrichment across depths and treatments (Table 2.1). However, there was consistent statistically significant  $\delta^{15}\text{N}$  enrichment across all treatments and depths, but it required a full two years post-treatment to manifest itself (Figure 2.2). This lag in N processing may be due to a variety of factors, but we believe the most likely explanation is that N cycling was initially constrained by the pulse addition of high C organic matter when the immediate-post sampling occurred, before N-limitations begin to lift over time allowing for more N nitrification and leaching that results in an overall enrichment in  $\delta^{15}\text{N}$ . It's notable that surface BO treatment did not result in a statistically significant increase, likely due to the additions of abundant needle litter relatively abundant in N from above that were not present in either WT or WTFFC treatments. The consistent enrichment of  $\delta^{15}\text{N}$  in the subsoil suggests there is a N transport limitation even in BO treatments that N-rich needle litter could not buffer against. This is consistent with findings from a nearby conifer forest, where researchers found the dissolved

organic carbon signature from aboveground litter and forest floor was not reflected in mineral soil carbon signature (Crow et al., 2009b).

Tracing the sources of organic matter in soils from biomarker analysis has the potential to elucidate the mechanisms of SOC resilience following major perturbations. We hypothesized the composition of SOM would shift towards a more root-derived signature, and we find convincing evidence for this phenomenon in the surface soils across all treatments (Figure 2.3c, d). The ratio of cutin to suberin is an indicator for the relative contribution of leaf vs root-derived waxes, and both the BO and WTFFC surface soils showed statistically significant increases in Cutin:Suberin indicating a shift towards a root-derived signature (Figure 2.3c). The WT surface soils showed the same trend, but it was not significant. By examining the C-normalized suberin values, we see that all treatments shifted towards a greater contribution of suberin in the surface soil compared to pre-treatment (Figure 2.4d). These patterns in cutin and suberin were not present in the subsoil, likely due to the already high contribution of suberin and relatively low contribution of cutin in the subsoil. This observation is reinforced by a stable isotope-DOC leaching studies showing below-ground glucose additions are more efficient in being converted to stabilized carbon compared to aboveground additions (Sokol and Bradford, 2019), and that new attachments can occur on short timescales (hours) especially on clay-sized minerals (Vogel et al., 2014). Similar to the potential N transport limitation of BO needle litter being unable to buffer against changes in the  $\delta^{15}\text{N}$  signature, there may be an equally plausible O-horizon transport limitation to the subsoil (Sokol and Bradford 2019; Crow et al., 2009b). In addition to a shift towards a root-derived signature,

surface soil P:V ratios indicate all treatments had a shift in SOM composition towards a microbially processed origin compared to pre-harvest (Figure 2.4b). This pattern was only statistically significant for the WT surface and subsurface soils, but all treatments and depths trended towards a higher P:V ratio indicating higher likelihood of microbial origins.

These observations indicate that bulk SOC may not be resistant to biomass harvesting but highly resilient (e.g. rapid changes in SOC immediately post treatment, but SOC returning to approximately pre-treatment values two years later). This resilience follows a weak  $\delta^{13}\text{C}$  enrichment and a strong  $\delta^{15}\text{N}$  enrichment that requires at least two years to manifest, and that bulk SOM composition appears to shift towards a more root-derived signature that is also more microbially processed. These patterns are most pronounced in the surface soils, with some of this behavior occurring in the subsoils as well (mainly enrichment of  $\delta^{13}\text{C}$  and  $\delta^{15}\text{N}$ ).

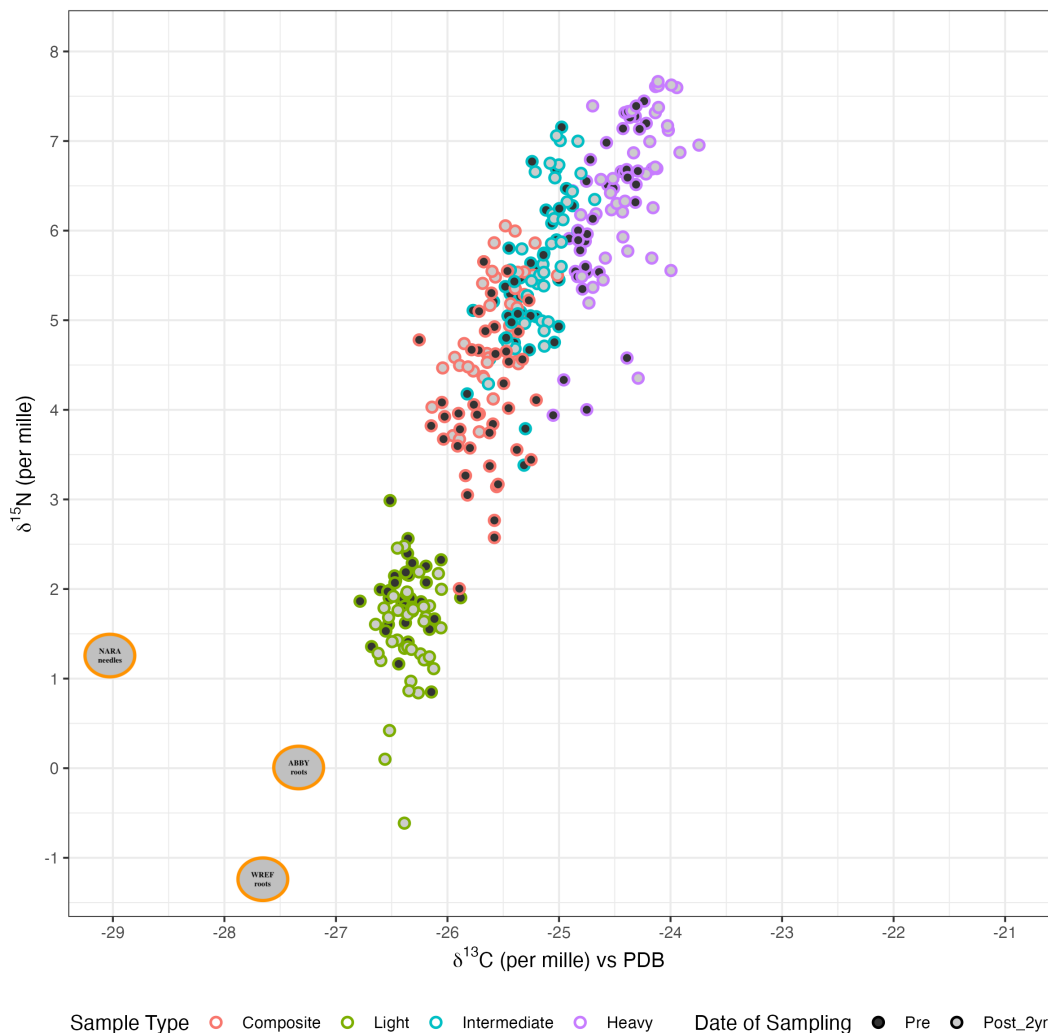


Figure 2.6: Figure 6. Carbon and nitrogen stable isotope data derived from bulk soils and density fractionation (light fraction  $>1.8$  g/cm<sup>3</sup>; intermediate fraction 1.8-2.5 g/cm<sup>3</sup>; heavy fraction  $>2.5$  g/cm<sup>3</sup>) for two periods of sample collection and both depths across all treatments at the NARA-LTSP site near Springfield, OR. We also present representative root and needle isotopic signatures from similarly situated forests. Needle litter from three-year old seedlings at this NARA-LTSP site (Littke, K. personal communication), and root data from two National Ecological Observatory Network sites that include the Wind River Experimental Forest (WREF) and Abby Road (ABBY) both in southern Washington containing an old-growth mixed conifer forest and Douglas-fir plantation forest respectively (NEON, 2022).

## 2.5.2 Density fraction responses

Our first hypothesis attributed the potential shifts in bulk SOC to losses in light fraction material derived from the presence (or lack thereof) residual surface biomass inputs. We assumed both the intermediate and heavy fraction, due to their proximity to mineral surfaces, would be more stable and less likely to be influenced by organic matter removals. Consistent with our hypothesis, there is overwhelming evidence that all treatments and depths experienced mass loss and decreases in C pool from the light fraction (Table 2.2). Light fraction CN ratios in surface soils all experienced significant increases (Figure 2.4), partially driven by a reduction in N pool size (Table 2.2), indicating fresh OM inputs were being incorporated into this SOM fraction. However, contrary to our first hypothesis, the greatest C pool losses were from the intermediate fraction (Table 2.2, Figure 2.4). The magnitude of light and intermediate fraction C losses were strongest in the WTFFC treatment, with this pattern also occurring in the subsoil, potentially highlighting the subsoil intermediate fraction being especially sensitive to aboveground biomass removals.

Light fraction stable isotope responses show a decoupling between the C and N cycles, and between the light and intermediate fractions. There is no evidence for surface or subsurface soil  $\delta^{13}\text{C}$  enrichment of the light fraction suggesting a lack of carbon limitation across all treatments and depths (Table 2.1, Figure 2.5). However, statistically significant depletion of BO light fraction  $\delta^{15}\text{N}$  suggests new N was entering the 0-15 and 15-30 cm horizons. This  $\delta^{15}\text{N}$  depletion pattern is similar, but not statistically significant, in both depths of the WT and WTFFC treatments also suggesting new nitrogen is being added to the light fraction. Additionally, needle

litter of three-year old seedlings at this site were collected resulting in average values across all treatments of -29.1 for  $\delta^{13}\text{C}$ , and +1.2 for  $\delta^{15}\text{N}$  (Littke, K. personal communication). Two similarly situated forests in the Pacific Northwest provided stable isotope signatures of living and dead roots; the Wind River Experimental Forest had average root values of -27.9 for  $\delta^{13}\text{C}$ , and -1.1 for  $\delta^{15}\text{N}$  and the Abby Road forest? was -27.4 for  $\delta^{13}\text{C}$ , and -0.1 for  $\delta^{15}\text{N}$  (NEON, 2022). This strongly suggests the depletion in light fraction  $\delta^{15}\text{N}$  is due to root additions because there was no change in the light fraction  $\delta^{13}\text{C}$  signature that would have indicated a conifer needle signal (Figure 2.6). This is supported by research from a nearby conifer forest finding dissolved organic nitrogen was 10 times higher from root litter compared to needle or wood litter (Yano et al., 2005). Taken together, we find senesced roots required at least six months to release their stored nitrogen, accounting for the delay in N depletion signal, and the stable isotopic signature of light fraction appears more root-derived compared to needle derived (Figure 2.6).

An alternative explanation to light fraction depletion and MAOM enrichment  $\delta^{15}\text{N}$ , considering significant light fraction N pool losses across both depths, could be that all treatments are exhibiting a light fraction positive priming response. As new N is added to the system, old N is being preferentially lost in greater quantities than replacement N can buffer against. Paradoxically, the 0-15 cm intermediate fraction shows statistically significant  $\delta^{15}\text{N}$  enrichment in the WTFFC treatment ( $p=0.040$ ), suggestive evidence in WT removals ( $p=0.116$ ), and no evidence in the BO treatment ( $p=0.753$ ). But these are more consistent  $\delta^{15}\text{N}$  enrichment responses in the subsoil. Taken holistically, this indicates that treatment with more natural

N additions (BO>WT>>WTFFC) encourages a priming effect that is strongest in the light fraction, but remains present in the surface and subsurface soil intermediate fractions emphasizing concerns that bulk soil observations are not capturing potential N losses that may present themselves in the future unless site fertilization commensurate with the pool losses occurs.

Heavy fraction behavior could be misinterpreted unless the full suite of response variables are considered. For example, heavy fraction C pool sizes and CN ratios appeared not to change two years post-treatment (Figure 2.4). This is consistent with the idea that MAOM, especially at this site where Fe/Al being a prominent mineral constituent, is more likely to exhibit ligand-sorption phenomena that are considered more thermodynamically stable leading to longer residence times (Newcomb et al., 2017; von Lutzow et al., 2007). However, there was statistically significant enrichment of heavy fraction  $\delta^{13}\text{C}$  across all treatments and both depths (Figure 2.5) indicating that mineral-association does not prevent participation in SOM transfers. It is more likely that enrichment occurred on mineral surfaces with pre-existing OM attachments and mineral clusters (Vogel et al., 2014). If there was an expansion of the total mineral area with newly added root or needle litter we would observe HF  $^{13}\text{C}$  depletion to match the more depleted  $^{13}\text{C}$  signature of input sources (Figure 2.6). But in fact we see the opposite, HF enrichment indicates that despite the large pulse of new inputs, they were not transferred onto the heavy fraction. Equally possible is the exterior layer of HF organic matter in the “onion model” framework was preferentially lost, indicating the presence of multiple pools of SOM cycling within the heavy fraction (Sollins et al., 2005).

If only examining the density fraction mass or C pools from the heavy fraction, one would incorrectly conclude that the mineral-associated C is excluded from short-term SOM dynamics. At this site there are heavy fraction C transfers (enrichment of  $\delta^{13}\text{C}$ ), occurring on relatively rapid timescales (2 years), that are not statistically detectable in the size of the HF pool (Table 2.2). However, in this andic-influenced forest soil these responses should be less likely to occur given the higher active Fe and Al species present in these soils that would theoretically protect MAOM from destabilization (Possinger et al., 2021; Bailey et al., 2019). This unexpected dynamism in heavy fraction carbon cycling in a high Fe/Al site is in tension with the implicit assumption in modeling frameworks today (e.g. MEMS, Roth-C, Century), that organic matter on heavy fraction material is resistant to losses. This result also provides more evidence to consider carbon turnover times as a distribution of responses with a right skew (e.g. resulting in median carbon turnover times that may not be representative of the majority of the soil carbon pool) that recognizes the short turnover times are present as part of the soil system-age distribution (Sierra et al., 2017; Sierra et al., 2018). Although the soil system-age distribution concept is relatively new and focused on bulk soils, as other researchers suggest (Heckman et al., 2021), a similar framework needs to be considered for the ‘stable’ heavy fraction organic matter.

### 2.5.3 Pacific Northwest forest organic matter cycling

Previous work by Gallo et al (2022) observed large temperature increases in the top 100 cm profile following organic matter removals at this location, with the 0-30 cm WTFFC growing season temperature increasing 2.5°C compared to BO removals. The proportional temperature increase in the WTFFC treatment, compared to BO or WT, partially explains why the response of  $\delta^{13}\text{C}$  enrichment was greatest. These temperature responses also lacked moisture limitations leading to increased soil growing degree days by 3-6 times in treated areas compared to unharvested controls which helps to explain why seedlings on the WTFFC treatment had the highest diameter growth and foliar nitrogen on this study location (Littke et al., 2021). On a similar soil in Washington, Strahm et al (2008) found three times as much nitrogen leaching past 100 cm in BO vs WT removals. Considering this NARA LTSP location reached optimal temperatures for nitrification to occur (25-35°C) on the WTFFC treatment (Gallo et al., 2022; Brady and Weil, 2010), it's plausible these extreme treatments lost significant portions of N that are not captured in bulk soil observations (Table 2.1).

These favorable conditions for microbial activity (higher temperatures with adequate moisture throughout most of the growing season) may have allowed the thermodynamic threshold of Fe/Al bound OM to be crossed such that MAOM was subsequently destabilized (Possinger et al., 2021). Indeed, across all treatments and both depths, the light fraction N pool was reduced by -1.4 mg N/g soil two years post-treatment compared to average N losses in the intermediate fraction of -1.6 mg N/g soil (Table 2.2). Furthermore, FLF  $\delta^{15}\text{N}$  became depleted (compared to all other

fractions and isotopes across both depths becoming generally enriched) suggesting fresh N inputs were replacing FLF material but not in large enough quantities to offset pool losses. This FLF  $\delta^{15}\text{N}$  depletion effect was strongest and statistically significant in BO surface and subsurface horizons where N additions are expected to be greatest (Strahm et al., 2018), but all treatments and depths experienced similar patterns likely attributed to a high production of dissolved organic nitrogen from root litter (Yano et al., 2005) (Figure 2.5). Because nitrogen likely plays a crucial role as the nucleation point of organo-mineral sorption phenomenon (Possinger et al., 2020), losses of any mineral-bound N may also reduce soil's ability to retain carbon and thus be resilient to future harvests.

#### 2.5.4 Soil organic matter response to perturbations, and management

Harvesting meta analyses have shown remarkable resilience of soil to extreme organic matter removals (Powers et al., 2005; Nave et al., 2022), although deep soils remain understudied as they tend to show larger SOC losses (James and Harrison, 2018; Gross and Harrison, 2019). Long-term litter manipulation studies also show soil to be remarkably resilient to bulk SOC changes (Man et al., 2022). However, bulk soil observations likely mask the rapid and substantial energy transfers within and between unique pools of soil organic matter (Heckman et al., 2022). As suggested by Powers et al. (2005) in a decade of LTSP results, they posit forest carbon resilience is driven by the root C pools. Using density fractions, stable isotopes, and biomarker tracing techniques, we believe there is convincing evidence that roots are indeed

providing that forest carbon resilience to harvesting rather than aboveground inputs. This is consistent with many other findings across ecosystem types (Heckman et al., 2021; Xu et al., 2021; Sokol and Bradford, 2019; Rasse et al., 2005; Ghafoor et al., 2017; Jackson et al., 2017; Crow et al., 2009b). An important note to consider, is that although dead roots material is a large contributor to SOC pools, living roots can also destabilize mineral carbon (Pierson et al., 2021; Keiluweit et al., 2015), even in deep soils with long-lived C (Shahzad et al., 2018). The tradeoff likely depends on many ecosystem-specific parameters, but the overwhelming majority of soil architecture is not rhizosphere-influenced, with deep soils being especially void of live-root influences, so the potential benefit of increasing SOC stores from greater root production and senescence likely outweighs the potential losses.

We studied a unique site with a high degree of inherent productivity containing large root carbon stores from prior ecosystems, as a form of biological legacy, that may not translate to other locations. Ongoing forest management may appear more resilient because of these legacy carbon and nutrient stores. We stress that the observed dynamism of soil biogeochemical cycling seen here is likely occurring across the landscape following timber harvesting. If modern successive rotation lengths allow enough time for root C pools to re-establish, and any lost nitrogen to be amended by fertilization, it is feasible for current forest management practices to fulfill increasing wood product demands while remaining sustainable. It is therefore essential to continue long-term monitoring of these locations to examine if the resilience identified here remains robust, or if there are other more concerning patterns that emerge which place our forests at risk of future declines in productivity.

## 2.6 Conclusions

Six-months following treatment the surface and subsurface soils increased soil organic carbon (SOC) stocks by 8-42%. Two years later surface soils returned to pre-treatment values but subsoils lost 8-17% of their original SOC stocks.

Six-months following treatments, 0-15 cm soil carbon stores increased between 8-42%, but two years after treatments they returned to pre-treatment values. Subsoil carbon losses became apparent only two years post-treatment resulting in 8-17% decreases compared to pre-treatment levels. This rapid carbon input, and loss, within two years signals a dynamism of soil nutrient cycling that would not be apparent if only examining soil carbon stocks years after treatments. Using stable isotopes we identified a decoupling between the FLF and MAOM characteristics. We observed a slow enrichment over time of bulk soil  $\delta^{13}\text{C}$ , largely driven by the MAOM fractions. Bulk soil nitrogen enrichment required two years to show statistically significant differences and was also driven by the MAOM fractions. But FLF N was significantly more depleted in the BO treatment, with other treatments exhibiting similar trends, suggesting roots as a primary contributor to the light fraction pool rather than needle litter from aboveground. Biomarker analysis indicates the remaining soil carbon after two years shifted towards a more root-derived signature (decreasing cutin:suberin ratio) that was also more heavily processed by microbes (higher P:V ratio). These shifts in compound chemistry were apparent in the surface horizon of all treatments, but the effect was less pronounced in the subsurface. Conversely, stable isotope trends of surface and subsurface soils were more often consistent with each other.

Taken holistically, we find evidence that following experimental biomass harvests

there is a large pool of carbon added to the system that rapidly cycles and returns forest soil carbon to pre-treatment levels suggesting a resilience. This resilience is likely due to root-derived pools rapidly decomposing, that is independent of other factors such as aboveground biomass retained or increases in soil temperature. While there was a general trend of increasing biomass removals seeing larger effect sizes (subsoil carbon loss, stable isotope enrichment, etc.), the most extreme treatments with no aboveground inputs (WTFFC) behave similarly as more conventional forms of forest harvesting (WT, BO). This suggests that these western cascade forests have a robust resilience mechanism, the legacy root-carbon pool, that may only be sustained if there is an adequate amount of time allowed for the root-carbon pool to rebuild prior to the next harvest interval. Should harvest rotations get shorter without replacing lost carbon and nitrogen then soil carbon resilience, and thus sustained forest productivity, may not be as robust into the future.

## 2.7 References

Bailey, V., C. Pries, and K. Lajtha. 2019. What do we know about soil carbon destabilization? *Environ. Res. Lett.* 14(8). Available at <http://dx.doi.org/10.1088/1748-9326/ab2c11>.

Bates, D.M. 2005. Fitting linear mixed models in R. *R News* 5(May): 27–30.

Brady, N., and R. Weil. 2010. *Elements of the Nature and Properties of Soils*, Person Educations, Bookmens,. 3rd ed. Prentice Hall, New Jersey.

Compton, J.E., and R.D. Boone. 2000. Long-term impacts of agriculture on soil carbon and nitrogen in New England forests. *Ecology* 81(8): 2314–2330.

Crow, S.E., T.R. Filley, M. McCormick, K. Szlávecz, D.E. Stott, D. Gamblin, and G. Conyers. 2009a. Earthworms, stand age, and species composition interact to influence particulate organic matter chemistry during forest succession. *Biogeochemistry* 92(1–2): 61–82.

Crow, S.E., K. Lajtha, R.D. Bowden, Y. Yano, J.B. Brant, B. a. Caldwell, and E.W. Sulzman. 2009b. Increased coniferous needle inputs accelerate decomposition of soil carbon in an old-growth forest. *For. Ecol. Manage.* 258(10): 2224–2232. Available at <http://linkinghub.elsevier.com/retrieve/pii/S0378112709000280> (verified 18 October 2013).

Crow, S.E., K. Lajtha, T.R. Filley, C.W. Swanston, R.D. Bowden, and B.A. Caldwell. 2009c. Sources of plant-derived carbon and stability of organic matter in soil: Implications for global change. *Glob. Chang. Biol.* 15(8): 2003–2019.

Crow, S.E., C.W. Swanston, K. Lajtha, J.R. Brooks, and H. Keirstead. 2007. Density fractionation of forest soils: methodological questions and interpretation

of incubation results and turnover time in an ecosystem context. *Biogeochemistry* 85(1): 69–90. Available at <http://link.springer.com/10.1007/s10533-007-9100-8> (verified 18 October 2013).

Dalal, R.C., and R.J. Mayer. 1986. Long-term trends in fertility of soils under continuous cultivation and cereal cropping in southern Queensland: Loss of organic carbon for different density functions. *Aust. J. Soil Res.* 24: 301–309.

Evans, J. 1992. *Plantation Forestry in the Tropics*.

Food and Agriculture Organization. 2006. *Global Forest Resources Assessment 2005: Progress towards sustainable forest management*. Rome, Italy.

Fox, T.R. 2000a. Sustained productivity in intensively managed forest plantations. *For. Ecol. Manage.* 138(1–3): 187–202. Available at [http://linkinghub.elsevier.com/retrieve/pii,](http://linkinghub.elsevier.com/retrieve/pii/S0926669000000000)

Fox, T.R. 2000b. Sustained productivity in intensively managed forest plantations. *For. Ecol. Manage.* 138(1–3): 187–202. Available at [http://linkinghub.elsevier.com/retrieve/pii,](http://linkinghub.elsevier.com/retrieve/pii,S0926669000000000)

Gallo, A.C. 2016. Response of Soil Temperature, Moisture, and Respiration Two Years Following Intensive Organic Matter and Compaction Manipulations in Oregon Cascade Forests.

Gallo, A.C., S.M. Holub, K. Littke, K. Lajtha, D. Maguire, and J.A. Hatten. 2022. Short-term Effects of Organic Matter and Compaction Manipulations on Soil Temperature, Moisture, and Soil Respiration for Two Years in the Oregon Cascades. *Soil Sci. Soc. Am. J.* In Press. Available at <https://acsess.onlinelibrary.wiley.com/doi/10.1002/saj2.204>

Ghafoor, A., C. Poeplau, and T. Kätterer. 2017. Fate of straw- and root-derived carbon in a Swedish agricultural soil. *Biol. Fertil. Soils* 53(2): 257–267. Available at <http://dx.doi.org/10.1007/s00374-016-1168-7>.

Goñi, M.A., J.A. Hatten, R.A. Wheatcroft, and J.C. Borgeld. 2013. Particulate organic matter export by two contrasting small mountainous rivers from the Pacific Northwest, U.S.A. *J. Geophys. Res. Biogeosciences* 118(1): 112–134.

Goñi, M.A., and J.I. Hedges. 1990. Cutin-derived CuO reaction products from purified cuticles and tree leaves. *Geochim. Cosmochim. Acta* 54: 3065–3072.

Goñi, M.A., and J.I. Hedges. 1992. Lignin dimers: Structures, distribution, and potential geochemical applications. *Geochim. Cosmochim. Acta* 56(11): 4025–4043.

Goñi, M.A., and J.I. Hedges. 1995. Sources and reactivities of marine-derived organic matter in coastal sediments as determined by alkaline CuO oxidation. *Geochim. Cosmochim. Acta* 59(14): 2965–2981.

Goñi, M.A., N. Monacci, R. Gisewhite, J. Crockett, C. Nittrouer, A. Ogston, S.R. Alin, and R. Aalto. 2008. Terrigenous organic matter in sediments from the Fly River delta-clinoform system (Papua New Guinea). *J. Geophys. Res. Earth Surf.* 113(1). Available at <https://agupubs.onlinelibrary.wiley.com/doi/pdf/10.1029/2006JF000653>.

Goñi, M., and S. Montgomery. 2000. Alkaline CuO Oxidation with a microwave digestion system: Lignin analysis of geochemical samples. *Anal. Chem.* 72: 3116–3121.

Goñi, M.A., and S. Montgomery. 2000. Alkaline CuO oxidation with a microwave digestion system: Lignin analyses of geochemical samples. *Anal. Chem.* 72(14): 3116–3121.

Goñi, M.A., and K.A. Thomas. 2000. Sources and transformations of organic matter in surface soils and sediments from a tidal estuary (North Inlet, South Carolina, USA). *Estuaries* 23(4): 548–564.

Gross, C.D., and R.B. Harrison. 2019. The Case for Digging Deeper: Soil Organic Carbon Storage, Dynamics, and Controls in Our Changing World. *Soil Syst.* 3(2): 28.

Hatten, J., M. a. Goñi, and R. a. Wheatcroft. 2012. Chemical characteristics of particulate organic matter from a small, mountainous river system in the Oregon Coast Range, USA. *Biogeochemistry* 107: 43–66. Available at <http://link.springer.com/10.1007/s10533-010-9529-z>.

Heckman, K., C.E. Hicks Pries, C.R. Lawrence, C. Rasmussen, S.E. Crow, A.M. Hoyt, S.F. von Fromm, Z. Shi, S. Stoner, C. McGrath, J. Beem-Miller, A.A. Berhe, J.C. Blankinship, M. Keiluweit, E. Marín-Spiotta, J.G. Monroe, A.F. Plante, J. Schimel, C.A. Sierra, A. Thompson, and R. Wagai. 2022. Beyond bulk: Density fractions explain heterogeneity in global soil carbon abundance and persistence. *Glob. Chang. Biol.* 28(3): 1178–1196. Available at <https://doi.org/10.1111/gcb.16023>.

Heckman, K.A., C.W. Swanston, M.S. Torn, P.J. Hanson, L.E. Nave, R.C. Porras, U. Mishra, and M. Bill. 2021. Soil organic matter is principally root derived in an Ultisol under oak forest. *Geoderma* 403(April): 115385. Available at <https://doi.org/10.1016/j.geoderma.2021.115385>.

Hedges, J.I., R.A. Blanchette, K. Weliky, and A.H. Devol. 1988. Effects of fungal degradation on the CuO oxidation products of lignin: A controlled laboratory study. *Geochim. Cosmochim. Acta* 52(11): 2717–2726.

Hedges, J.I., and J.R. Ertel. 1982. Characterization of Lignin by Gas Capillary Chromatography of Cupric Oxide Oxidation Products. *Anal. Chem.* 54(2): 174–178.

Hedges, J.I., and D.C. Mann. 1979a. The lignin geochemistry of marine sedi-

ments from the southern Washington coast. *Geochemica Cosmochim.* 43: 1809–1818.

Hedges, J.I., and D.C. Mann. 1979b. The characterization of plant tissues by their lignin oxidation products. *Geochemica Cosmochim.* 43(2): 1803–1807.

Helbling, E., D. Pierson, and K. Lajtha. 2021. Sources of soil carbon loss during soil density fractionation: Laboratory loss or seasonally variable soluble pools? *Geoderma* 382(October 2020): 114776. Available at "https://www.sciencedirect.com/science/article/pii/S016763692100114776".

Holub, S.M., and J.A. Hatten. 2019. Soil Carbon Storage in Douglas-Fir Forests of Western Oregon and Washington Before and After Modern Timber Harvesting Practices. *Soil Sci. Soc. Am. J.* 83(S1): 175–186.

Jackson, R.B., K. Lajtha, S.E. Crow, G. Hugelius, M.G. Kramer, and G. Piñeiro. 2017. The Ecology of Soil Carbon: Pools, Vulnerabilities, and Biotic and Abiotic Controls. *Annu. Rev. Ecol. Evol. Syst.* 48: 419–445.

James, J., and R. Harrison. 2016. The effect of harvest on forest soil carbon: A meta-analysis. *Forests* 7(12).

James, J.N., N. Kates, C.D. Kuhn, C.E. Littlefield, C.W. Miller, J.D. Bakker, D.E. Butman, and R.D. Haugo. 2018. The effects of forest restoration on ecosystem carbon in western North America: A systematic review. *For. Ecol. Manage.* 429(July): 625–641.

Keiluweit, M., J.J. Bougoure, P.S. Nico, J. Pett-Ridge, P.K. Weber, and M. Kleber. 2015. Mineral protection of soil carbon counteracted by root exudates. *Nat. Clim. Chang.* 5(6): 588–595. Available at <http://www.nature.com/doi/10.1038/nclimate2580>.

King, J. 1966. Site index curves for Douglas-fir in the Pacific Northwest. Centralia, WA.

Kogel-Knabner, I. 2002. The macromolecular organic composition of plant and microbial residues as inputs to soil organic matter. *Soil Biol. Biochem.* 34: 139–162.

Kramer, M.G., K. Lajtha, G. Thomas, and P. Sollins. 2009. Contamination effects on soil density fractions from high N or C content sodium polytungstate. *Biogeochemistry* 92(1–2): 177–181.

Lavallee, J.M., J.L. Soong, and M.F. Cotrufo. 2019a. PREPRINT Conceptualizing soil organic matter into particulate and mineral-associated forms to address global change in the 21st century. *Glob. Chang. Biol.*: 1–40.

Lavallee, J.M., J.L. Soong, and M.F. Cotrufo. 2019b. Conceptualizing soil organic matter into particulate and mineral-associated forms to address global change in the 21st century. *Glob. Chang. Biol.* (July): 1–13.

Lehmann, J., and M. Kleber. 2015. The contentious nature of soil organic matter. *Nature* 528: 60–68. Littke, K.M., S.M. Holub, R.A. Slesak, W.R. Littke, and E.C. Turnblom. 2021. Five-year growth, biomass, and nitrogen pools of Douglas-fir following intensive forest management treatments. *For. Ecol. Manage.* 494(April): 119276. Available at <https://doi.org/10.1016/j.foreco.2021.119276>.

von Lützow, M., and I. Kögel-Knabner. 2009. Temperature sensitivity of soil organic matter decomposition-what do we know? *Biol. Fertil. Soils* 46(1): 1–15.

von Lützow, M., I. Kögel-Knabner, K. Ekschmitt, H. Flessa, G. Guggenberger, E. Matzner, and B. Marschner. 2007. SOM fractionation methods: Relevance to functional pools and to stabilization mechanisms. *Soil Biol. Biochem.* 39(9): 2183–2207. Available at <http://linkinghub.elsevier.com/retrieve/pii/S0038071707001125> (verified 17 January 2014).

Man, M., D. Pierson, R. Chiu, M. Tabatabaei, R. Ye, K. Lajtha, and M.J. Simpson. 2022. Twenty years of litter manipulation reveals that above - ground litter quantity and quality controls soil organic matter molecular composition. *Biogeochemistry* (0123456789). Available at <https://doi.org/10.1007/s10533-022-00934-8>.

Nave, L.E., K. Delyser, G.M. Domke, S.M. Holub, M.K. Janowiak, B. Kittler, T.A. Ontl, E. Sprague, E.B. Sucre, B.F. Walters, and W. Christopher. 2022. Disturbance and management effects on forest soil organic carbon stocks in the Pacific Northwest. *Ecol. Appl.* 32(6): e2611.

Nave, L.E., C.W. Swanston, U. Mishra, and K.J. Nadelhoffer. 2013. Afforestation Effects on Soil Carbon Storage in the United States: A Synthesis. *Soil Sci. Soc. Am. J.* 77(3): 1035. Available at <https://www.soils.org/publications/sssaj/abstracts/77/3/1035>.

Nave, L.E., E.D. Vance, C.W. Swanston, and P.S. Curtis. 2010. Harvest impacts on soil carbon storage in temperate forests. *For. Ecol. Manage.* 259(5): 857–866. Available at <http://linkinghub.elsevier.com/retrieve/pii/S0378112709008780> (verified 25 March 2014).

Nave, L.E., E.D. Vance, C.W. Swanston, and P.S. Curtis. 2011. Fire effects on temperate forest soil C and N storage. *Ecol. Appl.* 21(4): 1189–1201.

NEON. 2022. Root biomass and chemistry. Root biomass Chem. Megapit. Available at <https://data.neonscience.org>.

Newcomb, C.J., N.P. Qafoku, J.W. Grate, V.L. Bailey, and J.J. De Yoreo. 2017. Developing a molecular picture of soil organic matter–mineral interactions by quantifying organo–mineral binding. *Nat. Commun.* 8. Available at <http://dx.doi.org/10.1038/s41467-017-00407-9>.

Paz, L.W. 2001. Soil-Water Characteristics and Hydrologic Implications Following Forest Soil Disturbance: The Relative Influence of Organic Residue and Soil Compaction on Permeability and Moisture Capacity. A study on the Cohasset soil in the Sierra Nevada mixed conifer . Dissertation.

Pierson, D., L. Evans, K. Kayhani, R.D. Bowden, K. Nadelhoffer, M. Simpson, and K. Lajtha. 2021. Mineral stabilization of soil carbon is suppressed by live roots , outweighing influences from litter quality or quantity. *Biogeochemistry* 9. Available at <https://doi.org/10.1007/s10533-021-00804-9>.

Pinheiro J, B. D, D. S, S. D, and R Core Team. 2014. nlme: Linear and Nonlinear Mixed Effects Models. R package(2015).

Possinger, A.R., T.L. Weiglein, M.M. Bowman, A.C. Gallo, J.A. Hatten, K.A. Heckman, L.M. Matosziuk, L.E. Nave, M.D. Sanclements, C.W. Swanston, and B.D. Strahm. 2021. Climate Effects on Subsoil Carbon Loss Mediated by Soil Chemistry. *Environ. Sci. Technol.*

Possinger, A.R., M.J. Zachman, A. Enders, B.D.A. Levin, D.A. Muller, L.F. Kourkoutis, and J. Lehmann. 2020. Organo–organic and organo–mineral interfaces in soil at the nanometer scale. *Nat. Commun.* 11(1): 1–11.

Powers, R.F. 1990. Are we maintaining the productivity of forest lands? Establishing guidelines through a network of long-term studies. p. 70–81. In *Symposium on Management and Productivity of Wester-Montane Forest Soils*. Boise.

Powers, R.F., D. Andrew Scott, F.G. Sanchez, R. a. Voldseth, D. Page-Dumroese, J.D. Elioff, and D.M. Stone. 2005. The North American long-term soil productivity experiment: Findings from the first decade of research. *For. Ecol. Manage.*

220(1–3): 31–50. Available at <http://linkinghub.elsevier.com/retrieve/pii/S037811270500469X> (verified 21 September 2013).

R Core Team. 2022. R Core Team 2021 R: A language and environment for statistical computing. R foundation for statistical computing. <https://www.R-project.org/>. R Found. Stat. Comput. 2: 2019.

Rasse, D.P., C. Rumpel, and M.F. Dignac. 2005. Is soil carbon mostly root carbon? Mechanisms for a specific stabilisation. *Plant Soil* 269(1–2): 341–356.

Shahzad, T., M.I. Rashid, V. Maire, S. Barot, N. Perveen, G. Alvarez, C. Mougin, and S. Fontaine. 2018. Root penetration in deep soil layers stimulates mineralization of millennia-old organic carbon. *Soil Biol. Biochem.* 124(June): 150–160. Available at <https://doi.org/10.1016/j.soilbio.2018.06.010>.

Sierra, C.A., A.M. Hoyt, Y. He, and S.E. Trumbore. 2018. Soil Organic Matter Persistence as a Stochastic Process: Age and Transit Time Distributions of Carbon in Soils. *Global Biogeochem. Cycles* 32(10): 1574–1588.

Sierra, C.A., M. Müller, H. Metzler, S. Manzoni, and S.E. Trumbore. 2017. The muddle of ages, turnover, transit, and residence times in the carbon cycle. *Glob. Chang. Biol.* 23(5): 1763–1773.

Soil Survey Staff. 2015. Official soil series descriptions.

Sokol, N.W., and M.A. Bradford. 2019. Microbial formation of stable soil carbon is more efficient from belowground than aboveground input. *Nat. Geosci.* 12(1): 46–53. Available at <http://dx.doi.org/10.1038/s41561-018-0258-6>.

Sollins, P., M.G. Kramer, C. Swanston, K. Lajtha, T. Filley, A.K. Aufdenkampe, R. Wagai, and R.D. Bowden. 2009. Sequential density fractionation across soils of

contrasting mineralogy: evidence for both microbial- and mineral-controlled soil organic matter stabilization. *Biogeochemistry* 96(1–3): 209–231. Available at <http://link.springer.com/10.1009-9359-z> (verified 18 October 2013).

Sollins, P., C. Swanston, M. Kleber, T. Filley, M. Kramer, S. Crow, B. Caldwell, K. Lajtha, and R. Bowden. 2005. Organic C and N stabilization in a forest soil: evidence from sequential density fractionation. *Soil Biol. Biochem.* July(UCRL-JRNL-213892).

Sollins, P., C. Swanston, M. Kleber, T. Filley, M. Kramer, S. Crow, B. a. Caldwell, K. Lajtha, and R. Bowden. 2006. Organic C and N stabilization in a forest soil: Evidence from sequential density fractionation. *Soil Biol. Biochem.* 38(11): 3313–3324. Available at <http://linkinghub.elsevier.com/retrieve/pii/S0038071706001866> (verified 17 October 2013).

Strahm, B.D., and R.B. Harrison. 2008. Controls on the sorption, desorption, and mineralization of low-molecular-weight organic acids in variable-charge soils. *Soil Sci. Soc. Am. J.* 72(6): 1653–1664. Strid, A., B.S. Lee, and K. Lajtha. 2016. Homogenization of detrital leachate in an old-growth coniferous forest, OR: DOC fluorescence signatures in soils undergoing long-term litter manipulations. *Plant Soil* 408(1–2): 133–148. Available at <http://dx.doi.org/10.1007/s11104-016-2914-1>.

Swanston, C.W., M.S. Torn, P.J. Hanson, J.R. Southon, C.T. Garten, E.M. Hanlon, and L. Ganio. 2005. Initial characterization of processes of soil carbon stabilization using forest stand-level radiocarbon enrichment. *Geoderma* 128(1–2): 52–62. Available at <http://linkinghub.elsevier.com/retrieve/pii/S0016706104003258> (verified 6 May 2014).

Vogel, C., C.W. Mueller, C. Höschen, F. Buegger, K. Heister, S. Schulz, M. Schloter, and I. Kögel-Knabner. 2014. Submicron structures provide preferential spots for carbon and nitrogen sequestration in soils. *Nat. Commun.* 5: 1–7.

Wada, K. 1980. Mineralogical characteristics of Andisols. In Theng, B.K.G. (ed.), *Soils with Variable Charge*. New Zealand Society of Soil Science, Palmerston North, New Zealand.

Weiglein, T.L., B.D. Strahm, M.M. Bowman, A.C. Gallo, J.A. Hatten, K.A. Heckman, L.M. Matosziuk, L.E. Nave, A.R. Possinger, M.D. SanClements, and C.W. Swanston. 2021. Key predictors of soil organic matter vulnerability to mineralization differ with depth at a continental scale. *Biogeochemistry* 0123456789. Available at <https://doi.org/10.1007/s10533-021-00856-x>.

Xu, H., B. Vandecasteele, S. De Neve, P. Boeckx, and S. Sleutel. 2021. Contribution of above- versus belowground C inputs of maize to soil organic carbon: Conclusions from a  $^{13}\text{C}/^{12}\text{C}$ -resolved resampling campaign of Belgian croplands after two decades. *Geoderma* 383(March 2020): 114727. Available at <https://doi.org/10.1016/j.geoderma.2020.114727>.

Yano, Y., K. Lajtha, P. Sollins, and B.A. Caldwell. 2005. Chemistry and dynamics of dissolved organic matter in a temperate coniferous forest on andic soils: Effects of litter quality. *Ecosystems* 8(3): 286–300.

Zhang, L., C. Yu, B. Cheng, C. Yang, and Y. Chang. 2020. Mitigating climate change by global timber carbon stock: Accounting, flow and allocation. *Renew. Sustain. Energy Rev.* 131(June): 109996. Available at <https://doi.org/10.1016/j.rser.2020.109996>.

Zurr, A., E. Ieno, N. Walker, A. Saveliev, and G. Smith. 2008. *Mixed Effects Models and Extensions in ecology with R* (M Gail, K Krickeberg, J Samet, A Tsaitis,

and W Wong, Eds.). 1st ed. Springer, New York.

## 2.8 Supplemental Materials for Chapter 2

Upon request, the **massive** tables of statistical comparisons can be made available.

Chapter 3: Continental patterns in plant sources of soil organic  
matter across the National Ecological Observatory Network (NEON)  
and down soil profiles

Adrian C. Gallo

Expected Co-Authors: Yvan Alleau, Maggie Bowman, Kate Heckman, Kate  
Lajtha, Lauren Matosziuk, Luke Nave, Angela Possinger, Mike SanClements, Brian  
Strahm, Tyler Weiglein, Jeff Hatten

Expected Submission: Journal of Geophysical Research - Biogeosciences (American  
Geophysical Union)

### 3.1 Abstract

We leveraged full soil profile samples ( $n = 40$ ) originating from the installation of National Ecological Observatory Network across North America representing the most broad and deepest assessment of cupric oxidation (CuO) identified soil organic matter (SOM) that has ever been investigated. Our aim was to examine the trade-off between local biomass production (net primary productivity - NPP) and climatic controls on lignin content and plant waxes down soil profiles. In addition to analyzing bulk soils with average depths  $>1\text{m}$ , we separated all A-horizons by density and examined the SOM of the three density fractions. Across the NEON sites studied, we find A-horizons had significantly different SOM compositions compared to their associated subsoils. Within NEON sites, neither upper nor lower B-horizon SOM components were significantly different from each other, indicating organic matter additions have a weak imprint on subsoil SOM characteristics. Lignin contributions to the total SOM pool generally decrease with increasing soil depth, and lignin becomes more degraded in deeper horizons. Surprisingly, neither NPP or the tradeoff between precipitation inputs and plant water use helped to explain the proportions of SOM components extracted with the CuO method. Despite the wide range in the quality and quantity of plant inputs SOM appears to have homogenized - especially across A-horizons and across/within subsoils - to produce a somewhat uniform SOM composition across these North American ecosystems.

## 3.2 Introduction

Globally, soils down to 1 m hold more carbon ( $\approx 1,500$  Pg) than the atmospheric ( $\approx 867$  Pg) and terrestrial vegetation pools ( $\approx 560$  Pg) combined (Batjes, 2014; Lal, 2018). More than half of these soil carbon stocks are held below 30 cm (Batjes, 2014), and recent work estimating soil carbon stocks to 3 m suggests the true pool is as large as 3,000 Pg (Scharlemann et al., 2014). Despite the importance of deep soil carbon pools (Gross and Harrison, 2019; Button et al., 2022), published soil science literature has become more shallow over the past few decades (from 53cm in the 1990's to 24 cm today) and too often researchers do not even report soil sampling depth (Yost and Hartemink, 2020). Furthermore, it remains difficult to incorporate disparate studies into a holistic framework because analytical methods and soil sampling practices (if reported) too often differ to meaningfully integrate studies into a more holistic understanding. Although researchers need to be more systematic in their sampling methods for cross validation (Wendt and Hauser, 2013; Rhymes et al., 2020), we also need a large scale systematic study to limit confounding variables inherent in our current body of terrestrial biogeochemical literature.

Recent analytical tools have allowed researchers to estimate the relative contributions of plant and microbial sources to soil organic matter (SOM), but calculations vary greatly. Some estimate microbes and their necromass account for 30-80% of SOM (Liang, et al., 2019; Angst et al., 2021), while other researchers find plant sources to account for 20-70% of SOM (Whalen et al., 2022), and belowground inputs account for  $\approx 46\%$  of carbon retained as SOM (Jackson et al, 2017). One major limitation in these estimates is they are often combined from many different study

designs that use slightly different techniques leading to wide estimates of plant and microbial contributions to SOM. By leveraging a continental scale study design, with consistent methodologies that also sample deep soils, we hope to address this knowledge gap in the sources of SOM as a preliminary step to then infer how ecosystem processes may shift as climate warms and land management changes.

The two most abundant biopolymers on earth (cellulose and lignin) are produced by vascular plants (Filley et al., 2002) with some analytical tools able to consistently identify lignin across terrestrial and aquatic ecosystems (Goñi and Thomas, 2000; Goñi et al., 2008). The cupric oxidation (CuO) method allows researchers to trace plant-derived organic matter (OM), as well as specific plant/tree/grass species because they often contain a unique ratio of lignin phenols (Hedges and Mann, 1979). In addition to tracking lignin, the CuO procedure tracks lignin degradation indices and some unique plant components such as waxy coatings on leaves and roots (substituted fatty acids). Lignin degradation can also affect total CuO yield (e.g. lignin polymer degradation can lead to specific monomer exclusion from the analytical window). However, the trifecta of tracing lignin as an OM component present in all plants, tracking its relative degradation status, and identifying other plant components make the CuO method highly favorable to understand the sources of SOM across ecosystems and down soil profiles. By leveraging the installation of new long-term research sites across North America (National Ecological Observatory Network - NEON), we hope to elucidate how ecosystems may respond to a warming climate.

Soil organic matter is not a uniform pool of plant and microbially altered compounds, and there are a myriad of mineral-organic interactions that have resulted in

a paradigm shift in SOM dynamics (Kleber et al, 2015). Previous studies emphasized large molecular structures govern SOM recalcitrance, although that view has long been under question (Lehmann and Kleber, 2015). There are many new frameworks that are replacing the outdated humic substances paradigm, with the most convincing also being the most complex to model (Dungait et al., 2012; Lehmann et al., 2020). More recent frameworks involve the interaction of climate and clay-sized minerals (Rasmussen et al., 2018), the fragmentation of aboveground plant matter into soluble OM that can then become SOM (Cotrufo et al., 2013), and the density separation of bulk soils into operationally defined pools that have distinct responses to temperature and moisture shifts (Heckman et al., 2022; Schrumpf et al., 2013).

By separating soils based on density, there is an easier distinction between rapidly cycling and more stable forms of organic matter that cannot be obtained from bulk soils alone (von Lutzow et al., 2007; Sollins et al., 2009). Furthermore, because there is a continuum between fresh plant debris fragmenting into the light fraction, which is then [a]biotically oxidized into mineral-associated OM (MAOM), we can leverage the CuO method to track the unique plant components in various stages of decomposition and which - if any - are preferentially sorbed onto mineral particles. This attachment is crucial, because the MAOM fraction is low in carbon but can persist for many thousands of years compared to light fraction material which is high in carbon but only persists at the decadal timescale or less (Lavalle et al., 2019; Lehmann and Kleber, 2015; von Lutzow et al., 2007; Sollins et al., 2009; and Heckman et al., 2022). With a cross ecosystem synthesis of plant-derived contributions to this continuum of SOM, we hope to aid in the prediction of global climate change

modeling.

Based on our emerging understanding of soil organic matter cycling and the representative nature of these NEON sites, the objectives of this study are to examine the trade-off between local biomass production and distal climatic controls on lignin content and plant waxes down soil profiles. Our overarching hypotheses are (1) sites with more net primary productivity have a higher proportion of lignin and plant waxes, and (2) this relationship is consistent - but diminished - in the deepest soil horizons furthest away from plant inputs.

To address these questions, we examined proxies of lignin and plant waxes across 40 NEON sites, using A-horizon bulk soils and density fractions, and bulk soils from the upper most illuvial B horizon, and the deepest mineral B horizon present at each location. We modeled our observations of plant biomarkers proxies against NPP and a climate index that accounts for precipitation inputs and evaporative outputs for each site. The focus of this manuscript is not on soil carbon storage or vulnerability or persistence; those analyses that use these exact soils can be found in Nave et al (2021), Weiglein et al (2021), and Heckman et al (2022), respectively. For this manuscript, by accounting for both the local (biomass production) and distal (climate) factors, we hope to better understand which ecosystems retain the strongest plant-organic matter signatures throughout soil profiles.

### 3.3 Materials and Methods

#### 3.3.1 Site description and soil sampling

This study used a subset of 40 sites from the larger set of terrestrial NEON installations (Table 3.1). The sites are categorized by 20 unique ecoclimatic domains meant to capture a wide range of ecosystem factors representative of global systems (Thorpe et al., 2016). As described by Possinger et al. (2022), we obtained net primary productivity (NPP) ( $\text{kg C} / \text{m}^2 \cdot \text{yr}$ ) from MODIS, mean annual temperature (MAT) and a Hargreaves evaporation index (MAP-Eref) from the ClimateNA-MAP database (ORNL DAAC, 2008; Running et al., 2008; Wang et al., 2012). We use MAP-Eref as our “moisture availability” index in our modeling efforts which helps to incorporate abiotic and biotic factors more holistically. To more easily map these current sites onto conventional ecosystem types with long-term data (Campbell et al., 2022), we leverage Whittaker Biomes with only eight unique ecosystem types (Whittaker, 1970) (Table 3.1). Instrumentation at the sites span multiple spatial and temporal scales that sometimes require a high number of additional sampling points to obtain an accurate estimate of the mean (e.g. soil moisture and temperature) (Loescher 2014), but the types of observations are consistent across all locations. One instrument present at each NEON site is a flux tower. Within the tower airshed are five soil plots with additional automated-observation equipment. During construction of the Terrestrial Observation System (including the full suite of sensors and access trails), soil CO<sub>2</sub> sensors were installed in each soil plot within the tower footprint. These soil cores, that were systematically collected at each site

with ongoing automated and seasonal data collection which are publicly available (San Clements et al., 2019), were sent to Oregon State University on ice for further processing.

A full description of sample processing can be found in Nave et al. (2019). Briefly, we received two pairs of soil cores from five unique long-term soil plots ( $n=10$ ) within the tower footprint. One of the pairs ( $n=5$ ) was immediately archived in a freezer ( $-30^{\circ}\text{C}$ ) for later analysis. Soil core diameter was 3.5 cm, but length varied depending on the site (e.g. Rocky Mountain National Park soil cores were often less than 50 cm, Jornada Experimental Range cores exceeded 2 m in length). All sites were cored to a depth of refusal by the NEON team (9100 series Power Probe, AMS Inc.).

All cores arrived from the NEON team between March 2015 - June 2017 and were stored at  $4^{\circ}\text{C}$  until being processed, as long as eight weeks but often within ten days of arrival. Cores from permafrost areas (HEAL, DEJU, BARR) were 50 cm diameter and stored in freezers until processing, which was conducted entirely in a  $4^{\circ}\text{C}$  walk-in refrigerator to minimize thawing effects. Additional information on permafrost soil processing can be found in Rooney et al (2022).

Each soil core was described (e.g. moist soil color, root/pore quantity, clay films, redoximorphic features, carbonates, consistence, etc..) using standard NRCS procedures (Schoeneberger et al., 2012). However, due to the narrow diameter of the core not all characteristics could be described (e.g. boundary topography, coarse structural or root features). When in doubt, horizons with small differences in visual characteristics (e.g. root quantity) were split into multiple horizons to better accommodate the compositing scheme (see below). Each horizon sample was individually

weighed and stored at 4°C until all five cores per site were described. This yielded a total of 1,024 unique horizons (Supplementary Material).

Compositing of soils occurred on a genetic horizon basis by comparing all individual core-horizon characteristics, the NEON megapit horizonation, and NRCS SoilWeb data of expected soils in the area. Our aim was to produce three horizons representative of a continuum of pedologic processes experienced at each site that includes an: A-horizon, uppermost illuvial B-horizon, and the deepest B-horizon that approached parent material but was not a dominant C horizon. The individual horizons per core were composited across site (e.g. the A1 and A2 from core 1 was combined with the A from core 2), air dried, passed through a 2-mm sieve, and split using a riffle box (Model CL-244; Soiltest, Inc., Evanston, IL, USA) to ensure all collaborators received a similar particle size distribution of each horizon sample.

During the sieving process, we root picked each composited horizon that passed through the 2 mm sieve. If there were too few root samples for analysis, we also picked roots from the >2 mm fractions. Root samples should be considered ‘fresh’ or “living” roots due to the relatively high degree of structural integrity required to separate with tweezers from soils. A small set of sites did not yield enough roots (approximate minimum of  $\approx 3$  g dry weight) for analysis. The sites with sufficient root biomass are referred to as “Root” samples herein.

During the coring procedures at each NEON site, the dominant above ground living vegetation was also collected, one sample per soil plot, and sent with the soil cores on ice. The maximum diameter of vegetation stems were 2mm, but our samples were biased towards the conifer needles, small branches, and flowering bodies

of plants, rather than the bole of conifer or deciduous trees. All five vegetation bags were composited, coarse ground, subsampled, then ground to a fine powder for analysis. These are referred to as “Vegetation” samples herein. Neither the Root or Vegetation samples were run for total carbon or nitrogen, thus we present those data only requiring CuO compounds for analysis (e.g. substituted fatty acids to lignin ratio, lignin phenol acid to aldehyde ratios).

Further descriptions of sample analysis can be found in a variety of sources. Heckman et al., (2020) describes the density fractionation procedures (light vs heavy fraction cutoff was 1.65 g/cm<sup>3</sup>, with sonication of 750 J/g soil applied to obtain the occluded fraction),  $\Delta^{14}\text{C}$ , and specific surface area methods. Weiglein et al (2021) describes year long soil incubation experiments, selective metal dissolutions procedures,  $\delta^{13}\text{C}$  and  $\delta^{15}\text{N}$  stable isotope observation, magnetic susceptibility, and soil pH methods. The original benzene polycarboxylic acid (BPCA) method for quantification of pyrogenic carbon can be found in Matosziuk (2019), with testing of extraction efficiencies for the wide range of mineralogies in NEON sites detailed in Matosziuk (2020 GRSM). Sequential aqueous and organic solvent extractions were also analyzed for FTICR-MS by Bowman (2021).

Site Abbreviation	Full NEON Site Name	Whittaker's Biome Type	Dominant Vegetation Type	Site Management	NPP (kgC/m <sup>2</sup> /yr)	Mean Annual Temperature (°C)	Mean Annual Precipitation (cm)	Mean Annual Activity Index (MAP - Erc)	Active Layer Depth (cm)	Upper Bt Horizon Midpoint (cm)	Lower Bt Horizon Midpoint (cm)	Soil Series Parent Material	USDA Soil Taxonomy	Ascendant Lands
ABRY	Abri Road	Temperate rain forest	Young Douglas fir forest	harvesting	0.343	9.0	225.0	1850.0	10.1	44.0	98.9	volcanic ash	Fine-loamy - isotic - mesic - Andic Humudults	
BARB	Duggs & Barrow	Tundra	Polynesian tundra	wildland	NA	-12.0	11.0	72.0	23.1	79.5	90.7	NA	NA	
BART	Barlett Experimental forest	Temperate seasonal forest	Mixed forest	wildland	0.753	7.0	122.3	545.0	5.8	98.6	143.4	residuum derived from limestone, calcareous shale, siltstone, and/or sandstone	Coarse-bony - isotic - frigid Aquic Haploblebbs	
BLAN	Bladly Experimental Farm	Woodland/shrubland	Fallow scrubland	fallow scrubland	0.669	12.0	99.1	-112.0	10.3	34.5	56.7	NA	Fine - mixed - subactive - mesic Udic Haploblebbs	
BONA	Caribou Pelter	Boreal forest	Shrub forest	unburned wildland	NA	-3.0	26.0	15.0	26.9	97.4	155.7	meadows less over weathered schist bedrock	NA	
CLBJ	Lynan B. Johnson Natural Grassland	Woodland/shrubland	Oak savannah	prescribed fire	0.315	18.0	86.0	-524.0	19.2	67.8	98.3	Sediments and residuum from Cretaceous sedimentary deposits	NA	
CFER	Central Plains Experimental Station	Temperate grassland/shrubland	Shortgrass prairie	grazing	0.218	9.0	36.7	-626.0	10.2	52.1	89.8	alkaline to neutral alluvium, colluvium, and residuum	Fine-loamy - mixed - supereactive - mesic Ariclic Haploblebbs	
DCJS	Duke-Corona	Woodland/shrubland	Poplar park	low intensity grazing	0.463	4.0	43.8	-303.0	12.5	122.8	140.9	alkaline glacial till and alluvium	Fine-loamy - mixed - supereactive - frigid Typic Haploblebbs	
DEJU	Delta Junction	Boreal forest	Spruce forest	wildland	NA	-3.0	31.0	69.0	5.8	165.9	184.1	meadows less over acid glacio-fluvial materials or till	NA	
DELA	Deer Lake	Temperate seasonal forest	Woods/Wetlands	wildland	0.496	18.0	140.0	25.0	11.7	53.8	84.0	meadows less over acid glacio-fluvial materials or till	Fine - mixed - semiactive - thermic Aquic Blebduhls	
DSNY	Dixey	Tropical seasonal forest/savanna	Regenerating long leaf pine	prescribed fire	0.602	22.0	122.0	-269.0	8.0	79.4	103.6	acid to slightly alkaline marine sediments	Stuhy - siltstone - hyperthermic Aricic Aksoquos	
GRSM	Great Smokey Mountains National Monument	Temperate seasonal forest	Eastern deciduous forest	wildland	0.576	13.0	138.8	307.0	6.0	37.6	93.2	colluvium and residuum from mesosedimentary sandstone, siltstone, and shale	Loamy-skeletal - isotic - mesic Typic Humudults	
HARV	Harvard Forest	Temperate seasonal forest	Regenerating forest	wildland	0.731	8.0	100.2	330.0	12.8	70.3	150.7	isotic glacial till	Loamy-skeletal - isotic - mesic Typic Humudults semiactive - frigid Oxyaquic Dystrudults	
HEAL	Healy	Boreal forest	Tussock tundra	wildland	NA	-1.0	37.0	NA	13.0	46.4	59.2	Neuman gravel, poorly consolidated gravels and conglomerate	NA	
JORN	Jornada	Temperate grassland/shrubland	Desert shrubland	wildland	0.117	18.0	27.3	-1230.0	23.8	66.0	93.0	Coarse-bony - mixed - supereactive - thermic Typic Kermudults		
KONA	Kona Agriculture	Woodland/shrubland	Cultivated tallgrass prairie	farming	0.363	13.0	88.7	-181.0	14.9	36.5	90.4	residuum derived from limestone or alkaline shale	Fine - smectitic - mesic Pacific Vertic Argiudolls	
KONZ	Kona Core	Woodland/shrubland	submontane tallgrass prairie	wildland	0.372	13.0	89.1	-157.0	14.3	55.8	89.4	moderately acid to slightly alkaline iron-oxalate rich alluvium	Fine - smectitic - mesic Pacific Udic Argiudolls	
LENO	Lenox Landing	Temperate seasonal forest	Pine oak mixed forest	wildland	0.378	18.0	151.2	-41.0	7.9	134.3	144.7	alluvial, coastal, and terrace deposits, Holocene	Fine - mixed - active - acid - thermic Vertic Epiaquops	
MILS	Mountain Lake	Temperate seasonal forest	Eastern deciduous forest	wildland	0.836	8.0	104.2	309.0	5.7	200.7	232.6	residuum or alluvium derived from sandstone, siltstone, and shale	Coarse-bony - mixed - semiactive - frigid Epiaquops	
MOAB	Moab	Temperate grassland/shrubland	Desert shrubland	wildland	0.142	10.0	31.4	-255.0	18.1	49.7	76.1	alkaline alluvium and aeolian deposits over sandstone	Coarse-bony - mixed - supereactive - mesic Udic Haploblebbs	
NGPR	Northern Great Plains Research Laboratory	Woodland/shrubland	Grassland Prairie	wildland	0.407	5.0	42.9	-341.0	20.4	54.7	77.5	neutral to alkaline loess over glacial till	Fine-loamy - mixed - supereactive - frigid Typic Haploblebbs	
NWJO	Noroot Ridge	Boreal forest	Alpine tundra	wildland	0.333	-4.0	68.0	339.0	15.8	94.6	102.7	alluvium, colluvium, and glacial till derived from acid igneous rocks	Argiudolls	
OAES	Oakes	Woodland/shrubland	Grassland pasture	grazing	0.296	14.0	70.1	10.3	139.0	157.1	157.1	Loamy, mixed, active, thermic, Udic Haploblebbs		
ONAO	Onaga-Auk Skappe	Temperate grassland/shrubland	Sage shrubland	grazing	0.170	9.0	29.4	-727.0	16.8	50.9	102.2	alluvium and colluvium derived from basic igneous and sedimentary rocks	Fine-loamy - mixed - supereactive - mesic Xeric Haploblebbs	
ORNL	Oak Ridge	Temperate seasonal forest	Eastern deciduous forest	wildland	0.617	15.0	123.3	190.0	4.5	165.8	196.4	residuum, alluvium derived from limestone and shale	Fine - loamitic - thermic Typic Pakudolls	
OSHS	Odyssey-Swabber	Temperate seasonal forest/savanna	Long-leaf pine forest	prescribed fire	0.761	20.0	129.8	-192.0	13.3	37.2	73.5	acid, iron-containing, alluvial, aeolian, and marine deposits	Hyperthermic - uncolored Typic Quartzipsums	
RANP	Rocky Mtn National Park	Temperate seasonal forest	Pine forest	wildland	0.475	7.0	49.2	55.0	10.7	31.5	72.3	Granite and gneiss. Mesogeotomic	NA	
SCBI	Sierra Nevada Bishop Institute	Temperate seasonal forest	High Poplar forest	wildland	0.719	13.0	104.1	-29.0	14.1	55.2	89.9	residuum and colluvium of basic igneous rocks	Fine-loamy - mixed - active - mesic Aquic Haploblebbs	
SERC	Savannah Environmental Research Center	Temperate seasonal forest	Coastal tulip poplar and ash	wildland	0.697	13.0	110.1	34.0	7.5	50.4	109.1	acid alluvial, fluvial, marine deposits	Fine-loamy - mixed - active - mesic Aquic Haploblebbs	
SOAP	Sagepost-Saddle	Woodland/shrubland	Poplar mesquite-grassland	prescribed fire	0.453	13.0	96.0	-408.0	27.1	45.2	54.1	granite-derived residuum	NA	
SRES	Santa Rita	Subtropical desert	Desert shrubland	wildland	0.126	22.0	39.4	-1221.0	17.1	105.3	150.2	slightly acid to strongly alkaline alluvium	Coarse-bony - mixed - calcareous - thermic Typic Torrifluvents	
STEI	Steigwald	Temperate seasonal forest	conifer forest	wildland	0.671	5.0	88.7	NA	25.6	91.1	196.9	acidic glacial till	Loamy-silty - mixed - supereactive - frigid Udic Haploblebbs	
STER	Stirling	Woodland/shrubland	Pasture	agriculture - dryland farming	0.230	10.0	42.5	-551.0	10.6	39.2	39.2	neutral to alkaline alluvial, aeolian, and glacio-fluvial deposits	Fine-silty - mixed - supereactive - mesic Pacific Haploblebbs	
TALL	Taliskaga	Temperate seasonal forest	Longleaf pine forest	prescribed fire	0.367	15.0	145.3	70.0	6.8	35.2	99.2	acidic, iron-containing alluvial, fluvial, and glacio-fluvial deposits	Fine-loamy - siltstone - subactive - thermic Typic Argiudolls	
TOOL	Toolik	Tundra	Tussock tundra	wildland	NA	-9.0	32.0	NA	26.2	51.7	78.0	acidic glacial till	NA	
TRIE	Trethewey	Temperate seasonal forest	N. hardwood forest	selective logging	0.667	5.0	81.0	NA	25.1	79.4	113.4	NA	Coarse loamy, mixed, supereactive, frigid Alfic Epiaquops	
UNDE	University of Notre Dame Ecosystem Research Center	Temperate seasonal forest	Northern hardwood forest	wildland	0.647	5.0	84.7	130.0	6.2	32.8	48.2	isotic glacial till and acid acidium deposits	Coarse-bony - mixed - supereactive - frigid Argic Epiaquops	
WOOD	Woodworth	Woodland/shrubland	Regenerating post oak prairie	re-seeding	0.430	4.0	42.0	-312.0	11.6	31.7	47.9	neutral to alkaline glacial till and glacio-fluvial deposits	Coarse-bony over sandy or sandy-skeletal - mixed - supereactive - frigid Typic Haploblebbs	
WREF	Wet River Experimental Watershed	Temperate rain forest	Wet-growth Douglas fir	wildland	0.773	9.0	222.0	NA	28.7	56.6	79.1	acidic-skeletal mesic Pacific Mollinamentum, Loamy-skeletal mixed Pacific Haploblebbs	Acidic-skeletal mesic Pacific Mollinamentum, Loamy-skeletal mixed Pacific Haploblebbs	

Table 3.1: Site information for a subset (n=39) of the National Ecological Observatory Network (NEON). Soil horizon depths were calculated from cores collected at the five soil plots within the flux tower footprint, and represent three distinct pedogenic horizons.

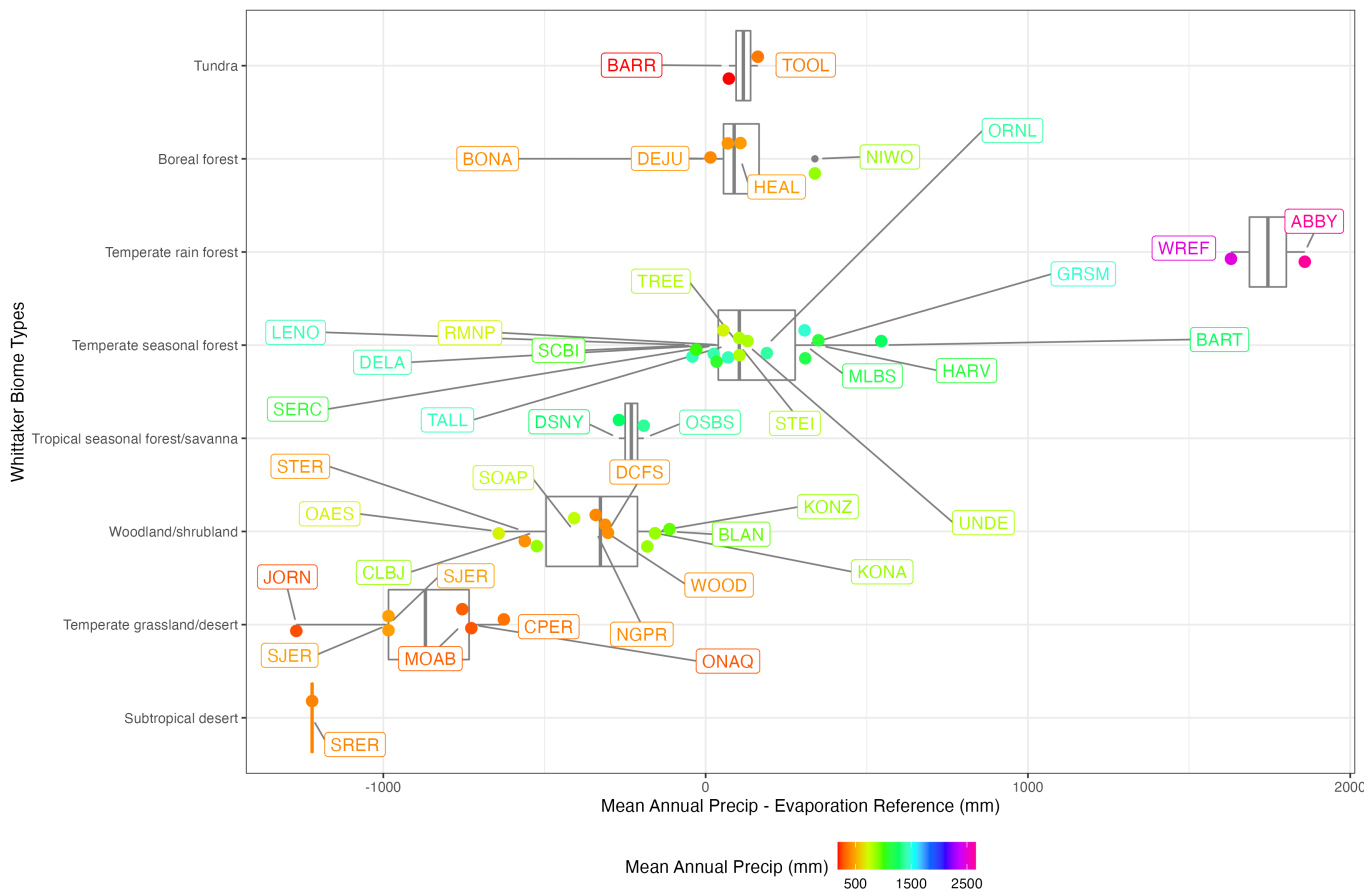


Figure 3.1: Hydroclimatic patterns across a subset ( $n=39$ ) of the National Ecological Observatory Network (NEON). Whittaker Biomes were used to increase the number of sites with each ecosystem category rather than the ecoclimatic domains used by NEON which only contain 1-3 sites per domain. See Table 1 for a full site description corresponding to the four-letter codes.

### 3.3.2 Cupric oxidation procedures

Both Weiglein (2021) and Heckman (2020) briefly describe the cupric oxidation (CuO) method, but additional details are below. We used the CuO procedure to identify biomarkers that allow us to trace the sources of soil organic matter, especially from unique plant-tissue components (Hedges and Mann 1979). The procedure was originally developed by Hedges and Ertel (1982), modified by Goñi and Hedges (1992), and finally refined into our current working method by Goñi and Montgomery (2000). Due to practical constraints, CuO analysis was conducted on the three representative mineral horizons per site, the dominant aboveground vegetation, and belowground root samples when available. A subset of A-horizon density fractions were available for CuO analysis, however, due to limitations in sample masses only 22 occluded fractions were available.

Briefly, each 55 mL Teflon bomb vessel (MARS Xpress) contains approximately 5 mg of organic carbon combined with cupric oxide, ferrous ammonium sulfate, and N<sub>2</sub> degassed NaOH before microwave digestion (CEM Mars 6 Xpress) for 1.5 hours at 150°C. Following the microwave-induced oxidation, internal recovery standards (ethyl vanillin and cinnamic acid) are added from a shared source before a quantitative transfer into centrifuge tubes with an additional NaOH rinse. The solution is then centrifuged (Thermo Scientific, Sorvall Legend XTR) with the supernatant transferred and acidified to pH 1. Two rounds of ethyl acetate (HPLC grade) additions are used to extract the organic matter, with the organic supernatant transferred to 12 mL vials for efficient evaporation under heat (50°C) and N<sub>2</sub> purging (LabConco RapidVac Vertex Evaporator). The dried solution is then re-dissolved with pyridine

and stored in amber vials in a refrigerator until final analysis.

For more efficient sample behavior in the gas chromatograph, a 50 uL subsample was derivatized with 50 uL BSTFA (+ 1% TCMS), vortexed, and heated to 40°C for 30 minutes. We used a Hewlett Packard (6890 series) gas chromatograph fitted to a Agilent Technologies (5973 Network) mass spectrometer with a DB-5 column (Agilent Technologies, 30 m length, 0.25 mm internal diameter, 0.25 um film thickness) for all analysis. We employed a six point calibration curve with concentrations ranging from 1-50 ug standard / mL. The calibration contained 22 commercially available compounds that include all CuO oxidation products presented herein.

Recovery of internal standards (ethyl vanillin and cinnamic acid) varied between sample types (Supplemental Materials). Vegetation, root, bulk soil samples of all horizons, and free light fraction samples recovered a similar proportion of both internal standards ( $\approx 65\%$ ), but occluded fraction and heavy fractions recovered 20-40% of ethyl vanillin and only 5-50% cinnamic acid. As a result, we refrain from interpreting any CuO indices on occluded or heavy fractions that rely on exclusive differences between acid:aldehyde, and exhibit caution in interpreting other CuO data from these density fractions.

We present data for the following CuO oxidation products: lignin (the sum of the vanillyl, syringyl, and cinnamyl phenols) (Hedges and Mann 1979, Hatten et al., 2012), cutin (16-hydroxyhexadecanoic acid, 8,16-dihydroxydecanoic acid, 9,16-dihydroxydecanoic acid, 10,16-Dihydroxydecanoic acid, 7-hydroxyhexadecane-1,16-dioic acid, 8-hydroxyhexadecane-1,16-dioic acid, 18-hydroxyoctadec-9-enoic acid) (Hatten et al., 2012, Goñi and Hedges 1995; Goñi and Hedges, 1990; Crow et al., 2009a),

suberin (hexadecanedioic acid and  $\omega$ -hydroxyoctadecenoic acid) (Crow et al., 2009a), and non-lignin para-phenols that are designated with the letter P (the sum of p-hydroxybenzaldehyde, p-hydroxyacetophenone, p-hydroxybenzoic acid) (Goñi et al., 2008). We normalized lignin to organic carbon content, and use the phrase "lignin content" to represent lignin contributions to the total soil organic carbon pool.

Both cutin and suberin were combined into the substituted fatty acid category - generally representing plant wax compounds - and normalized to lignin (SFA:Lig). The individual lignin monomers are used for tracing different plant types. For example, gymnosperms produce  $\approx 90\%$  vanillyl (V) phenols and near zero syringyl (S) phenols, angiosperms produce 25-40% V phenols and 50-75% S phenols, and the litter of pine trees only produce  $\approx 14\%$  cinnamyl (C) phenols while grasses overwhelmingly produce C phenols (Goñi and Thomas, 2000; Hedges and Mann, 1973). Normalizing individual monomers aids in organic matter tracing, high S:V is indicative of flowering plants (angiosperms) and lower values indicates a tree source (gymnosperms). High C:V values indicate non-woody biomass (grasses) while low values indicate more woody inputs (branches, trees). We also present a lignin decomposition product (3,5-dihydroxybenzoic acid) and normalize it to lignin with higher values indicating greater lignin degradation. Similarly, the ratio between acid and aldehyde forms of S and V phenols indicate the relative oxidation state of these phenol classes (Kogel, 1986), with higher values indicating greater lignin degradation. The para-phenols (P) are non-lignin products, and of predominantly microbial origin (Goñi et al., 2008), with higher P:V ratios indicating more microbial processing of lignin products. Illustrations of these lignin structures can be found in Hedges et

al (1988), and non-lignin structures can be found in Goñi and Thomas (2000) and Kogel-Knabner (2002).

### 3.3.3 Statistics

We first leverage Spearman's Rank correlation matrices to assess the influence of NPP, moisture availability, and root biomass on lignin and SFA compounds. Each horizon (A, upper B, and lower B horizons) was performed separately (n=35, 27, and 24 respectively for each horizon type). Only correlations with  $p < 0.1$  are presented. Spearman's correlations were selected rather than Pearson's due to monotonic relationships between climatic variables across biome types. This is a similar procedure as other researchers working with identical soils (i.e. Heckman et al., 2020; Possinger et al., 2022). This framework helps to identify how either climatic variables (moisture availability) or local plant production (NPP) influence SOM properties.

Second, linear mixed-effect models were used to compare CuO products of horizon types using paired two-sided t-tests. All models included horizon type (A, upper B, lower B-horizon) as a fixed effect, and NPP and moisture availability as random effects. This framework allows us to test whether the SOM properties within an individual site are significantly different as you move down the soil profile into either B-horizon. Using both frameworks allows us to better understand if distal climate properties or local plant communities are controlling SOM patterns, and if within-site characteristics control the (dis)similarity of SOM down soil profiles. All statistical analysis was conducted in R (v.4.0.3) in RStudio (v2022.07.1+554) using base R

(Bates, 2005; Zurr et al., 2008; Pinheiro et al., 2014; R Core Team, 2022).

### 3.4 Results

Based on the CuO products studied, we find a remarkably narrow range of SOM composition despite a diverse collection of ecosystems. We also find the SOM patterns of A-horizons are significantly different from either B-horizon, but that no B-horizons were significantly different from each other (Table 3.2). Both Spearman's Rank correlation matrices and linear models generally suggest neither the moisture availability or NPP were influential in explaining the patterns of CuO products across sites or down soil profiles.

Sample and Horizon Type	Total Organic Carbon		CN	Lignin:C	Lignin:N	3,5-Benzozic Acid:Lignin	P:V	Syringyl (Acid: Aldehyde)	Vanillyl (Acid: Aldehyde)	Cutin:C	Suberin:C	Substituted Fatty Acids (SFA):C	Substituted Fatty Acids (SFA):Lignin	Total Extractable Material
	%	mg/100 mg OC												
Organic	-	-	-	-	-	-	-	-	-	-	-	-	-	-
Vegetation	-	-	-	-	-	-	-	-	-	-	-	-	-	-
Roots	-	-	-	-	-	-	-	-	-	-	-	-	-	-
A-Horizon	5.91 (±1.53)a	18.69 (±1.57)a	-	0.98 (±0.07)a	21.78 (±3.48)a	0.08 (±0.01)	0.5 (±0.05)	1.19 (±0.3)	0.58 (±0.03)	0.52 (±0.05)a	0.24 (±0.02)a	0.77 (±0.07)a	0.44 (±0.04)	-
Upper B-Horizon	2.02 (±0.59)a	23.23 (±6.07)ab	-	1.01 (±0.21)b	21.19 (±4.05)b	0.09 (±0.01)a	0.62 (±0.06)a	3.22 (±0.3)a	1.22 (±0.07)a	0.75 (±0.17)b	0.31 (±0.07)b	1.06 (±0.23)b	0.76 (±0.02)a	5.88 (±0.52)a
Lower B-Horizon	1.59 (±0.63)a	14.02 (±1.68)b	-	1.18 (±0.35)b	11.12 (±1.04)b	0.11 (±0.02)b	0.67 (±0.12)b	5.42 (±0.51)b	1.05 (±0.04)b	0.94 (±0.31)b	0.39 (±0.12)b	1.31 (±0.44)b	0.96 (±0.03)b	7.52 (±1.65)b
FLF	28.92 (±1.03)	31.98 (±3.75)	-	2.36 (±0.18)	75.59 (±10.72)	0.08 (±0.00)	0.51 (±0.04)	1.73 (±0.21)	0.97 (±0.05)	0.90 (±0.05)	0.43 (±0.03)	1.33 (±0.08)	0.99 (±0.05)b	15.35 (±6.70)b
Density Fraction (A-Horizon)	34.4 (±1.75)	35.59 (±6.31)	-	6.77 (±0.98)	289 (±48.40)	0.12 (±0.00)	0.40 (±0.01)	13.33 (±2.14)	2.33 (±0.12)	5.41 (±0.94)	2.17 (±0.34)	7.98 (±1.18)	1.11 (±0.03)	53.04 (±6.00)
OCC	1.88 (±0.29)	13.53 (±1.17)	-	1.69 (±0.21)	26.63 (±5.85)	0.11 (±0.001)	0.48 (±0.04)	8.92 (±1.52)	2.14 (±0.23)	1.20 (±0.17)	0.90 (±0.07)	1.70 (±0.23)	1.00 (±0.03)	12.19 (±1.64)
HF	-	-	-	-	-	-	-	-	-	-	-	-	-	-

Table 3.2: Summary of cupric oxidation products for all sample types, bulk soil horizons, and A-horizon density fractions. Bulk soil horizons were meant to encapsulate representative horizons for each site with the widest pedogenic influence down soil profiles. Letters indicate significant differences ( $p < 0.1$ ) between bulk soil horizons. Due to logistical constraints, organic samples were not analyzed for elemental carbon or nitrogen analysis and thus could not be carbon normalized.

### 3.4.1 Lignin contributions

A-horizon lignin content (i.e. lignin normalized to the soil organic carbon pool) had a moderately negative correlation with root biomass (-0.36,  $p=0.056$ ). Neither NPP or the moisture availability had any correlation with A horizon or upper B horizon lignin content. Surprisingly, lower B horizon lignin content was negatively correlated with the moisture availability (-0.64,  $p=0.001$ ). There is suggestive evidence of a negative relationship between NPP and lignin content (-0.36,  $p=0.141$ ) and NPP with substituted fatty acid content (-0.35,  $p=0.157$ ) of lower B horizons. When controlling for NPP and the moisture availability, we find lignin contributions of A-horizons are significantly different from upper B (+0.97,  $p<0.01$ ), and lower B-horizons (+1.33,  $p<0.01$ ) (Table 3.2).

Despite a wide range of MAP, MAT, and NPP, representing Whittaker biome types that include tundras, subtropical deserts, grasslands, and temperate rain forests, soil lignin content fell with a remarkably narrow range of values (0.5 - 1.5 mg Lignin / 100 mg OC) (Figure 3.2). For example, the A horizon lignin content for a temperate desert (JORN) and a temperate seasonal forest (DELA) was 0.68 and 0.66 (mg Lignin/100 mg OC), respectively. Furthermore, the lower B-horizon from a boreal forest (BONA Cfgjj horizon) and an upper B-horizon from a temperate desert (ONAQ Bk1 horizon) was 0.63 and 0.64 (mg Lignin/100 mg OC), respectively. The BONA sample is a loess-dominated (C) mineral horizon with frozen water layers (f), with evidence of gleying (g) and cryoturbation (jj) with an approximate midpoint depth of 125 cm. The ONAQ sample is a yellowish brown (10 YR 6/4) mineral B horizon with a 50 cm midpoint depth and enough calcium carbonate (k) to have vio-

lent effervescence to the application of 10% v/v HCl. Despite their many differences, the contribution of lignin as a proportion of the total SOC pool is nearly identical.

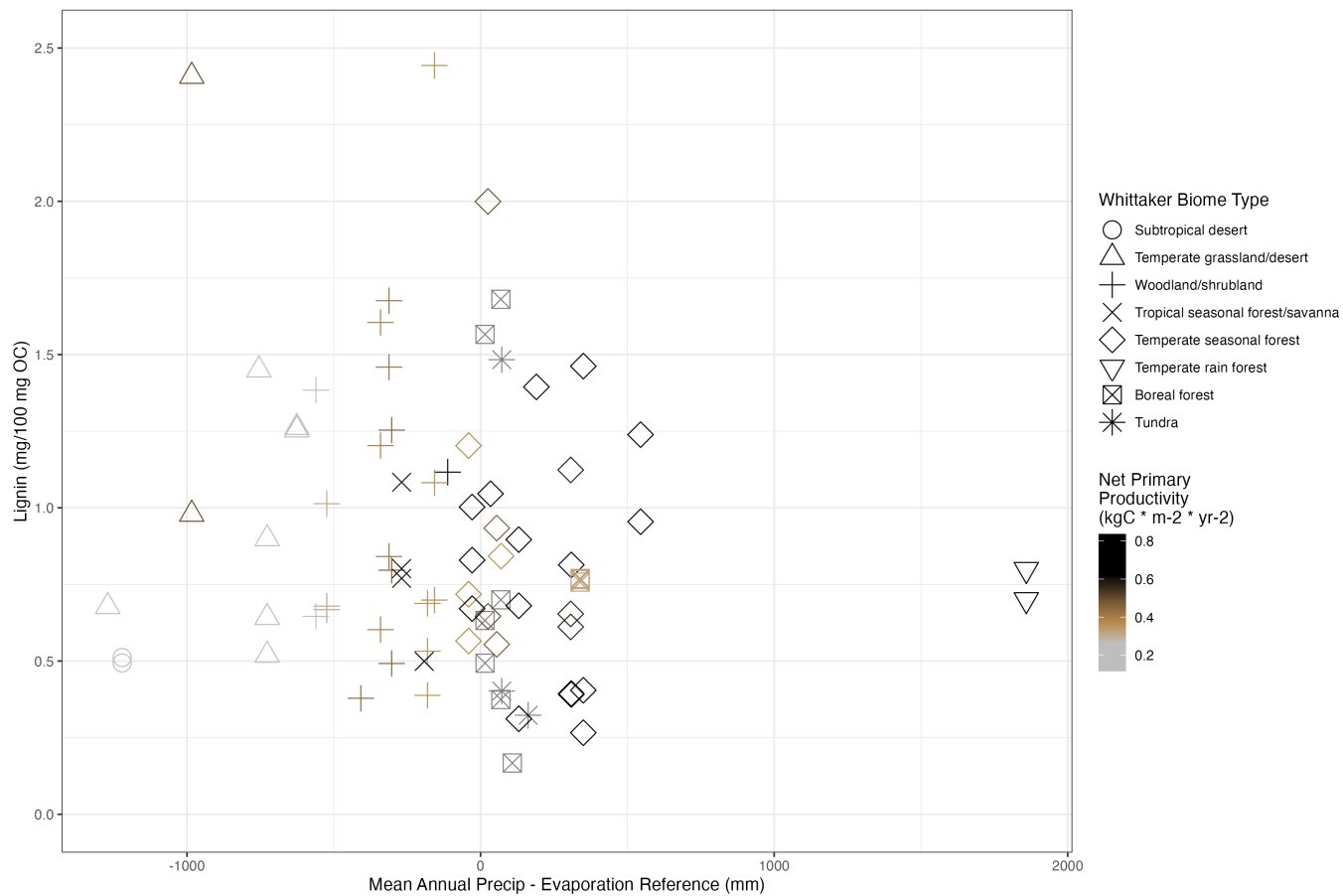


Figure 3.2: Carbon normalized lignin contributions to bulk soils (A, upper and lower B-horizons) relative to a hydroclimatic moisture index for a subset (n=39) of the National Ecological Observatory Network (NEON) sites.

We also explored a more stoichiometric relationship between lignin:carbon:nitrogen, however only 12% of samples exceeded 0.5 mg Lignin:C:N with the overwhelming majority of samples clustering within values of 0.1-0.25 (Supplementary Materials). Those samples with higher Lignin:C:N ratios spanned A, upper, and lower B horizons, and tended to be moderately dry ecosystems such as temperate grassland/deserts (n=4), woodland/shrublands (n=3), and temperate seasonal forest (n=2).

Although lignin content across sites are within a narrow range of values, there is an overall decrease in lignin content with increasing depth and substantial influences depending on density fraction category (Figure 3.3). Heavy fractions from A-horizons had approximately 70% more lignin than bulk soil A-horizons, and the occluded fraction contained  $\approx 2.5$  times more lignin than bulk A-horizons.

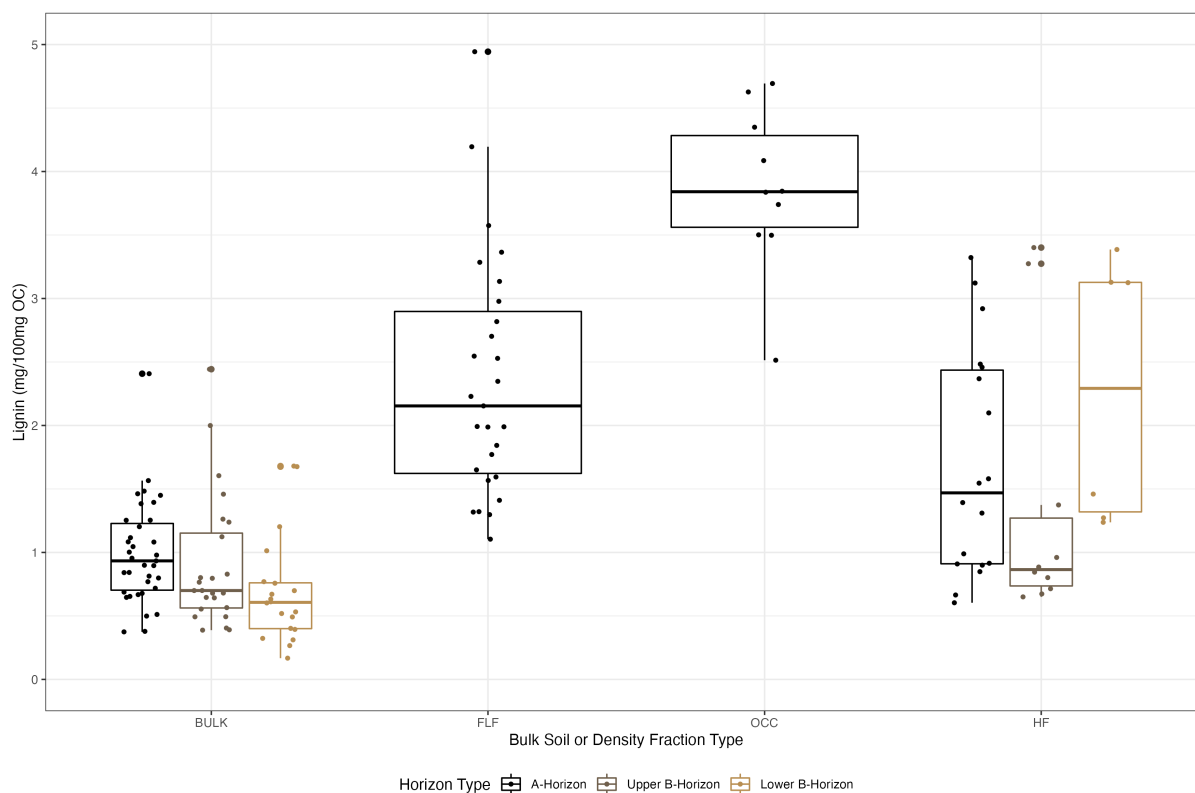


Figure 3.3: Carbon normalized lignin contributions to bulk soils (A, upper and lower B-horizon) and density fractions (FLF: free light, OCC: occluded; HF: heavy fraction) for a subset (n=31) of the National Ecological Observatory Network (NEON) sites. Due to logistical constraints, not all bulk soils yielded enough occluded fraction mass to be both analyzed for elemental carbon and cupric oxidation. We opportunistically included a subset of upper B and lower B-horizons but they are not meant to be representative sample sets.

### 3.4.2 Lignin degradation

Across all three bulk soil horizon types we see a trend of less lignin content with increasing depth (Figure 3.3), and as depth increases we also find higher degrees of soil organic matter processing (Figure 3.4a), greater lignin degradation (Figure 3.4c,d), but similar degrees of microbial contribution relative to lignin (Figure 3.4b). When controlling for NPP and the moisture availability, we find A-horizons have significantly less organic matter processing (3,5-benzoic acid:lignin) and greater lignin degradation (syringyl and vanillyl acid:aldehyde ratios) compared to either upper or lower B-horizons, but neither B horizons were significantly different from one another (Table 3.2).

Organic matter degradation state is represented by 3,5-benzoic acid normalized to lignin to control for different quantities of lignin, with higher values indicating greater degree of organic matter degradation (Figure 3.4a). Both vegetation samples, and free light fraction samples have the lowest degradation index. Root samples exhibit a widest range of organic matter degradation states, and bulk soil samples having the lowest variance of any sample types. Due to differential recoveries of our acid and aldehyde internal standards on occlude and heavy fraction sample types (Supplemental Materials), we refrain from drawing any conclusions that leverage only acids in the denominator of any ratio (Figure 3.4c,d). We can however interpret microbial contributions across all sample types (Figure 3.4b).

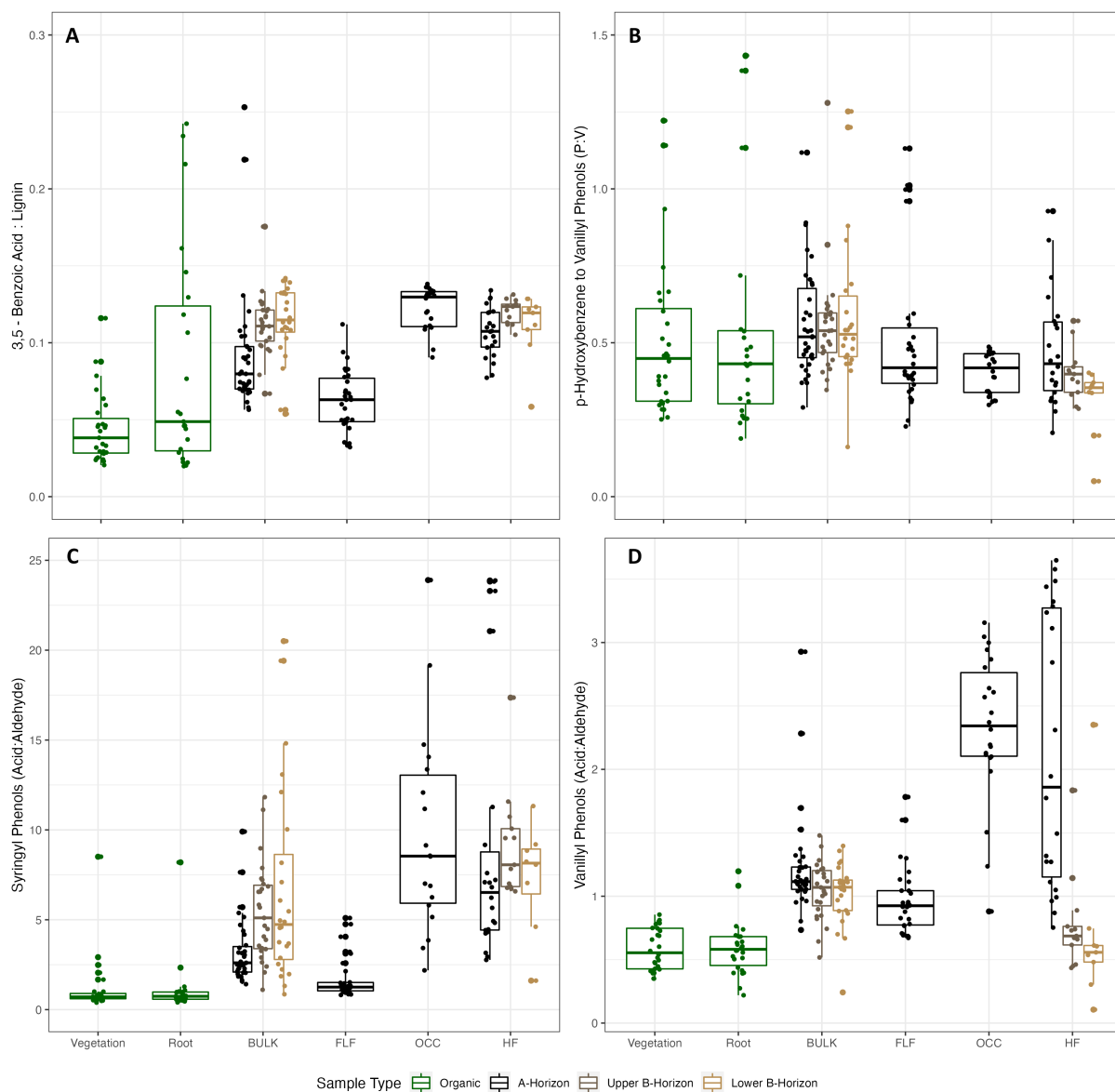


Figure 3.4: Lignin and non-lignin cupric oxidation product yields for all sample types, horizons, and density fractions available from the National Ecological Observatory Network (NEON). We present four panels that include (A) lignin degradation index with higher values indicating greater lignin degradation, (B) microbial to plant biomarker index with higher values indicating higher microbial processing of lignin, and (C, D) the acid to aldehyde ratios of two lignin phenols with higher values indicating greater lignin oxidation. Due to unequal recovery of internal standards, the observed occluded and heavy fraction data may be underestimating the amount of acid phenols relative to aldehyde phenols, and these data should be viewed with caution.

The category of p-hydroxybenzene (P) phenols incorporates compounds of a dominant microbial origin such as algae, fungi, bacteria, and some vascular plants (Goñi et al., 2008), and when normalized to a lignin phenol (vanillin) it can be used as a proxy of microbial contributions to organic matter and for organic matter sourcing techniques (Goñi and Hedges, 1995; Goñi et al., 2000). We find similar amounts of P:V in vegetation, roots, and all three density fraction sample types (Figure 3.4b). However, bulk mineral soils of all three horizon types have an overall greater P:V ratio indicating higher microbial contributions. It is notable that the occluded fraction has the smallest variance of any sample type, and bulk soils of all three depths show similar degrees of microbial contributions to soil organic matter.

Syringyl phenols are almost exclusively produced by angiosperms, with angiosperms containing 25-50% of their lignin as vanillyl phenols and gymnosperms contribute 90-95% of their lignin as vanillyl phenols. By comparing the acid:aldehyde ratio of these lignin-specific phenols we can interpret the relative degradation state of lignin. Both phenols suggest vegetation and root sample types had the lowest degree of lignin degradation, with higher degradation in bulk soils (Figure 3.4c,d). Syringyl phenols were progressively more degraded with increasing soil depth, but the free light fraction resembled fresh vegetation or root signatures. Conversely, vanillyl phenols appeared to have similar degrees of degradation in all three bulk soil types, but were still more degraded than either vegetation or root samples. The free light fraction showed intermediate degradation between vegetation and bulk mineral samples.

### 3.4.3 Substituted fatty acids (SFA)

Due to their similar molecular structures, the combination of cutin (exterior leaf waxy coatings) and suberin (exterior root waxy coatings) are considered substituted fatty acids, and normalizing them to lignin (SFA:Lig) allows for a more consistent comparison of the relative plant contributions to organic matter across ecosystems (Goñi and Hedges, 1990; Crow et al. 2009b). As expected, both vegetation and roots have similar SFA:Lig ratios (Figure 3.5). The free light fractions present intermediate values with some overlap between vegetation/roots and A-horizons. As the depth of the horizon increases there is a higher contribution of SFA:Lig with significant differences between the A and either B horizons (Table 3.2). When controlling for NPP and moisture availability, A-horizons had significantly less SFA contributions compared to either B-horizon, but neither B-horizon was significantly different from each other.

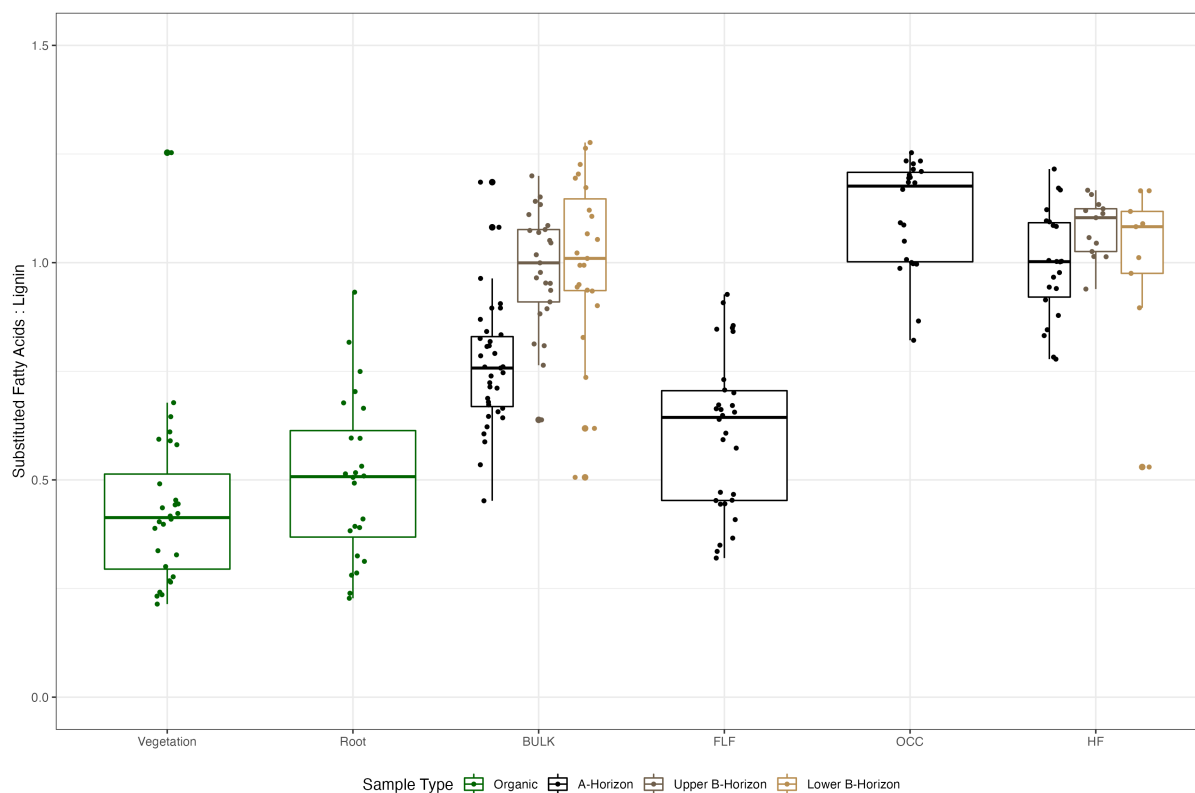


Figure 3.5: Plant wax yields (substituted fatty acids) from the cupric oxidation procedure for all sample types, horizons, and density fractions available from the National Ecological Observatory Network (NEON). Due to unequal recovery of internal standards, the observed occluded and heavy fraction data may be underestimating the amount of acid phenols relative to aldehyde phenols, and these data should be viewed with caution.

### 3.4.4 Alternative biomarkers for sourcing techniques

Although not the primary intent of this manuscript, the CuO procedure is often used for tracing how organic matter varies from different plant types. The ratio of cinnamyl to vanillyl (C:V) is used as an indication of non-woody (higher ratio) compared to woody plants (lower ratio). The ratio of syringyl to vanillyl (S:V) is used as an indication of gymnosperms (higher ratio) compared to angiosperms (lower ratio). There remains strong evidence that C:V ratios can be used to trace woody vs non-woody plants in A-horizons, but the signal becomes diminished in both upper and lower B-horizons (Supplemental Materials). Similarly, S:V ratio of A-horizons captures angiosperms vs gymnosperm organic matter signatures (Supplemental Materials). When controlling for NPP and moisture availability, both C:V and S:V of A-horizons were significantly different from either B-horizon, but neither B-horizon was significantly different from each other.

## 3.5 Discussion

Our overarching hypotheses were that (1) sites with higher NPP would result in higher lignin and plant wax contribution to the SOM, and (2) lignin and plant wax contributions of deeper horizons would mirror surface horizons where plant inputs are greatest. Based on the CuO biomarker products we examined, we find nearly all A horizons differ in their composition of SOM compared to any upper or lower B horizons which were independent of either NPP or climatic factors. We also find that the composition of either B horizon are not statistically different from each other

(Table 3.2). Thus we have limited evidence to support our first or second hypotheses. Partially consistent with our first hypothesis, we do find evidence that lignin content is highest in A-horizons and decreases down soil profile, but plant waxes increase in deeper soil horizons (see discussion below). Contrary to our second hypothesis, we have strong consistent evidence that A-horizons are unique from either B-horizon, but that both B-horizon are similar to each other. Finally, the CuO procedure remains robust to tracking specific plant-types (woody vs nonwoody, angiosperms vs gymnosperms), however this signal is only robust in A-horizons (Supplemental Materials).

Considering all the evidence, this suggests local biomass production generates A-horizons that retain some of the plant community organic matter signal, but across a wide range of hydroclimate regimes the lower soil horizons no longer retain the aboveground plant organic matter characteristics. It's important to note that the estimated midpoint depths of our soil horizons are 18, 56, and 91 cm for the A, upper B and lower B-horizons respectively. Our upper B-horizons are deeper than the reported maximum soil depths for four prominent high impact soil journals spanning over 1,100 articles; since the 1990's the maximum soil depth has decreased from  $\approx 53$  cm, to only  $\approx 24$  cm in 2000's (Yost and Hartemink, 2020). If researchers continue to sample only surface soils, we are unlikely to be able to predict whole-ecosystem carbon responses to climate change because more than half of soil carbon is below 30 cm (Batjes, 2014; Lal, 2018). To the author's knowledge, this is both the most broad systematic organic matter inventory and deepest soil horizon assessment that have ever been investigated.

### 3.5.1 Vegetation endmembers and surface soil lignin contributions

Despite a wide range of plant community types (e.g., grasses, shrubs, conifers) many CuO indexes for decomposition suggest the dominant aboveground vegetation and belowground roots are at similar degradation states (Figure 3.4b,c,d). The exception is 3,5-benzoic acid normalized to lignin, indicating roots have a much wider range of degradation states compared to vegetation endmembers (Figure 3.4a). The nature of root collection (that include living and dead roots, collected after potentially weeks since coring and sample processing) may explain the higher rates of root decomposition compared to the fresh and still living vegetation that was collected and frozen until processed. Alternatively, it's likely greater root degradation is a true property of soils due to ongoing root turnover. Regardless of the mechanism, this suggests that 3,5-benzoic acid is likely a more sensitive indicator of soil organic matter degradation compared to other CuO indices studied.

Surprisingly, surface soil lignin content did not follow a pattern in NPP (Figure 3.2). We expected ecosystems with large aboveground woody additions (e.g. temperate rain forests, temperate seasonal rain forests) would have increased lignin contributions to the surface soils, and that SOM would have a stronger woody-gymnosperm signal (low C:V and low S:V). We could not identify a clear pattern with forested ecosystems containing more lignin (Figure 3.2). Some forested sites contain SOM with a stronger woody-gymnosperm signal (ABBY, SERC, UNDE), but not all forested sites followed this pattern (Supplemental Materials).

Examining the relationship between C:V and S:V can aid in separating out vegetation endmembers from their mixing zones (e.g. Goñi et al, 2013; Crow et al,

2009 plant-source). Broadly speaking, many site-SOM appeared closer to root-litter chemistry (ABBY, SERC, UNDE, DEJU, LENO, NIWO), but some SOM appeared more like aboveground vegetation (JORN, SOAP, TALL), a mixture between the two vegetation endmembers (DCFS, HARV, ONAQ), and some endmembers were so similar they are not obviously decipherable from each other (CLBJ, MLBS, SRER, WOOD) (Supplemental Materials). This is likely a limitation of both the sampling and the CuO method. Most, but not not all, vegetation samples were provided upon soil core shipment. A larger number of sites do not have root end-members due to (a) our inability to find any roots in the small-diameter cores, (b) the roots were so fragile on collection we could not physically collect them, or (c) there simply was not enough root biomass present for grinding and analysis. The combination of (b) and (c) likely contributed the most to the lack of root samples. Alternatively, our inability to distinguish SOM from its endmembers may be a limitation in the CuO method. White-rot fungi degrade lignin in a way that excludes it from the GCMS analytical window and thus is not fully captured by the CuO method (Filley et al., 2002), likely underestimating the woody contributions to SOM, especially in forested ecosystems. In a deciduous and conifer ecosystem Crow et al. (2009b) found needle endmembers had the largest cinnamyl (C) component, which is considered the more easily degradable compared to other lignin monomers due to ester linkages that are easily hydrolyzable (Bahri et al., 2006). This may further lead to an underestimation of aboveground contributions to SOM, especially in forested ecosystems.

### 3.5.2 Deep soil lignin and SFA patterns

Our lignin degradation results reinforce previous research findings. Based on deep soil lignin phenol degradation indices, we find acid:aldehyde ratios of vanillin were insensitive to increasing soil depth compared to syringal phenols (Figure 3.4cd, Supplemental Materials). Our observations further supports the notion that vanillyl phenols are more resistant to degradation than syringyl phenols (Hedges et al, 1988, Bahri et al., 2006; Angst et al., 2021).

As a proportion of the total SOM pool, overall lignin contributions decrease with depth. This could be due to a number of possibilities including: a true loss of lignin due to higher microbial degradation at greater depth, stronger mineral retention of organic matter in deeper soil samples, or lignin compounds being lost out of our analytical window. The higher organic matter degradation state (Figure 3.4a), greater microbial contributions to SOM (Figure 3.4b), and higher higher lignin acid:aldehyde ratios (Figure 3.4cd, Supplemental Materials) suggest this is a true decrease in lignin contributions with depth due to microbial degradation. While there may be stronger organic matter binding mechanisms with depth due to higher Fe and Al oxide phases in wetter ecosystems, drier ecosystem soil carbon concentration content was predicted by abundant cation bridging from calcium and magnesium (Rasmussen et al., 2018; Heckman et al., 2020). Using a subset (n=34) of these NEON sites, Heckman et al. (In review, 2022) found root mass distributions were significantly lower in arid compared to humid sites (when MAP/potential evapotranspiration > 1) and MAOM carbon persistence ( $\Delta^{14}\text{C}$ ) can be explained by depth in humid systems but not in arid systems. They attribute this decoupling to moisture transport limitations of

OM in arid systems. Despite the robust pattern in carbon persistence with depth and mechanistic explanation, it is surprising that lignin has a similar contribution to the SOM pool across these same NEON sites.

As noted by Weiglein et al (2021), using these same soil horizon samples for a year-long soil incubation experiment with temperature and moisture factors fully crossed, we also observe strong evidence that lignin becomes degraded with increasing depth. However, current degradation states of lignin are not always predictive of future lignin vulnerability. Weiglein et al (2021) shows that greater lignin degradation in A-horizons was predictive of lower SOM vulnerability (using cumulative specific respiration during the year long incubation period), but this relationship did not hold in upper B-horizons. Out of the  $\approx 129$  potential predictors variables, only seven were selected for predicting B-horizon cumulative specific respiration. The seven predictors include two climate variables, and five soil chemistry variables. The two highest importance rank of soil chemistry variables to predict B-horizon SOC vulnerability include the microbial contribution to the total SOC pool (measured as the mean chloroform extract double bond equivalents) and dissolved organic matter with a more degraded signature. Examining the wide range of sites present in this study design, we suggest that while microbial communities are undoubtedly influencing SOM characteristics, in the subsoil they have a somewhat universal imprint on SOM chemistry regardless of climate, vegetation, or parent materials. These observations also support a hypothesis set forth by Lian et al (2017), that microbial processing of unique plant inputs would result in homogenized SOM due to microbial anabolism and microbial biomass being more similar than the original plant inputs.

The increasing SFA:Lig ratio as soil depth increases (Figure 3.5) could be due to a true increase in the sum of SFA components, a decrease in lignin content, or a combination of both. We find evidence for both patterns occurring simultaneously; both B-horizons have less lignin:C compared to A-horizons, and SFA:C increase in both B-horizons relative to A-horizons (Table 3.2). Our inability to distinguish B-horizons from each other (using either SFA:C or SFA:Lig) could be due to consistent aboveground cutin inputs, belowground suberin inputs, or microbial recycling of SFA that can lead to accumulation of SFA. We observe cutin contributions nearly double or triple the suberin inputs across all sample and horizon types (Table 3.2). This is likely due to the cutin category composed of five unique CuO compounds compared to only three for suberin, but evidence suggests both cutin and suberin components degrade at similar rates (Angst et al., 2016; Feng et al., 2010). Furthermore, it is known that some of these plant waxes can have contributions from bacteria and fungi (Whalen et al., 2022 and references therein), and that microbial in vivo turnover of these products could eventually lead to most SOM being indistinguishable despite differing plant inputs (Liang et al., 2017).

Due to the broad range of sites with overlapping SFA signatures, a better application of the CuO method to determine SOM sources would require a site-specific root and shoot adjustment of individual CuO products to ascertain the signal from the noise. Such an endeavor was carried out by Crow et al. (2009 plant-source), however they used a highly controlled biomass manipulation study in two forests with multiple site-specific OM endmembers that contained intermediate stages of plant decomposition allowing them to make strong inferences on SOM sourcing. It's

possible such a task can be implemented, but it could only be done on the subset of locations with both root and shoot endmembers, which is out of the scope of this study.

### 3.5.3 Density fractions

Due to the disparate recovery of our internal standards on occluded and heavy fractions, we refrain from interpreting CuO observations that exclusively leverage acids vs aldehydes. One index we can more confidently interpret is the P:V (Figure 3.4b) because both numerator and denominator contain acid, ketone, and aldehyde functional groups. We find both the free light and occluded fractions appear to have intermediate states of microbial processing greater than vegetation samples, but less than bulk soils. This is consistent with the MEMS hypothesis, that (aboveground or belowground) litter requires some amount of microbial processing before it can become stabilized on minerals (Cotrufo et al., 2013; Cotrufo et al., 2015; Lavalley and Cotrufo, 2018). The first stage of litter decomposition, according to the MEMS framework, will yield labile DOC that is efficiently used by microbes and contributes a disproportionate amount of litter OM to SOM. With the CuO method, we cannot examine these smaller molecule components, or more thoroughly investigate microbe-specific contributions (Whalen et al, 2022). Although additional research suggests that belowground litter input is more efficient at forming mineral-stabilized SOM compared to aboveground inputs (Sokol and Bradford, 2019), especially smaller molecule root exudates (Sokol et al., 2018).

### 3.5.4 Cupric oxidation (CuO) as a tool

A large proportion of terrestrial-based research using the CuO procedure is conducted in a single ecosystem transition zone (Crow et al., 2009a; Angst et al., 2016b), compares only pairs of factors such as plant type (Angst et al., 2016a) or parent material (Angst et al., 2018), or is constructed as a randomized controlled trial with organic matter manipulations (Angst et al., 2021b; Rumpel et al., 2014; Hatten and Goñi, 2016; Feng et al., 2010; Hedges et al., 1988; Chapter 2 of this dissertation).

This is one of the first studies that uses the CuO procedure as part of a large-scale observational study that was conceived to capture the widest range of climatic and environmental characteristics (Loescher et al., 2014). Although the CuO procedure is robust to tracking sources of organic matter during major transitions (e.g. plant, rock type, biomass manipulations), without these contrasts a surprising majority of mineral soils across North America have SOM qualities that are more similar than dissimilar. This suggests that although sources and quantities and rates of lignin additions to soil vary greatly, all observed ecosystems reach a steady state of how much lignin can contribute to the SOM pool. This contribution decreases with depth as lignin becomes more degraded. But the lack of ecosystems differentiation in the second most abundant biomolecule on the planet (Filley et al., 2002) further reinforces the view that that there is nothing inherently stable or recalcitrant about lignin (Schmidt et al., 2011; Lehmann and Kleber, 2015). The fact that overall lignin content decreases with depth, but that upper B and lower B-horizons are more similar to each other compared to their parent A-horizons also suggests a universal endpoint of microbial SOM processing that all deep soil environments follow.

It remains possible that within-site normalization of individual CuO products that accounts for the molecular fingerprint of pure end-members (e.g. vegetation, roots) could be a more sensitive approach to determine litter-contributions to SOM. Such a process has been successfully carried out in terrestrial ecosystems, but only a limited number of sites (Angst et al., 2016b) or very shallow soils (Crow et al., 2009b). Additional work is needed to specify individual CuO products, rather than a broad lignin or plant wax categories, to understand whether this method can be more precise at identifying within-site litter contributions to the free light or bulk soil fraction. This would help us better understand how future change to plant communities or climatic conditions could affect the presence and persistence of SOM compounds.

Given these cross-ecosystem and down-profile similarities, the authors question the rationale behind many global climate change models that continue to use Lignin:N as an input variable for predicting centennial-scale ecosystem responses to a changing climate (Dungait et al., 2012 and references therein). The initial usage of Lignin:N as input variable is due to litterbag studies revealing “leaf skeletons” after short incubation periods (months), and that the initial stage of litter decomposition is strongly controlled by lignin (Meentemeyer, 1978) and lignin:N (Adair et al., 2008). However, with the advancement of stable isotope tracing and larger synthesis studies finding that lignin may have an initially slow decomposition rate (Rasse et al., 2005), it can nearly fully decompose on decadal timescales (Dungait et al., 2012; Dignac et al., 2017; Hoffman et al., 2006; Thevenot et al., 2010). The narrow range of lignin content we find across a wide range of ecosystems, and the fact it’s one of

the most abundant biomolecules on earth, suggests that as much as there are high lignin litter inputs in some ecosystems, it cannot persist indefinitely and is instead being constantly undergoing turnover in soils.

It's also possible the CuO method is not suited for strict organic matter sourcing in the way it is currently being used. For example, some SFA components can be sourced from microbes or fungi, some lignin monomers exhibit unequal turnover kinetics, and mineral-matrix interference may affect some sites with high Fe/Al components more than others (Whalen et al., 2022 and references therein). However, the CuO method does have its strengths in riverine and oceanographic studies where plant species diverge more than on a single terrestrial NEON site. Aqueous transport of POM, and its subsequent collection, also does not have as much mineral-matrix interference as we observe in deep soil horizons, occluded fractions, and heavy fractions (Supplemental Materials).

The CuO method continues to have strong applications in terrestrial ecosystems, especially in biomass manipulation studies, or plant-transition zones, or other locations where there is a strong gradient in a small number of biochemically distinct organic matter sources. One opportunity for a potentially viable source of novel information using the CuO method is to consider analyzing the post-incubation temperature/moisture controlled soils conducted by Weiglein et al. (2021). Further analysis of those incubations show carbon vulnerability in humid systems is more sensitive to temperature increases but arid system carbon vulnerability is more sensitive to moisture shifts (Possinger et al., 2021). It remains possible that compound-specific vulnerabilities are influenced by temperature or oxygen availability, which could be

rigorously addressed with CuO analysis of these post-incubation samples. However, as a general application to determine the overall sourcing of soil organic matter in natural systems without experimental controls, especially in regards to its non-lignin products, the CuO extraction procedure may not be a robust method for that application.

### 3.5.5 Implications for SOM patterns across ecosystems

Despite a wide range in ecosystems, climates, geology, plant types and soil types present in this study we observe remarkably similar patterns in soil-derived CuO products. It is well established that pure litters produce a unique composition of water extractable organic matter (McKnight et al., 2001), but lysimeter collection of soil water produced homogenized organic matter signatures (Yano et al., 2005), even after 17 years of above and belowground litter manipulations (Strid et al., 2016). This suggests soil biotic and abiotic processes are acting like a chemostat on dissolved organic matter; a variety of unique litter inputs (e.g. initial degradation products) are processed by soil microbes and result in a homogenized output of dissolved organic matter. This theoretical framework has been implemented in biorefineries to convert a range of woody biomass into homogenized co-products for biofuel production (Linger et al., 2014), and has been hypothesized to occur in natural systems by Liang et al (2017).

Based on our observations, we suggest this framework of unique POM-derived inputs resulting in similar-DOM outputs should be extended to also include lignin

contributions to SOM as a homogenized endmember independent of climate, NPP, or plant community composition. For example, seven NEON A-horizons have lignin contributions between  $\approx 1.0$ - $1.2$  mg Lig/100 mg OC that include temperate seasonal forests (SCBI, SERC), woodlands/shrublands (KONZ, NGPR), a tropical seasonal savanna regenerating into a long-leaf pine forest (DSNY), a temperate grassland/desert (SJER), and a fallow scrubland (BLAN). These seven sites span a three-fold range in MAP (38 cm SJER; 122 cm DSNY), a four-fold range in MAT ( $5^{\circ}\text{C}$  NGPR;  $22^{\circ}\text{C}$  DSNY), and the A-horizons nearly span an entire order of magnitude in organic carbon values (0.56% SJER; 4.83% SCBI). Despite the wide range in ecoclimatic variables of these seven sites, CuO identified plant contributions to the SOM pool are nearly identical.

Our inability to explain the differences in lignin contributions to soils across ecosystems also suggests SOM composition could be viewed through a stochastic framework. Similar to how researchers are now considering  $\Delta^{14}\text{C}$  as a stochastic process, with a probability distribution of values that cannot be sufficiently captured in a single median value (Sierra et al., 2017; Sierra et al., 2018), it seems equally possible for this concept to apply to SOM composition. That lignin contributions to SOM are generally consistent (71% of all bulk soils within 0.25-1.0 mg Lig/100 mg OC), but not precisely predictable at the site or horizon scale. Due to this ecosystem inertia in homogenizing SOM components, we caution against ongoing efforts seeking to increase single plant compound(s) to increase SOC (e.g. genetically engineering plants to increase their suberin contributions at the Salk Institute) because they may not result in a meaningful change to long-term soil carbon stores. On the multi-

decadal timescale we humans are all temporarily not soil, it is similarly possible that all SOM - regardless of its source or current ecosystem - are temporarily not carbon dioxide.

### 3.6 Conclusion

We leveraged full soil profile samples originating from the installation of National Ecological Observatory Network that will be in operation for at least the next 30 years, representing the deepest assessment of CuO extracted SOM across nearly all North American ecosystems. A-horizons across ecosystems had significantly different SOM compositions compared to their associated subsoils. However, within sites, neither upper or lower B-horizon SOM components were significantly different from each other. We find lignin content (Lig:Carbon) decreases and down soil profiles and that organic matter degradation (3,5 benzoic acid:Lig), lignin degradation (syringyl phenol acid:aldehyde ratios), and plant waxes (SFA:Lig) generally increases. However, neither NPP or the tradeoff between precipitation inputs and plant water use exports (moisture availability) were predictive of SOM components extracted with the CuO method. Lignin contributions to SOM are greatest in the free light fraction and occluded fraction, with the free light fraction resembling intermediate SOM characteristics between site-specific vegetation and root endmembers and bulk soils. We find certain CuO indexes more sensitive to detecting organic matter degradation (3,5 benzoic acid:lignin) and consistent with other research findings that vanillyl phenols are more resistant to degradation compared to syringyl phenols. We caution that

mineral-matrix interferences minimize the interpretations of some CuO products for the occluded and heavy fractions. Overall we find the cross-ecosystem similarity in CuO extracted SOM products to provide evidence for the homogenizing effect on SOM that biotic and abiotic soil processes have from unique litter inputs. Similar to heterogenous litter-DOM being converted into a homogenous DOM once entering soils, we suggest a similar process occurs with unique litter-POM inputs converting to a more uniform SOM composition across all North American ecosystems.

### 3.6.1 Acknowledgements

This study was funded by the U.S. National Science Foundation Macrosystems, BIO Directorate, Division of Environmental Biology Program (Award No. EF- 1340681). Raven Chavez and Maylita Brougher of Oregon State University were instrumental in conducting the soil characterizations and laboratory analyses. We would like to acknowledge the National Ecological Observatory Network Systems Installation and Verification Team for the collection of soil cores. The National Ecological Observatory Network is a project sponsored by the National Science Foundation and managed under cooperative agreement by Battelle.

### 3.7 Supplemental Materials

There are four items of supplementary materials, they include:

1. Supplemental Figure 1. CuO Internal Standard Recoveries
2. Supplemental Figure 2. C:V Ratios (non-woody v woody) index
3. Supplemental Figure 3. S:V Ratios (flowering v seed cones) index
4. Supplemental Figure 4. Acid:Aldehyde ratios of S and V phenols down soil profiles

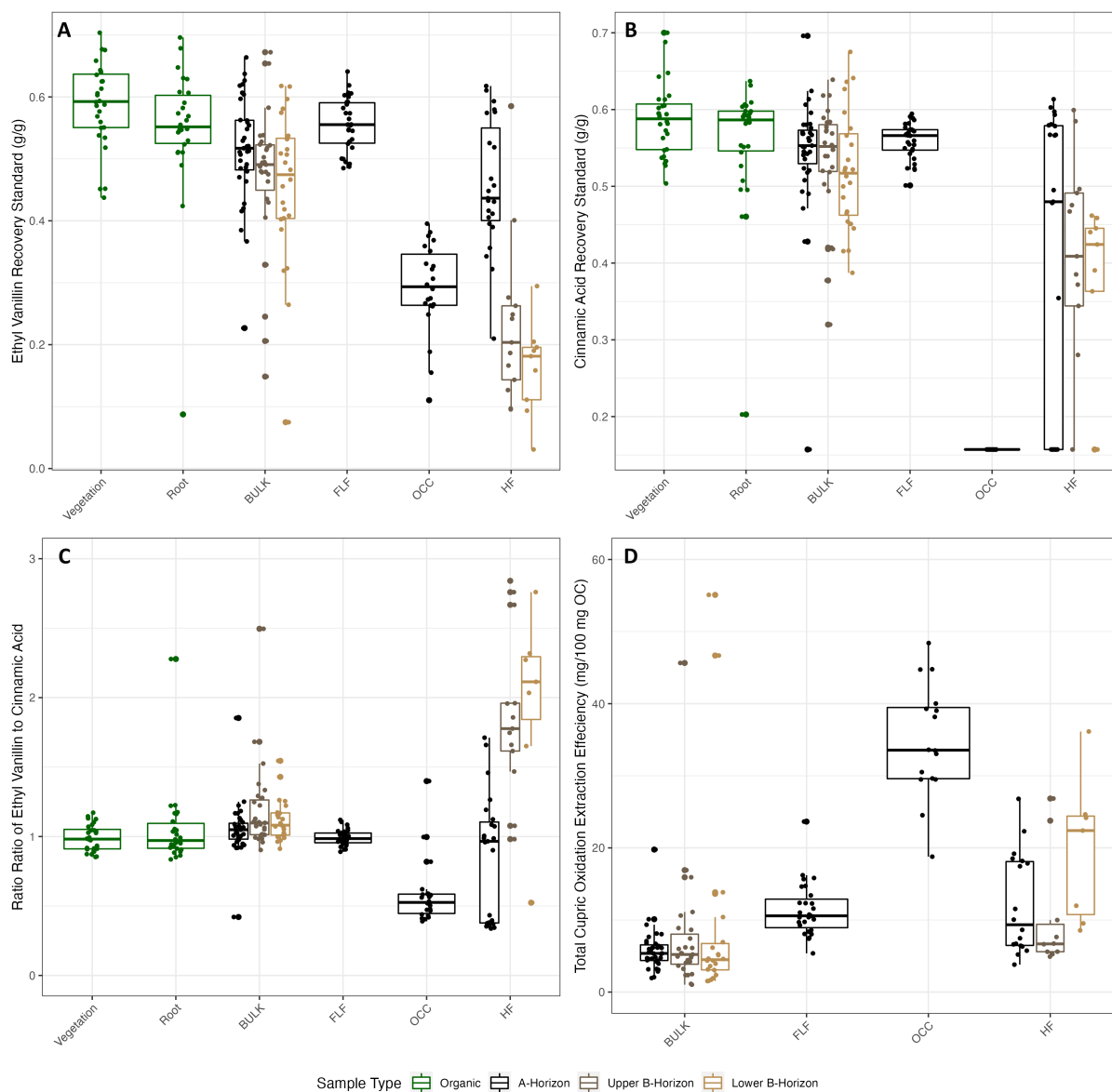


Figure 3.6: Plant wax yields (substituted fatty acids) from the cupric oxidation procedure for all sample types, horizons, and density fractions available from the National Ecological Observatory Network (NEON). Due to unequal recovery of internal standards, the observed occluded and heavy fraction data may be underestimating the amount of acid phenols relative to aldehyde phenols, and these data should be viewed with caution.

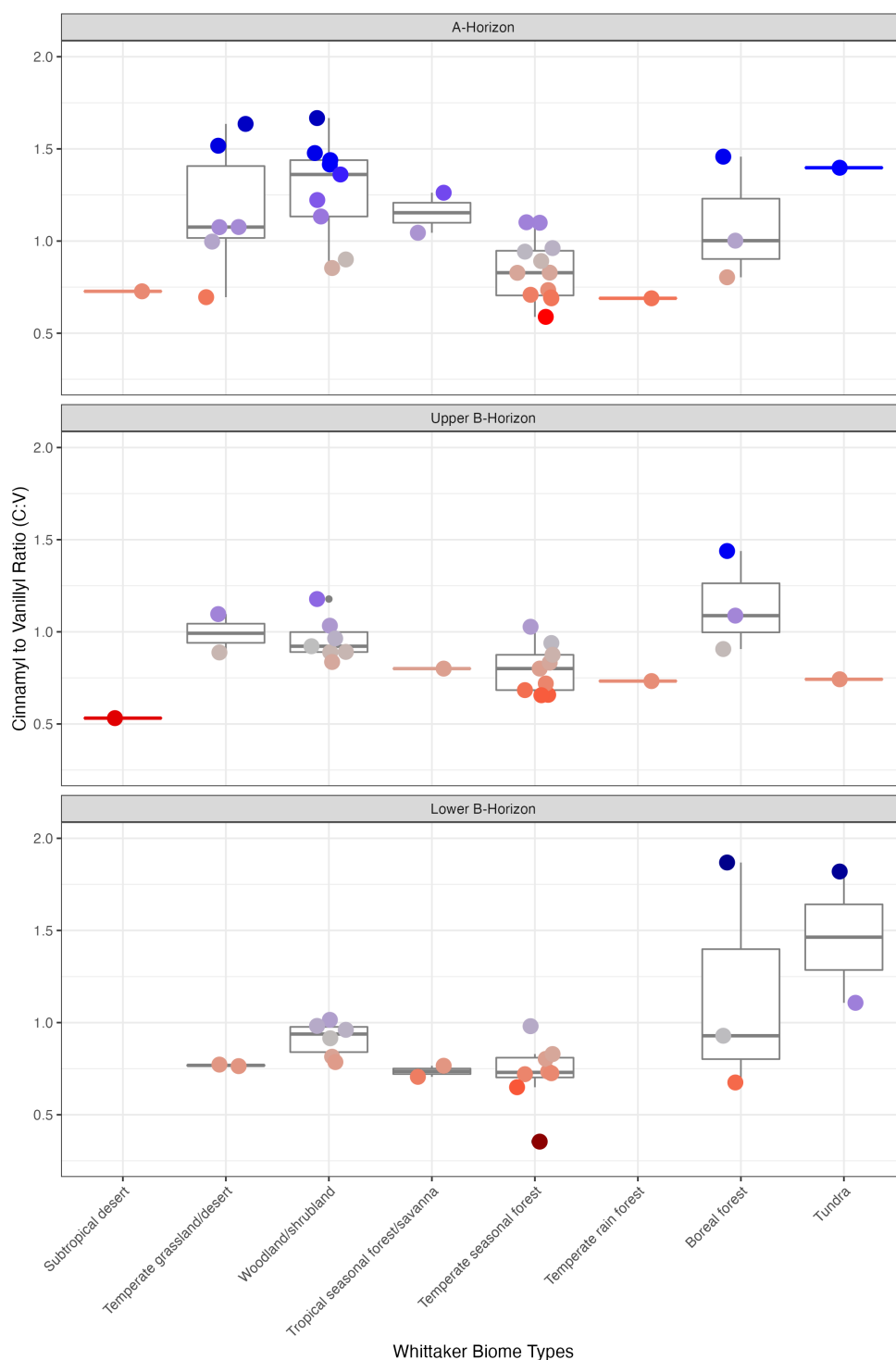


Figure 3.7: Comparing two lignin phenol categories from bulk soils of the National Ecological Observatory Network (NEON). Higher values indicate a non-woody source of lignin, and lower values indicate a woody source. The C:V ratio correctly identifies the biomes that dominate in grasses/shrubs vs trees in the A horizon, but the aboveground biomarker signal diminishes with increasing depth. See Table 2 for estimated midpoint depths for all three horizons meant to capture representative horizons for each site with the widest pedogenic influence down soil profiles

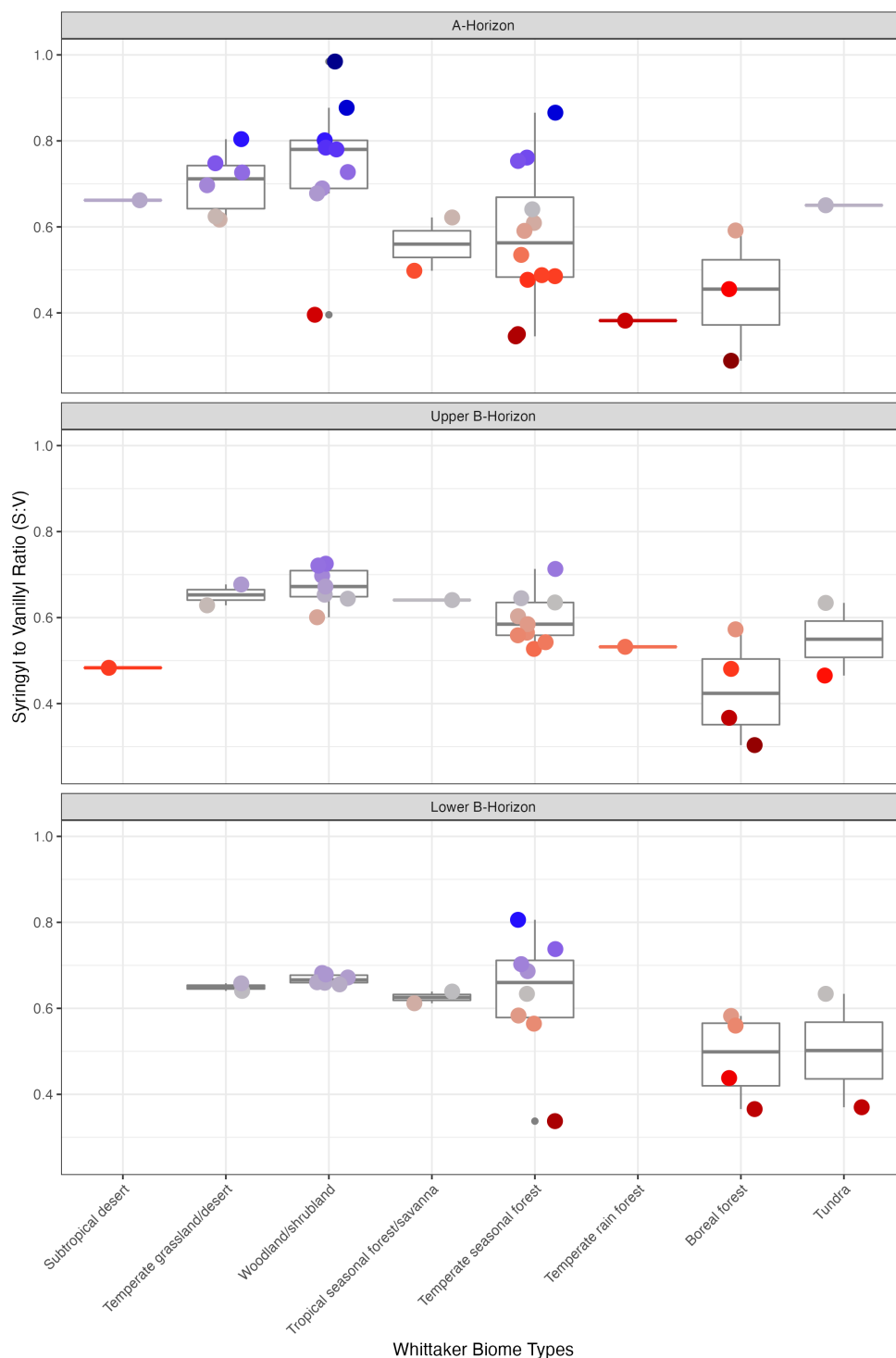


Figure 3.8: Comparing two lignin phenol categories from bulk soils of the National Ecological Observatory Network (NEON). Higher values indicate an angiosperm (flowers, grasses) source of lignin, and lower values indicate a gymnosperm (tree) source. The S:V ratio correctly identifies the biomes that dominate in grasses/shrubs vs trees in the A horizon, but the aboveground biomarker signal quickly diminishes with increasing depth. See Table 2 for estimated midpoint depths for all three horizons meant to capture representative horizons for each site with the widest pedogenic influence down soil profiles

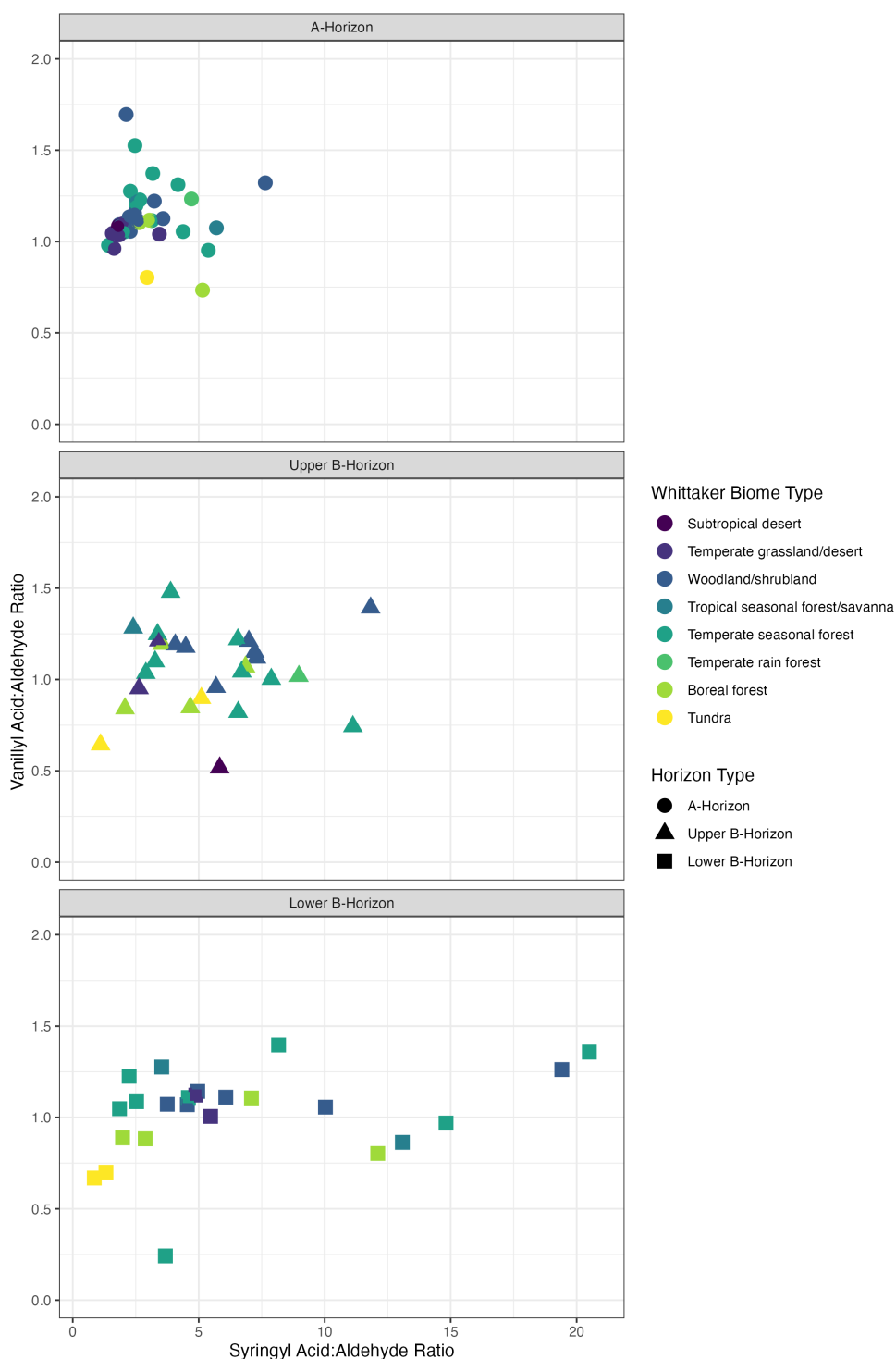


Figure 3.9: Comparing acid to aldehyde ratios of two lignin phenol categories from all three bulk soil types from the National Ecological Observatory Network (NEON). As depth of soils increase, research shows the organic matter is generally more decomposed (characterized by more -OH functional groups substituted onto SOM). Higher acid:aldehyde ratios indicate greater oxidation of those lignin phenols. Vanillyl phenols may persist longer, or are less vulnerable to oxidation, compared to syringyl phenols which observe expected patterns of increased degree of oxidation as depth of soil increases.

### 3.8 References

Adair, E.C., W.J. Parton, S.J. Del Grosso, W.L. Silver, M.E. Harmon, S.A. Hall, I.C. Burke, and S.C. Hart. 2008. Simple three-pool model accurately describes patterns of long-term litter decomposition in diverse climates. *Glob. Chang. Biol.* 14(11): 2636–2660.

Angst, G., L. Heinrich, I. Kögel-Knabner, and C.W. Mueller. 2016a. The fate of cutin and suberin of decaying leaves, needles and roots - Inferences from the initial decomposition of bound fatty acids. *Org. Geochem.* 95: 81–92. Available at <http://dx.doi.org/10.1016/j.orggeochem.2016.02.006>.

Angst, G., S. John, C.W. Mueller, I. Kögel-Knabner, and J. Rethemeyer. 2016b. Tracing the sources and spatial distribution of organic carbon in subsoils using a multi-biomarker approach. *Sci. Rep.* 6(June): 1–12.

Angst, G., J. Messinger, M. Greiner, W. Häusler, D. Hertel, and K. Kirfel. 2018. Soil organic carbon stocks in topsoil and subsoil controlled by parent material, carbon input in the rhizosphere, and microbial-derived compounds. *Soil Biol. Biochem.*: 1–2.

Angst, G., K.E. Mueller, K.G.J. Nierop, and M.J. Simpson. 2021a. Plant- or microbial-derived? A review on the molecular composition of stabilized soil organic matter. *Soil Biol. Biochem.*: 135907. Available at <https://doi.org/10.1016/j.soilbio.2021.108189>.

Angst, G., J. Pokorný, C.W. Mueller, I. Prater, S. Preusser, E. Kandeler, T. Meador, P. Straková, T. Hájek, G. van Buiten, and Š. Angst. 2021b. Soil texture affects the coupling of litter decomposition and soil organic matter formation. *Soil Biol. Biochem.* 159(November 2020).

Bahri, H., M.F. Dignac, C. Rumpel, D.P. Rasse, C. Chenu, and A. Mariotti. 2006. Lignin turnover kinetics in an agricultural soil is monomer specific. *Soil Biol. Biochem.* 38(7): 1977–1988.

Bates, D.M. 2005. Fitting linear mixed models in R. *R News* 5(May): 27–30.

Batjes, N.H. 1994. Landmark papers. *Eur. J. Soil Sci.*

Bowman, M.M. 2021. Investigating the role of organo-mineral and organo-metal stabilization of soil organic matter using diverse organic matter sources and model soil B horizons. Available at TBD.

Button, E.S., J. Pett-Ridge, D. V. Murphy, Y. Kuzyakov, D.R. Chadwick, and D.L. Jones. 2022. Deep-C storage: Biological, chemical and physical strategies to enhance carbon stocks in agricultural subsoils. *Soil Biol. Biochem.* 170(February): 108697. Available at <https://doi.org/10.1016/j.soilbio.2022.108697>.

Campbell, J.L., C.T. Driscoll, J.A. Jones, E.R. Boose, H.A. Dugan, P.M. Groffman, C.R. Jackson, J.B. Jones, P. Glenn, N.R. Lottig, and J.K. Zimmerman. 2022. Forest and Freshwater Ecosystem Responses to Climate Change and Variability at US LTER Sites. *Biosci. - Spec. Sect. LTER Clim. Chang.* 72(9): 851–870.

Cotrufo, M.F., J.L. Soong, A.J. Horton, E.E. Campbell, M.L. Haddix, D.H. Wall, and W.J. Parton. 2015. Formation of soil organic matter via biochemical and physical pathways of litter mass loss. *Nat. Geosci.* 8(10): 776–779. Available at <http://www.nature.com/doi/10.1038/ngeo2520>.

Cotrufo, M.F., M.D. Wallenstein, C.M. Boot, K. Denef, and E. Paul. 2013. The Microbial Efficiency-Matrix Stabilization (MEMS) framework integrates plant litter decomposition with soil organic matter stabilization: do labile plant inputs

form stable soil organic matter? *Glob. Chang. Biol.* 19(4): 988–995. Available at <http://doi.wiley.com/10.1111/gcb.12113>.

Crow, S.E., T.R. Filley, M. McCormick, K. Szlávecz, D.E. Stott, D. Gamblin, and G. Conyers. 2009. Earthworms, stand age, and species composition interact to influence particulate organic matter chemistry during forest succession. *Biogeochemistry* 92(1–2): 61–82.

Dignac, M.-F., D. Derrien, P. Barré, S. Barot, L. Cécillon, C. Chenu, T. Chevalier, G.T. Freschet, P. Garnier, B. Guenet, M. Hedde, K. Klumpp, G. Lashermes, P.-A. Maron, N. Nunan, C. Roumet, and I. Basile-Doelsch. 2017. Increasing soil carbon storage: mechanisms, effects of agricultural practices and proxies. A review. *Agron. Sustain. Dev.* 37(2): 14. Available at <http://link.springer.com/10.1007/s13593-017-0421-2>.

Dungait, J. a J., D.W. Hopkins, A.S. Gregory, and A.P. Whitmore. 2012. Soil organic matter turnover is governed by accessibility not recalcitrance. *Glob. Chang. Biol.* 18(6): 1781–1796.

Feng, X., Y. Xu, R. Jaffé, W.H. Schlesinger, and M.J. Simpson. 2010. Turnover rates of hydrolysable aliphatic lipids in Duke Forest soils determined by compound specific <sup>13</sup>C isotopic analysis. *Org. Geochem.* 41(6): 573–579. Available at <http://dx.doi.org/10.1016/j.orggeochem.2010.02.013>.

Filley, T.R., G.D. Cody, B. Goodell, J. Jellison, C. Noser, and A. Ostrofsky. 2002. Lignin Demethylation and Polysaccharide Decomposition in Spruce Sapwood. *Org. Geochem.* 33: 111–124.

Goñi, M.A., and J.I. Hedges. 1990. Cutin-derived CuO reaction products from

purified cuticles and tree leaves. *Geochim. Cosmochim. Acta* 54: 3065–3072.

Goñi, M.A., N. Monacci, R. Gisewhite, J. Crockett, C. Nittrouer, A. Ogston, S.R. Alin, and R. Aalto. 2008. Terrigenous organic matter in sediments from the Fly River delta-clinoform system (Papua New Guinea). *J. Geophys. Res. Earth Surf.* 113(1). Available at <https://agupubs.onlinelibrary.wiley.com/doi/pdf/10.1029/2006JF000653>.

Goñi, M.A., and K.A. Thomas. 2000. Sources and transformations of organic matter in surface soils and sediments from a tidal estuary (North Inlet, South Carolina, USA). *Estuaries* 23(4): 548–564.

Gross, C.D., and R.B. Harrison. 2019. The Case for Digging Deeper: Soil Organic Carbon Storage, Dynamics, and Controls in Our Changing World. *Soil Syst.* 3(2): 28.

Hatten, J., and M. Goñi. 2016. Cupric Oxide (CuO) Oxidation Detects Pyrogenic Carbon in Burnt Organic Matter and Soils. *PLoS One* 11(3): e0151957 Available at <http://dx.plos.org/10.1371/journal.pone.0151957>.

Hatten, J., M. a. Goñi, and R. a. Wheatcroft. 2012. Chemical characteristics of particulate organic matter from a small, mountainous river system in the Oregon Coast Range, USA. *Biogeochemistry* 107: 43–66. Available at <http://link.springer.com/10.1007/s10533-010-9529-z>.

Heckman, K., C.E. Hicks Pries, C.R. Lawrence, C. Rasmussen, S.E. Crow, A.M. Hoyt, S.F. von Fromm, Z. Shi, S. Stoner, C. McGrath, J. Beem-Miller, A.A. Berhe, J.C. Blankinship, M. Keiluweit, E. Marín-Spiotta, J.G. Monroe, A.F. Plante, J. Schimel, C.A. Sierra, A. Thompson, and R. Wagai. 2022a. Beyond bulk: Density fractions explain heterogeneity in global soil carbon abundance and persistence.

Glob. Chang. Biol. 28(3): 1178–1196. Available at <https://doi.org/10.1111/gcb.16023>.

Heckman, K.A., L.E. Nave, M. Bowman, A. Gallo, J.A. Hatten, L.M. Matosziuk, A.R. Possinger, M. SanClements, B.D. Strahm, T.L. Weiglein, C. Rasmussen, and C.W. Swanston. 2020. Divergent controls on carbon concentration and persistence between forests and grasslands of the conterminous US. *Biogeochemistry* 0123456789. Available at <https://doi.org/10.1007/s10533-020-00725-z>.

Heckman, K.A., A.R. Possinger, B.D. Badgley, M.M. Bowman, A.C. Gallo, J.A. Hatten, L.E. Nave, M.D. SanClements, C.W. Swanston, T.L. Weiglein, W.R. Weider, and B.D. Strahm. 2022b. In Review: Moisture-driven divergence in mineral-associated soil carbon persistence. *Proc. Natl. Acad. Sci.*

Hedges, J.I., R.A. Blanchette, K. Weliky, and A.H. Devol. 1988. Effects of fungal degradation on the CuO oxidation products of lignin: A controlled laboratory study. *Geochim. Cosmochim. Acta* 52(11): 2717–2726.

Hedges, J.I., and D.C. Mann. 1979. The characterization of plant tissues by their lignin oxidation products. *Geochemica Cosmochim.* 43(2): 1803–1807.

Hofmann, A., H. Alexander, and M.W.I. Schmidt. 2006. Lignin degradation in arable soils: a 15-year time series.

Jackson, R.B., K. Lajtha, S.E. Crow, G. Hugelius, M.G. Kramer, and G. Piñeiro. 2017. The Ecology of Soil Carbon: Pools, Vulnerabilities, and Biotic and Abiotic Controls. *Annu. Rev. Ecol. Evol. Syst.* 48: 419–445.

Janzen, H.H., K.J. van Groenigen, D.S. Powlson, T. Schwinghamer, and J.W. van Groenigen. 2022. Photosynthetic limits on carbon sequestration in croplands. *Geoderma* 416(March): 115810. Available at <https://doi.org/10.1016/j.geoderma.2022.115810>.

Jones, J.A., and C.T. Driscoll. 2022. Long-Term Ecological Research on Ecosystem Responses to Climate Change. *Bioscience*: 1–13.

Kleber, M., K. Eusterhues, M. Keiluweit, C. Mikutta, R. Mikutta, and P.S. Nico. 2015. *Mineral-Organic Associations: Formation, Properties, and Relevance in Soil Environments*. Elsevier Ltd.

Kogel-Knabner, I. 2002. The macromolecular organic composition of plant and microbial residues as inputs to soil organic matter. *Soil Biol. Biochem.* 34: 139–162.

Kögel, I. 1986. Estimation and decomposition pattern of the lignin component in forest humus layers. *Soil Biol. Biochem.* 18(6): 589–594.

Lal, R. 2018. Digging deeper: A holistic perspective of factors affecting soil organic carbon sequestration in agroecosystems. *Glob. Chang. Biol.* 24(8): 3285–3301.

Lavallee, J.M., and R.T.C.E.A.P.M.F. Cotrufo. 2018. Incorporation of shoot versus root-derived  $^{13}\text{C}$  and  $^{15}\text{N}$  into mineral-associated organic matter fractions: results of a soil slurry incubation with dual-labelled plant material. *Biogeochemistry*. Available at <https://doi.org/10.1007/s10533-018-0428-z>.

Lavallee, J.M., J.L. Soong, and M.F. Cotrufo. 2019. Conceptualizing soil organic matter into particulate and mineral-associated forms to address global change in the 21st century. *Glob. Chang. Biol.* (July): 1–13.

Lehmann, J., C.M. Hansel, C. Kaiser, M. Kleber, K. Maher, S. Manzoni, N. Nunan, M. Reichstein, J.P. Schimel, M.S. Torn, W.R. Wieder, and I. Kögel-Knabner. 2020. Persistence of soil organic carbon caused by functional complexity. *Nat. Geosci.* 13(8): 529–534. Available at <http://dx.doi.org/10.1038/s41561-020-0612-3>.

Lehmann, J., and M. Kleber. 2015. The contentious nature of soil organic matter. *Nature* 528: 60–68.

Liang, C., W. Amelung, J. Lehmann, and M. Kästner. 2019. Quantitative assessment of microbial necromass contribution to soil organic matter. *Glob. Chang. Biol.* 25(11): 3578–3590.

Liang, C., J.P. Schimel, and J.D. Jastrow. 2017. The importance of anabolism in microbial control over soil carbon storage. *Nat. Microbiol.* 2(8).

Linger, J.G., D.R. Vardon, M.T. Guarnieri, E.M. Karp, G.B. Hunsinger, M.A. Franden, C.W. Johnson, G. Chupka, T.J. Strathmann, P.T. Pienkos, and G.T. Beckham. 2014. Lignin valorization through integrated biological funneling and chemical catalysis. *Proc. Natl. Acad. Sci. U. S. A.* 111(33): 12013–12018.

Loescher, H., E. Ayres, P. Duffy, H. Luo, and M. Brunke. 2014. Spatial Variation in Soil Properties among North American Ecosystems and Guidelines for Sampling Designs. *PLoS One* 9(1).

von Lützow, M., I. Kögel-Knabner, K. Ekschmitt, H. Flessa, G. Guggenberger, E. Matzner, and B. Marschner. 2007. SOM fractionation methods: Relevance to functional pools and to stabilization mechanisms. *Soil Biol. Biochem.* 39(9): 2183–2207. Available at <http://linkinghub.elsevier.com/retrieve/pii/S0038071707001125> (verified 17 January 2014).

Masoom, H., D. Courtier-Murias, H. Farooq, R. Soong, B.P. Kelleher, C. Zhang, W.E. Maas, M. Fey, R. Kumar, M. Monette, H.J. Stronks, M.J. Simpson, and A.J. Simpson. 2016. Soil Organic Matter in Its Native State: Unravelling the Most Complex Biomaterial on Earth. *Environ. Sci. Technol.* 50(4): 1670–1680. Available

at <http://pubs.acs.org/doi/abs/10.1021/acs.est.5b03410>.

Matosziuk, L.M., Y. Alleau, B.K. Kerns, J. Bailey, M.G. Johnson, and J.A. Hatten. 2019. Effects of season and interval of prescribed burns on pyrogenic carbon in ponderosa pine stands in the southern Blue Mountains, Oregon, USA. *Geoderma* 348(December 2018): 1–11.

Matosziuk, L.M., A. Gallo, J. Hatten, K.D. Bladon, D. Ruud, M. Bowman, J. Egan, K. Heckman, M. SanClements, B. Strahm, and T. Weiglein. 2020. Short-Term Effects of Recent Fire on the Production and Translocation of Pyrogenic Carbon in Great Smoky Mountains National Park. *Front. For. Glob. Chang.* 3(February): 1–15. Available at <https://www.frontiersin.org/article/10.3389/ffgc.2020.00006/full>.

McKnight, D.M., E.W. Boyer, P.K. Westerhoff, P.T. Doran, T. Kulbe, and D.T. Andersen. 2001. Spectrofluorometric characterization of dissolved organic matter for indication of precursor organic material and aromaticity. *Limnol. Oceanogr.* 46(1): 38–48.

Meentemeyer, V. 1978. Macroclimate the Lignin Control of Litter Decomposition Rates. *Ecology* 59(3): 465–472.

Nave, L.E., M. Bowman, A. Gallo, J.A. Hatten, K.A. Heckman, L. Matosziuk, A.R. Possinger, M. SanClements, J. Sanderman, B.D. Strahm, T.L. Weiglein, and C.W. Swanston. 2021. Patterns and predictors of soil organic carbon storage across a continental-scale network. *Biogeochemistry* 9. Available at <https://doi.org/10.1007/s10533-020-00745-9>.

Nave, L.E., A. Covarrubias Ornelas, P.E. Drevnick, A. Gallo, J.A. Hatten, K.A. Heckman, L. Matosziuk, M. Sanclements, B.D. Strahm, T.J. Veverica, T.L. Weiglein,

and C.W. Swanston. 2019. Carbon-Mercury Interactions in Spodosols Assessed through Density Fractionation, Radiocarbon Analysis, and Soil Survey Information. *Soil Sci. Soc. Am. J.* 83(1): 190–202.

ORNL DAAC (Oak Ridge National Lab Distributed Active Archive Center). 2018. MODIS and VIIRS Land Products Fixed Sites Subsetting and Visualization Tool. (31 January 2020).

Pinheiro J, B. D, D. S, S. D, and R Core Team. 2014. nlme: Linear and Nonlinear Mixed Effects Models. R package(2015).

Possinger, A.R., K.A. Heckman, M.M. Bowman, A.C. Gallo, J.A. Hatten, L.M. Matosziuk, L.E. Nave, M.D. Sanclements, C.W. Swanston, T.L. Weiglein, B.D. Strahm, and U.F. Service. 2022. Lignin and fungal abundance modify manganese effects on soil organic carbon persistence at the continental scale. *Geoderma* 425(June): 116070. Available at <https://doi.org/10.1016/j.geoderma.2022.116070>.

Possinger, A.R., T.L. Weiglein, M.M. Bowman, A.C. Gallo, J.A. Hatten, K.A. Heckman, L.M. Matosziuk, L.E. Nave, M.D. Sanclements, C.W. Swanston, and B.D. Strahm. 2021. Climate Effects on Subsoil Carbon Loss Mediated by Soil Chemistry. *Environ. Sci. Technol.*

R Core Team. 2022. R Core Team 2021 R: A language and environment for statistical computing. R foundation for statistical computing. <https://www.R-project.org/>. *R Found. Stat. Comput.* 2: 2019.

Rasmussen, C., K. Heckman, W.R. Wieder, M. Keiluweit, C.R. Lawrence, A. Asefaw, J.C. Blankinship, S.E. Crow, J.L. Druhan, C.E. Hicks, J.P. Schimel, E.M. Alain, and F.P. Christina. 2018. Beyond clay: towards an improved set of variables

for predicting soil organic matter content. *Biogeochem. Lett.*

Rasse, D.P., C. Rumpel, and M.F. Dignac. 2005. Is soil carbon mostly root carbon? Mechanisms for a specific stabilisation. *Plant Soil* 269(1–2): 341–356.

Rhymes, J., I. Cordero, M. Chomel, J. Lavallee, A. Straathof, D. Ashworth, H. Langridge, M. Semchenko, F. de Vries, D. Johnson, and R. Bardgett. 2020. Are researchers following best storage practices for measuring soil biochemical properties? *SOIL Discuss.* (3): 1–15.

Rooney, E.C., V.L. Bailey, K.F. Patel, M. Dragila, A.K. Battu, A.C. Buchko, A.C. Gallo, J. Hatten, A.R. Possinger, O. Qafoku, L.R. Reno, M. SanClements, T. Varga, and R.A. Lybrand. 2022. Soil pore network response to freeze-thaw cycles in permafrost aggregates. *Geoderma* 411: 115674. Available at <https://doi.org/10.1016/j.geoderma.2021.115674>.

Rumpel, C., K. Eusterhues, and I. Kögel-Knabner. 2004. Location and chemical composition of stabilized organic carbon in topsoil and subsoil horizons of two acid forest soils. *Soil Biol. Biochem.* 36: 177–190.

Running, S., Q. Mu, and M. Zhao. 2022. MODIS. MOD17A3H MODIS/Terra Net Prim. Prod. Yrly. L4 Glob. 500m SIN Grid V006 NASA EOSDI

SANCLEMENTS, M., R.H. LEE, E. AYRES, K. GOODMAN, M. JONES, D. DURDEN, K. THIBAUT, R. ZULUETA, J. ROBERTI, C. LUNCH, and A. GALLO. 2020. Collaborating with NEON. *Bioscience* 70(2): 2020.

Scharlemann, J.P.W., E.V.J. Tanner, R. Hiederer, and V. Kapos. 2014. Global soil carbon: Understanding and managing the largest terrestrial carbon pool. *Carbon Manag.* 5(1): 81–91.

Schmidt, M.W.I., M.S. Torn, S. Abiven, T. Dittmar, G. Guggenberger, I. a

Janssens, M. Kleber, I. Kögel-Knabner, J. Lehmann, D. a C. Manning, P. Nannipieri, D.P. Rasse, S. Weiner, and S.E. Trumbore. 2011. Persistence of soil organic matter as an ecosystem property. *Nature* 478(7367): 49–56 Available at <http://www.ncbi.nlm.nih.gov/pubmed/21> (verified 6 November 2013).

Schoeneberger, P.J., D.A. Wysocki, and E.C. Benham. 2012. *Field Book for Describing and Sampling Soils*. Natl. Soil Surv. Cent. 3.0.

Schrumpf, M., K. Kaiser, G. Guggenberger, T. Persson, I. Kögel-Knabner, and E.D. Schulze. 2013. Storage and stability of organic carbon in soils as related to depth, occlusion within aggregates, and attachment to minerals. *Biogeosciences* 10(3): 1675–1691.

Sierra, C.A., A.M. Hoyt, Y. He, and S.E. Trumbore. 2018. Soil Organic Matter Persistence as a Stochastic Process: Age and Transit Time Distributions of Carbon in Soils. *Global Biogeochem. Cycles* 32(10): 1574–1588.

Sierra, C.A., M. Müller, H. Metzler, S. Manzoni, and S.E. Trumbore. 2017. The muddle of ages, turnover, transit, and residence times in the carbon cycle. *Glob. Chang. Biol.* 23(5): 1763–1773.

Six, J., R.T. Conant, E. a Paul, and K. Paustian. 2002. Stabilization mechanisms of soil organic matter: Implications for C-saturatin of soils. *Plant Soil* 241: 155–176.

Sokol, N.W., and M.A. Bradford. 2019. Microbial formation of stable soil carbon is more efficient from belowground than aboveground input. *Nat. Geosci.* 12(1): 46–53 Available at <http://dx.doi.org/10.1038/s41561-018-0258-6>.

Sokol, N.W., S.E. Kuebbing, E. Karlsen-Ayala, and M.A. Bradford. 2018. Evidence for the primacy of living root inputs, not root or shoot litter, in forming soil

organic carbon. *New Phytol.* Available at <http://doi.wiley.com/10.1111/nph.15361>.

Sollins, P., M.G. Kramer, C. Swanston, K. Lajtha, T. Filley, A.K. Aufdenkampe, R. Wagai, and R.D. Bowden. 2009. Sequential density fractionation across soils of contrasting mineralogy: evidence for both microbial- and mineral-controlled soil organic matter stabilization. *Biogeochemistry* 96(1–3): 209–231 Available at <http://link.springer.com/10.1009-9359-z> (verified 18 October 2013).

Strid, A., B.S. Lee, and K. Lajtha. 2016. Homogenization of detrital leachate in an old-growth coniferous forest, OR: DOC fluorescence signatures in soils undergoing long-term litter manipulations. *Plant Soil* 408(1–2): 133–148 Available at <http://dx.doi.org/10.1007/s11104-016-2914-1>.

Thevenot, M., M.-F. Dignac, and C. Rumpel. 2010. Fate of lignins in soils: A review. *Soil Biol. Biochem.* 42(8): 1200–1211 Available at [http://linkinghub.elsevier.com/retrieve/pii/S0038-0717\(10\)00100-0](http://linkinghub.elsevier.com/retrieve/pii/S0038-0717(10)00100-0) (verified 16 July 2014).

Thorpe, A.S., D.T. Barnett, S.C. Elmendorf, E.L.S. Hinckley, D. Hoekman, K.D. Jones, K.E. Levan, C.L. Meier, L.F. Stanish, and K.M. Thibault. 2016. Introduction to the sampling designs of the National Ecological Observatory Network Terrestrial Observation System. *Ecosphere* 7(12): 1–11. Wang, T., A. Hamann, D.L. Spittlehouse, and T.Q. Murdock. 2012. ClimateWNA-high-resolution spatial climate data for western North America. *J. Appl. Meteorol. Climatol.* 51(1): 16–29.

Weiglein, T.L., B.D. Strahm, M.M. Bowman, A.C. Gallo, J.A. Hatten, K.A. Heckman, L.M. Matosziuk, L.E. Nave, A.R. Possinger, M.D. SanClements, and C.W. Swanston. 2021. Key predictors of soil organic matter vulnerability to mineralization differ with depth at a continental scale. *Biogeochemistry* 0123456789 Available at

<https://doi.org/10.1007/s10533-021-00856-x>.

Wendt, J.W., and S. Hauser. 2013. An equivalent soil mass procedure for monitoring soil organic carbon in multiple soil layers. *Eur. J. Soil Sci.* 64(1): 58–65.

Whalen, E.D., A.S. Grandy, N.W. Sokol, M. Keiluweit, J. Ernakovich, R.G. Smith, and S.D. Frey. 2022. Clarifying the evidence for microbial- and plant-derived soil organic matter, and the path towards a more quantitative understanding. *Glob. Chang. Biol.*: 0–2.

Whittaker, R.H. 1970. *Communities and Ecosystems*. Macmillan, New York.

Yost, J.L., and A.E. Hartemink. 2020. How deep is the soil studied – an analysis of four soil science journals. *Plant Soil* 452(1–2): 5–18.

Zurr, A., E. Ieno, N. Walker, A. Saveliev, and G. Smith. 2008. *Mixed Effects Models and Extensions in ecology with R* (M Gail, K Krickeberg, J Samet, A Tsaitis, and W Wong, Eds.). 1st ed. Springer, New York.

Chapter 4: Assessing the biochemical relationships between litter  
endmembers, surface horizons, and the ability to predict deep soil  
characteristics across the National Ecological Observatory Network  
(NEON)

Adrian C. Gallo

Expected Co-Authors: Yvan Alleau, Maggie Bowman, Kate Heckman, Lauren  
Matosziuk, Luke Nave, Angela Possinger, Mike SanClements, Brian Strahm, Tyler  
Weiglein, Jeff Hatten

Expected Co-Authors: Yvan Alleau, Maggie Bowman, Kate Heckman, Lauren  
Matosziuk, Luke Nave, Angela Possinger, Mike SanClements, Brian Strahm, Tyler  
Weiglein, Jeff Hatten

## 4.1 Abstract

We leveraged the installation of the National Ecological Observatory Network (NEON) to collect soils from the widest range of biomes to a depth of soil refusal, often reaching one-meter or more in depth. Using the Cupric Oxidation (CuO) method for three distinct soil horizons, and the dominant aboveground vegetation and belowground roots as organic matter (OM) endmembers, we examined the soil OM characteristics to determine the relative OM similarity between soils and their plant communities. To better leverage the  $\approx 70$  unique compounds identified by the CuO method, we used the Bray-Curtis ecological dissimilarity index to compare sample types. We find exactly half of A-horizons favor a root-derived SOM composition, and the remaining favoring an aboveground vegetation signal. Between the soil-only Bray-Curtis comparisons, we find upper vs lower B-horizons to have the greatest overlap in SOM composition, and A vs lower B-horizons to have the greatest SOM dissimilarity. However, there were no generalizable patterns as to which ecosystems, or biotic or abiotic factors that produced these patterns. This could be attributed to the very low Bray-Curtis values we calculated (generally  $< 0.2$ ), such that all A-horizon vs endmember comparisons are uniformly [dis]similar. Or that the CuO method prioritizes extracting plant-derived OM, thus microbial compounds are not sufficiently contributing to our observations and potentially deflating the unique nature of SOM across these NEON sites. We encourage more researchers to both dig deeper, and to conduct analysis that would capture both plant and microbially derived compounds to better understand the sources of soil organic matter across ecosystems and down soil profiles.

## 4.2 Introduction

Soils are integrators of past and present climates, geologies, and plant communities (Jenny, 1941). Soil carbon stores have been subject to losses following human agriculture activities (Sanderman et al., 2017), deforestation (Drake et al., 2019), industrial timber management (James and Harrison, 2016; Mayer et al., 2020), and many other natural disasters (Nave et al., 2011). Conversely, humans' large terrestrial footprint also provides an opportunity to increase soil carbon stores as a result of targeted agricultural management practices (Minasny et al., 2017; Lal, 2018), afforestation of degraded lands (Nave et al., 2013), and with a large potential in global reforestation activities to positively impact soil carbon stores (Nave et al., 2018). These management practices are not without their functional limitations (Poulton et al., 2018; Fleischman et al., 2020; Schlesinger, 2022), nutrient stoichiometric dilemmas (van Groenigen et al., 2006; van Groenigen et al., 2017), political hurdles (Sultana and Loftus, 2020; Fleischman 2021), or practical constraints to increase soil carbon stores (van Groenigen, 2018; Schlesinger and Amundson, 2019; Amundson et al., 2022). However, there is little doubt that on a human timescale we have lost soil organic matter on a scale relevant to climate mitigation aims that we naturally ask which organic matter sources are left in soils, and which plants have added the most carbon to soils?

Globally, the top 1 m of soil holds more carbon than the atmospheric and terrestrial vegetation pools combined, with more than half of the carbon below 30 cm (Batjes, 2014; Lal, 2018). Unfortunately, few studies focus on tracing carbon into deeper soil horizons (Dungait et al., 2012; Gregory et al., 2014), with other re-

searchers emphasizing the need for deep soil characterization (Gross and Harrison, 2019). With the advent of digital soil mapping and quantitative pedology techniques, we have the ability to map with some level of precision the soil processes that will produce unique soil types across landscapes (Ma et al., 2019). While this is essential to better understand the abiotic soil processes, we lack a similar ability to predict soil organic matter patterns across the landscape necessary for optimizing land management recommendations. There are multiple knowledge gaps that are present: a lack of consistent sampling methodology across wide bioclimatic regimes, a lack of deep soil collection, and a dearth of SOM characterization data available at either scale necessary for predicting ecosystem responses to ongoing climate change. As we expect land-uses to shift considerably in the near future (Lambin and Meyfroidy, 2011), the sources of organic matter that built up in soils over the holocene period are likely to shift in plant species and total quantity. Therefore it is essential to begin to develop procedures that will aid in the prediction of deep SOM characteristics from surface characteristics that are more easily obtained.

The primary objective of this manuscript is to evaluate the relative similarity of CuO extracted OM between vegetation, root, and bulk mineral soil samples. Our two questions will focus on (1) whether A-horizons have a SOM signature that is closer to either the dominant aboveground vegetation or the belowground roots and (2) whether upper and lower B-horizon SOM characteristics are simply diluted A-horizons. We hypothesized that A-horizons would have more similarity in their organic matter composition to aboveground vegetation due to the proximity of those inputs, and that aboveground vegetation may dilute the root-derived organic matter

signal. Furthermore, we expected A and upper B-horizons to be more similar due to their proximity and often physical connection in the soil profile, and that lower B-horizons would have the largest dissimilarity to either above horizons due to their physical distance and from a lack of above and belowground inputs.

## 4.3 Methods

### 4.3.1 Site description, design, and sampling

A full description of sample acquisition and processing can be found in the second chapter of this dissertation, and in Supplemental Materials. Briefly, we acquired soil cores and the dominant aboveground vegetation samples from the NEON terrestrial sites. Vegetation samples were homogenized, coarse ground, then ground to a fine powder. Individual soil cores were first described (Schoeneberger et al., 2012), then composited based on common genetic horizons that represent the A-horizon, upper most illuvial horizon (upper B-horizon), and the deepest B-horizon (lower B-horizon). The average midpoint depths for A, upper and lower B-horizons studied are 14.3, 72.8, and 109.0 cm (Supplementary Materials). Samples were combined, air dried, sieved and root picked, then homogenized and ground for analysis. Root sample collection required approximately 3 grams of dry material for processing, thus not all sites have available root samples for analysis. As described by Possinger et al. (2022), we obtained the mean annual temperature (MAT) and a Hargreaves reference evaporation (MAP-Eref) from the ClimateNA-MAP database (Wang et al., 2012). We use MAP-Eref as our “moisture availability” index in our modeling efforts which

helps to incorporate abiotic and biotic factors more holistically.

### 4.3.2 Cupric oxidation (CuO) procedures

Both Weiglein et al (2021) and Heckman et al (2020) briefly describe the cupric oxidation (CuO) method, with additional details available in Chapter 2 of this dissertation. Briefly, we used the CuO procedure to identify biomarkers that allow us to trace the sources of soil organic matter, especially from unique plant-tissue components (Hedges and Mann 1979). The procedure was originally developed by Hedges and Ertel (1982), modified by Goñi and Hedges (1992), and finally refined into our current working method by Goñi and Montgomery (2000). Due to practical constraints, CuO analysis was conducted on the three representative mineral horizons per site, the dominant aboveground vegetation, and belowground root samples when available.

The CuO procedure returns approximately 72 unique and quantifiable compounds, with others that are not quantified. For calculating the organic matter dissimilarity index (see below), each compound was retained in its original form without grouping. For easier interpretation of figures, standard groupings of compounds were conducted. These include: lignin (including the sum of vanillyl, syringyl, and cinnamyl phenols) (Hedges and Mann 1979, Hatten et al., 2012), cutin (16-hydroxyhexadecanoic acid, 9,16 and 10,16-dihydroxyhexadecanoic acid, 8-hydroxyhexadecandioic acid) (Goñi and Hedges, 1990; Crow et al., 2009), suberin (hexadecane-1,16-dioic acid, 18-hydroxyoctadec-9-enoic acid, hexadecanedioic acid and  $\omega$ -hydroxyoctadecenoic acid)

(Crow et al., 2009), 3,5-dihydroxybenzoic acid (Goñi and Hedges, 1995), C16 to C18 hydroxy fatty acids (including hydroxyhexadecanedioic acid, dihydroxyhexadecanoic acid, and trihydroxyoctadecanoic acid) (Hatten and Goñi 2012, Goñi and Hedges, 1995; Goñi and Hedges, 1990), and non-lignin para-phenols that are designated with the letter P (the sum of p-hydroxybenzaldehyde, p-hydroxyacetophenone, p-hydroxybenzoic acid) (Goñi et al., 2008). The remaining compounds that are not quantified were classified into the “Other” compound category. Illustrations of these lignin structures can be found in Hedges and Blanchette, et al (1988), and non-lignin structures can be found in Goñi and Thomas (2000) and Kogel-Knabner (2002).

### 4.3.3 Bray-Curtis Statistics

In order to better accommodate the numerous compounds produced in the CuO method, we identified Bray-Curtis ecological dissimilarity index to compare the composition of organic matter between sites and sample types (Bray and Curtis, 1957; Greenacre, 2018). There are two strengths of this method. First, it is relatively insensitive to zeros in the data set (e.g. if no plant was identified in the plot, it is not overweighted to skew the dissimilarity index). Second, it accounts for the presence and abundance of the entity in question to determine the amount of dissimilarity between samples (e.g. identifying 50 plants compared to 5 plants has a unique effect). The primary assumption for the Bray-Curtis method requires compound abundances from similarly sized samples. In the ecological context, this often requires normalizing the site area. For example, plant community surveys must have similarly sized

plots, or bird count data requires time of observation to be controlled. For this application, we normalized each unique CuO compound to the total CuO extracted for the sample. We do not reach 100% proportion, because there are some compounds that are not identified or quantified, although it is typically less than 4% of the total sample. This is a non-Euclidean statistical ecological tool, thus we refrain from using ‘distances’ in this manuscript. The Bray-Curtis dissimilarity index is calculated:

$$BC_{ij} = 1 - \frac{2C_{ij}}{T_i + T_j}$$

Where  $C_{ij}$  is the sum of the lesser CuO compound abundances only for the compounds that are shared between both samples.  $T_i$  and  $T_j$  are the total number of compound abundances identified in both samples. The Bray-Curtis dissimilarity values are between 0 and 1, where smaller values indicate less dissimilarity in compound abundances between samples, and larger values indicate greater dissimilarity. All statistical analysis was conducted in R (v.4.0.3) in RStudio (v2022.07.1+554), with vegan package used for Bray-Curtis calculations (Oksanen et al., 2020), and base R (Bates, 2005; Zurr et al., 2008; Pinheiro et al., 2014; R Core Team, 2020).

## 4.4 Results

### 4.4.1 Endmember organic matter composition

We find lignin contributions to the dominant aboveground vegetation and roots to be nearly equal to each other (Figure 4.1). Of the ten grouped compound classes,

the “Other” category generally contributes the greatest to the total CuO extracted sample. The range of lignin contributions for vegetation was between 18 to 38%, and for roots it was 15 to 40%.

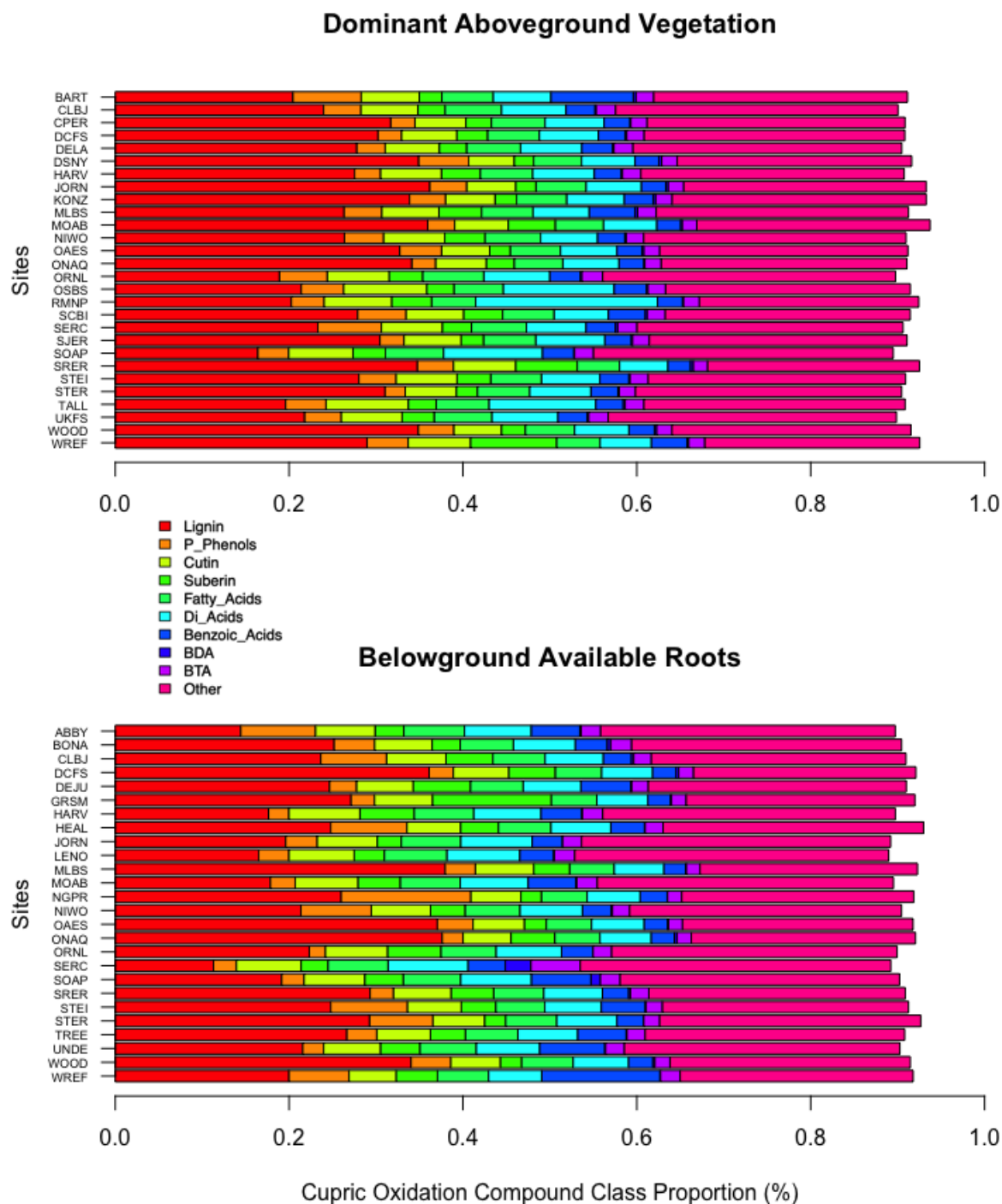


Figure 4.1: Proportion of cupric oxidation (CuO) extracted compound classes in available vegetation and root samples across the National Ecological Observatory Network. Individual CuO products ( $n=72$ ) are normalized to the total extracted material within each sample, and are grouped according to broad compound class. Abbreviations: P Phenols - para-hydroxybenzoic acid phenols; BDA - benzenedicarboxylic acids, BTA - benzenetricarboxylic acids.

#### 4.4.2 Soil organic matter composition

We find lignin contributions to the total SOM composition to decrease with depth, and rarely exceeding 18% (Figure 4.2). Across all three mineral soil depths, both cutin and suberin classes make up a larger proportion of OM pool compared to either vegetation or root samples. As depth of horizon increases, the proportion of “other” category increases from  $\approx 40\%$  in the A-horizon to over 50% in the lower B-horizon.

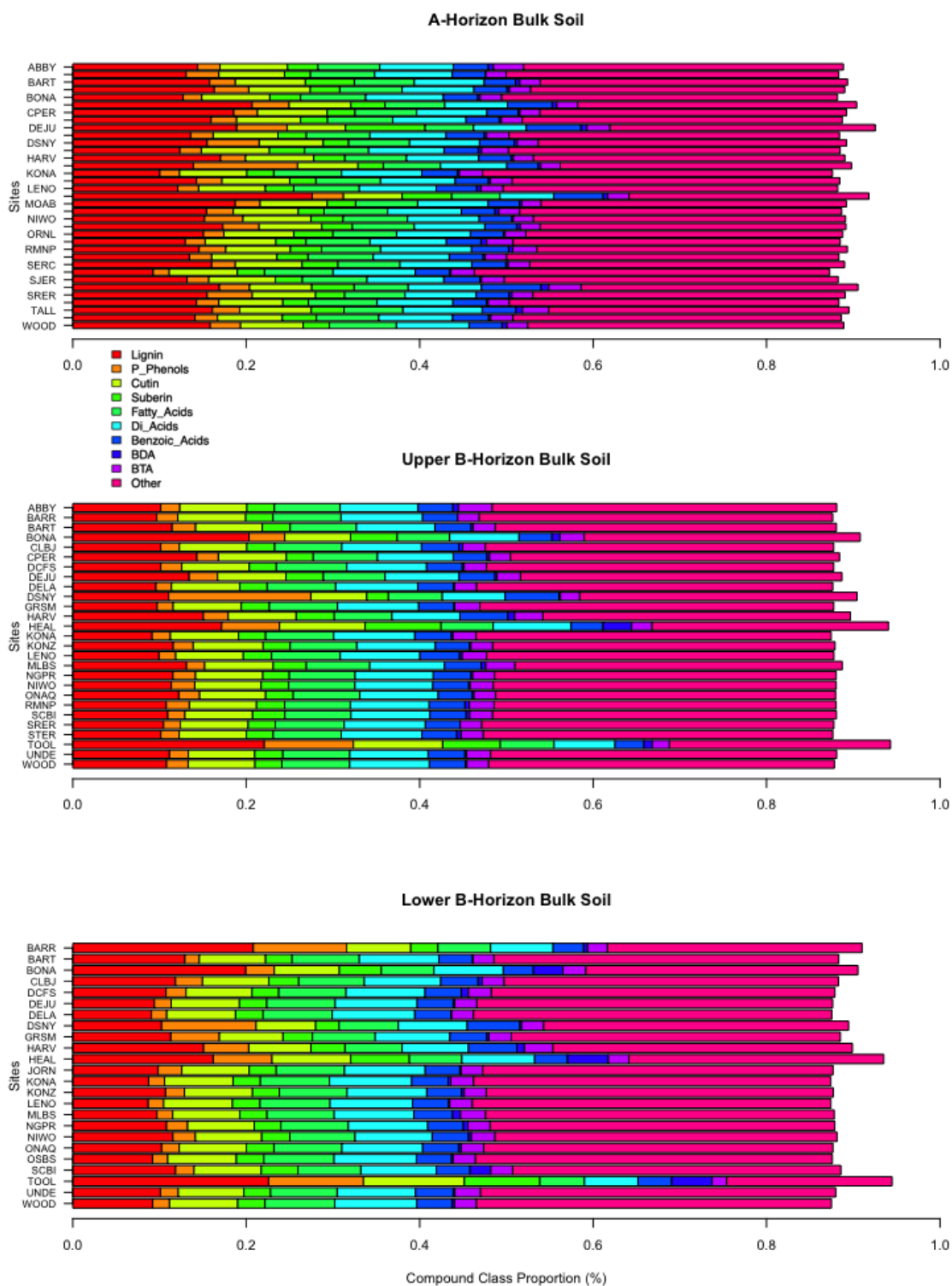


Figure 4.2: Proportion of cupric oxidation (CuO) extracted compound classes in available A-horizon, upper B-horizon, and lower B-horizons across the National Ecological Observatory Network. Individual CuO products ( $n=72$ ) are normalized to the total extracted material within each sample, and are grouped according to broad compound class. Abbreviations: P Phenols - para-hydroxybenzoic acid phenols; BDA - benzenedicarboxylic acids, BTA - benzenetricarboxylic acids.

### 4.4.3 Average Bray-Curtis dissimilarity index

Bray-Curtis values show the average dissimilarity between all vegetation and roots (0.178) to be nearly equal to the relative dissimilarity between either vegetation and A-horizons (0.159) or roots and A-horizons (0.184) (Table 4.1). The greatest similarity between any average endmember or average soil horizon comparisons was the within-root dissimilarity (0.222). There is nearly as much overlapping organic matter characteristics between the all vegetation average (0.132), and the vegetation vs A-horizon (0.159).

Within-soil horizon average dissimilarity values indicate A-horizons have the greatest similarity to each other across sites (0.083), with an nearly identical result for upper B-horizons (0.084) (Table 4.2). There was increasing dissimilarity as soil depth increased. The greatest dissimilarity values for averaged soil horizons are between A vs lower B horizon (0.110), and the within-horizon dissimilarity of all lower B-horizons (0.110).

	Vegetation	Root	A-Horizon
Vegetation	0.132	0.178	0.159
Root	0.178	0.222	0.184
A-Horizon	0.159	0.184	0.084

Table 4.1: Average Bray-Curtis ecological dissimilarity values for grouped organic matter endmembers and A-horizon soils from the National Ecological Observatory Network. Smaller values (closer to 0) indicate samples have less dissimilarity and share more organic matter composition abundances with each other, larger values (closer to 1) indicate samples have greater dissimilarity. Diagonals represent the dissimilarity *within* each sample class.

	A-Horizon	Upper B-Horizon	Lower B-Horizon
A-Horizon	0.083	0.096	0.110
Upper B-Horizon	0.096	0.084	0.096
Lower B-Horizon	0.110	0.096	0.110

Table 4.2: Average Bray-Curtis ecological dissimilarity values for grouped A-horizon, upper B-horizon, and lower B-horizon soils from the National Ecological Observatory Network. Smaller values (closer to 0) indicate samples have less dissimilarity and share more organic matter composition abundances with each other, larger values (closer to 1) indicate samples have greater dissimilarity. Diagonals represent the dissimilarity *within* each sample class.

#### 4.4.4 Unique within-site Bray-Curtis dissimilarity index

Generally we find very low Bray-Curtis values for any of the three endmember comparisons (A vs vegetation, A vs root, vegetation vs root), indicating the organic matter composition across all three sample types are relatively uniform (Table 4.3). Exactly half of the sites with available endmembers show A-horizon are more similar to vegetation, with the remaining half favoring a root OM signal. Most dissimilarity values are between 0.1 and 0.2, but the largest values (0.685) are driven by a vegetation sample (STER) comparison. We find even smaller Bray-Curtis values for soil horizon comparisons (A vs upper B, A vs lower B, upper vs lower B-horizons) (Table 4.4). Most values are between 0.05 and 0.1, with the greatest dissimilarity values comparing DEJU A vs lower B-horizons (0.292).

Site	A-Horizon vs Vegetation	A-Horizon vs Root	Vegetation vs Root
CLBJ	0.086	0.119	0.083
DCFS	0.152	0.240	0.099
HARV	0.119	0.076	0.108
JORN	0.243	0.117	0.184
MLBS	0.175	0.181	0.140
MOAB	0.188	0.175	0.188
NIWO	0.147	0.109	0.101
ONAQ	0.171	0.219	0.080
ORNL	0.094	0.094	0.094
SERC	0.181	0.140	0.181
SOAP	0.076	0.104	0.100
SRER	0.108	0.252	0.108
STER	0.685	0.169	0.685
WOOD	0.042	0.219	0.042

Table 4.3: Unique Bray-Curtis ecological dissimilarity values for all available organic matter endmembers and A-horizon soils from the National Ecological Observatory Network. Smaller values (closer to 0) indicate samples have less dissimilarity and share more organic matter composition abundances with each other, larger values (closer to 1) indicate samples have greater dissimilarity. Only sites with all three sample types are presented.

#### 4.4.5 Bray-Curtis relationship with climatic factors

We also examined the potential relationship between climatic factors and its influence on SOM compositional overlap between endmembers and other soil horizons. We

were unable to identify any consistent relationships between abiotic (MAP, MAT moisture availability) or biotic (NPP, root biomass) factors that explained the A-horizon dissimilarity between either vegetation or root endmembers (Figure 4.3). At the coarse scale, A-horizons from temperate seasonal forests (ORNL, HARV, SERC) tended to favor a more root-derived OM signature, although one seasonal forest (MLBS) favored the vegetation endmember. Woodland and shrubland A-horizons tended to favor vegetation organic matter composition (CLBJ, WOOD, SOAP, DCFS), but one favored a root signature (STER). Comparing only mineral soils to each other yielded similar results, we were unable to identify a generalizable abiotic or biotic factor that helped to explain the dissimilarity distributions in CuO extracted SOM (Figure 4.4).

Site	A vs Upper B-Horizon	A vs Lower B-Horizon	Upper vs Lower B-Horizon
ABBY	0.057	-	-
BARR	0.049	0.167	0.213
BART	0.083	0.117	0.045
BONA	0.150	0.146	0.048
CLBJ	0.157	0.127	0.034
CPER	0.054	-	-
DCFS	0.065	0.062	0.015
DEJU	0.222	0.292	0.076
DELA	0.057	0.063	0.007
GRSM	0.055	0.039	0.055
HARV	0.062	0.079	0.042
HEAL	-	-	0.092
JORN	-	0.139	-
KONA	0.012	0.018	0.010
KONZ	0.036	0.047	0.013
LENO	0.031	0.054	0.026
MLBS	0.202	0.248	0.056
NGPR	0.047	0.056	0.016
NIWO	0.071	0.069	0.009
ONAQ	0.078	0.102	0.025
OSBS	-	0.067	-
RMNP	0.081	-	-
SCBI	0.031	0.035	0.039
SRER	0.096	-	-
STER	0.050	-	-
TOOL	-	-	0.207
UNDE	0.049	0.060	0.015
WOOD	0.069	0.090	0.025

Table 4.4: Unique Bray-Curtis ecological dissimilarity values for all available A-horizon, upper B-horizon, and lower B-horizon soils from the National Ecological Observatory Network. Smaller values (closer to 0) indicate samples have less dissimilarity and share more organic matter composition abundances with each other, larger values (closer to 1) indicate samples have greater dissimilarity. Only sites with at least two sample types are presented.

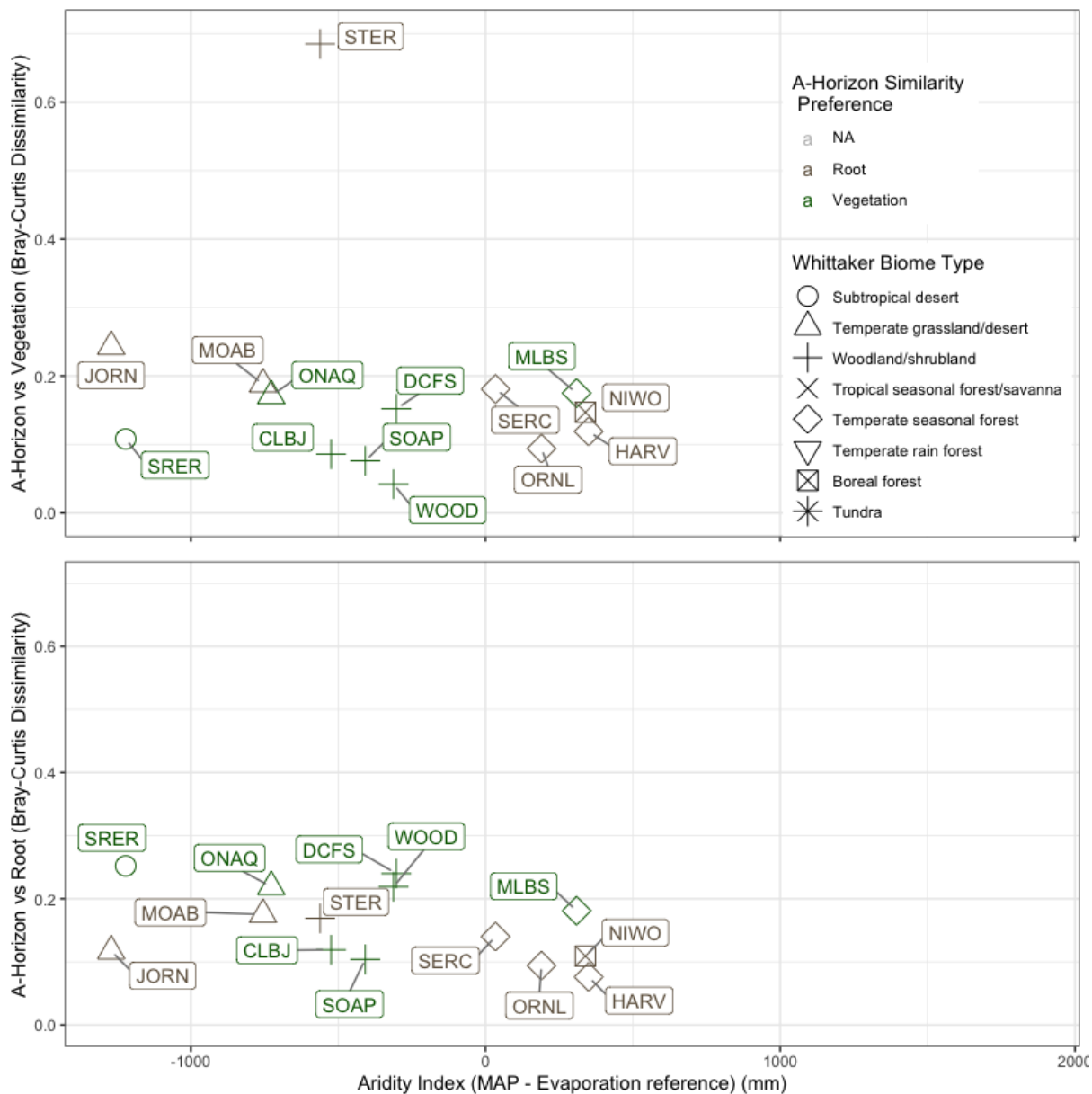


Figure 4.3: Unique Bray-Curtis ecological dissimilarity values for all available organic matter endmembers and A-horizon soils from the National Ecological Observatory Network. Smaller values (closer to 0) indicate samples have less dissimilarity and share more organic matter composition abundances with each other, larger values (closer to 1) indicate samples have greater dissimilarity. Only sites with all three sample types are presented. A-horizon similarity preference is determined by comparing the Bray-Curtis index of A vs Root and A vs Vegetation samples within each site.

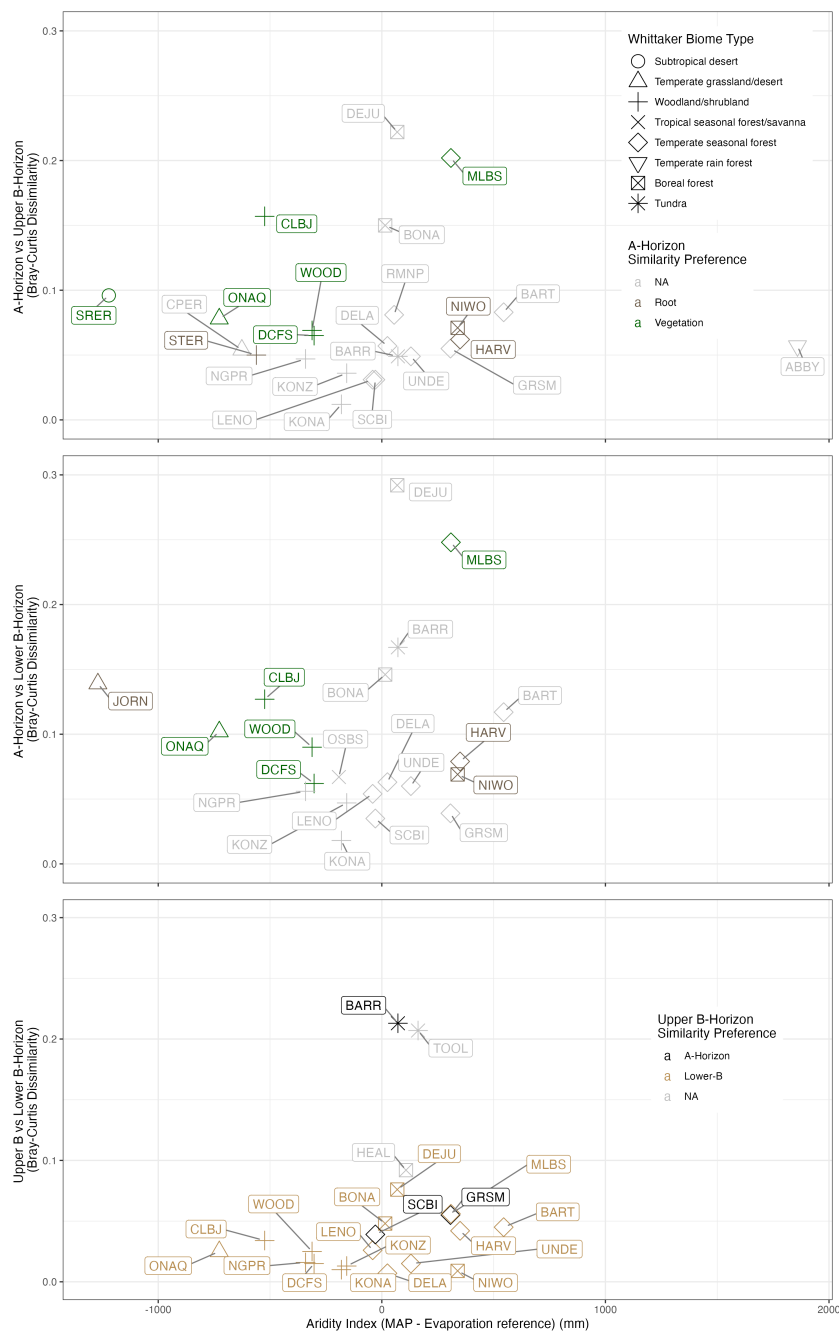


Figure 4.4: Unique Bray-Curtis ecological dissimilarity values for all available A, Upper, and Lower B-horizon soils from the National Ecological Observatory Network. Smaller values (closer to 0) indicate samples have less dissimilarity and share more organic matter composition abundances with each other, larger values (closer to 1) indicate samples have greater dissimilarity. Only sites with all three sample types are presented. A-horizon and B-horizon similarity preferences are determined by comparing the Bray-Curtis index of each endmember and soil sample type.

## 4.5 Discussion

We sought to rectify the knowledge gaps in both deep soil SOM characterization and how they relate to surface organic matter inputs. Despite a wide range of plant community types, root phenology, and soil forming factors present at these NEON sites, we generally find the CuO extracted organic matter composition across all samples and their associated soils to be relatively uniform.

We hypothesized that A-horizons would have greater similarity to the dominant aboveground vegetation; we find evidence to support this from the all-horizon average Bray-Curtis analysis (Table 4.1). However, within each site, we find many examples of A-horizon SOM to reflect a more root-derived composition (e.g. HARV, JORN, MOAB, NIWO, SERC, STER) (Table 4.2). Indeed, exactly 50% of the sites (7/14) with available samples (vegetation, roots, A-horizons) presented A-horizons with greater similarity to roots than aboveground, with the remaining half favoring vegetation. This illustrates the importance of site-specificity and limits and broadly generalizable patterns.

We also hypothesized that, due to their physical proximity, A and upper B-horizons would be more similar compared to any lower B-horizon. We find strong evidence to support this from both the all-horizon averages (Table 4.2), and within site Bray-Curtis values (Table 4.4). The average Bray-Curtis dissimilarity between A and upper B-horizons is low (indicating substantial overlapping SOM composition abundances), and less than 25% of any individual site deviated from this pattern (Table 4.4). Further supporting our second hypothesis, the majority (64%) of upper vs lower B-horizons are more dissimilar to each other compared to A vs upper B-

horizons (Table 4.4).

#### 4.5.1 A-horizon SOM signature relative to endmembers

Despite half of A-horizon SOM favoring roots, and the other half favoring vegetation, we were unable to identify any systematic mechanisms for these patterns. We expected grassland sites, due to their higher belowground biomass production compared to forests, to produce soils with greater overlap to root endmembers. Although we were unable to obtain all root samples from grassland sites, we generally find forests to have the smallest Bray-Curtis index with roots, indicating forest A-horizons appear more root-like than vegetation-like (Table 4.3; Figure 4.4; Supplementary Materials). For example, two eastern deciduous forests (HARV, ORNL), a boreal forest (NIWO), and a desert shrubland (JORN) had the smallest dissimilarity values, favoring roots more so than a vegetation signal. However, a ponderosa pine forest (SOAP) and an oak savannah (CLBJ) site had similar Bray-Curtis values even though their A-horizons favored a vegetation signal more so than roots (Figure 4.3, Table 4.3). These conflicting results reinforce the old adage on the importance of site specificity.

#### 4.5.2 Soil horizon SOM dissimilarity patterns

The importance of site-specificity is reinforced by the patterns in soil profile organic matter compositions. The two sites with the largest Bray-Curtis dissimilarity between A and lower B-horizons are a boreal/spruce forest (DEJU) and a pine/oak

forest (MLBS) (Figure 4.4). However, there is another boreal/tundra forest (NIWO), and numerous deciduous/conifer forests (GRSM, SCBI, DELA) that have much lower dissimilarity values. While there was a general pattern of lower B-horizons favoring SOM composition that was closer to upper B than A-horizons (Table 4.4; Figure 4.4), the two sites with cryoturbation (BARR, TOOL) had largest dissimilarity values. Soil cryoturbation in both BARR and TOOL sites were severe; of the five TOOL cores, all had cryoturbation beginning from 30-50 cm. BARR cryoturbation was not as severe, with only three of five cores experienced classic cryoturbation between 30-70 cm, but the remaining cores were almost exclusively organic-horizons mixing with themselves, thus not satisfying the official requirements of cryoturbation to include mixing between genetic horizons, rather than within genetic horizons. These two permafrost sites also highlight a potential maximum Bray-Curtis index that is possible for upper vs lower B-horizons. The mind strains to consider how a soil could become more physically and heterogeneously mixed together than the combination of somewhat recent glaciation coupled with O-horizon/mineral soil cryoturbation as deep as 196 cm for BARR, and 120 cm for TOOL.

### 4.5.3 Potential CuO method limitations

Soil science studies have almost exclusively focused on the upper horizon, rarely digging past 30 cm in depth (Yost and Hartemink, 2020) and seldom are this level of organic matter characterizations conducted on deep soils (Gross and Harrison, 2019). One limitation of this combined approach with CuO extraction and ecological dissim-

ilarity, is the inherent bias in the CuO procedures to capture plant-derived organic matter at the expense of microbially-derived organic matter. Some estimates suggest microbially derived organic matter can be as large as 80% (Liang and Balsler, 2011), with a more likely proportion between 11-15% in forests and 44-56% in agricultural areas (Angst, et al., 2021; Whalen et al., 2022 and references therein). Although some CuO compounds are microbial in nature (e.g. amino acids, some fatty acids and some diacids), there is a strong preferred bias towards plant-derived compounds. Even within the plant-component category, white-rot fungi degrade lignin in such a way that their degradation signature is not captured by the CuO method, potentially causing an underestimate in the amount of decayed wood to the lignin pool (Filley et al., 2002). The relative [dis]similarity in soils to endmembers presented should therefore be understood to not incorporate the potential variation induced by microbial and fungal communities. Especially in A-horizons, where microbial biomass is greatest, we may be over-estimating the relative [dis]similarity of SOM to either roots or vegetation endmembers.

Conversely, microbial-focused studies patterns in that community structure can vary more within a soil profile than between sites across a similar range of biomes presented here (Eilers, et al., 2021). Although those researchers were focused on soil microbial communities, not SOM composition, they also found that surface soil communities were more unique across sites but that deeper horizons had similar microbial communities regardless of biome or landscape position. Although we focus on CuO extracted material that is biased towards identifying more plant-derived organic matter, our patterns are somewhat consistent with a microbial focused study

potentially indicating a universal ecosystem inertia that pushes both microbial communities and their resulting organic matter processing to appear far more similar than dissimilar.

## 4.6 Conclusions

Overall, we find dominant aboveground vegetation and root organic matter compound class categories tend to be in different proportions compared to any soil horizon. Lignin in both endmembers contributed nearly twice as much to the total CuO extracted material compared to any lignin contribution in soil horizons. Conversely, soil horizons had nearly twice the cutin and suberin contributions to their CuO extracted SOM pool compared to any vegetation or root endmember. Using the Bray-Curtis ecological index, we generally find that comparing any endmember, upper, and lower soil horizon tends to show the OM abundances are relatively similar to each other (values  $<0.2$ ). Within the vegetation, root, and A-horizon categories the dissimilarity values were very small (0.083, 0.096, and 0.083 respectively), indicating there is little OM abundance variation within each sample type as observed with the CuO extraction procedure. We hypothesized A-horizons would have a stronger correlation with aboveground vegetation OM, but only half of the available sites exhibited this pattern with the remaining A-horizons favoring a more root-derived signal. We also hypothesized that A and upper B-horizons are more similar compared to A and lower B-horizons. We find strong evidence for this, where 75% of sites examined had A-horizons that favored upper B-horizon SOM composition com-

pared to lower B-horizons. Despite this, lower and upper B-Horizons comparison had the smallest dissimilarity index, suggesting subsoils are closer in SOM composition than A vs upper B-horizons. Because the overall dissimilarity values across all soil horizon comparisons are relatively small ( $<0.1$ ), we find evidence to suggest soils are acting like a dilution-inducing chromatographic column. Although absolute abundances are different in A, upper, and lower B-horizons, the relative contribution of CuO extracted SOM compounds are far more similar down soil profile than they are different. It should be noted, lower B-horizons exhibited the largest within-sample dissimilarity (0.110), that was larger than any between horizon dissimilarity but still relatively small for the Bray-Curtis index. We do exhibit caution in interpreting these results. Because the CuO method prioritizes plant-derived organic matter more so than microbially derived organic matter, and our endmembers are pure-vegetation or root-litter samples, we may be underestimating the SOM dissimilarity because of a missing (microbial) endmember. We encourage more researchers to both consider digging deeper, and to conduct analysis that would capture both plant and microbially derived compounds to better understand the sources of soil organic matter across ecosystems and down soil profiles.

#### 4.6.1 Acknowledgements

This study was funded by the U.S. National Science Foundation Macrosystems, BIO Directorate, Division of Environmental Biology Program (Award No. EF- 1340681). Raven Chavez and Maylita Brougher of Oregon State University were instrumental in conducting the soil characterizations and laboratory analyses. We would like to acknowledge the National Ecological Observatory Network Systems Installation and Verification Team for the collection of soil cores. The National Ecological Observatory Network is a project sponsored by the National Science Foundation and managed under cooperative agreement by Battelle.

## 4.7 Supplemental Materials

There is one table of supplementary materials, they include:

Site Abbreviation	Full NEON Site Name	Whittaker's Biome Type	Dominant Vegetation Type	Site Management	NPP (kgC/m <sup>2</sup> /yr)	Mean Annual Temperature (°C)	Mean Annual Precipitation (cm)	Mean Annual Activity Index (MAP - Erc)	Active Layer Depth (cm)	Upper Bt Horizon Midpoint (cm)	Lower Bt Horizon Midpoint (cm)	Soil Series Parent Material	USDA Soil Taxonomy	Ascendant Lands
ABRY	Abri Road	Temperate rain forest	Young Douglas fir forest	harvesting	0.343	9.0	225.0	1850.0	10.1	44.0	86.9	volcanic ash	Fine-loamy - isotic - mesic - Andic Humudults	
BARB	Duggs & Barrow	Tundra	Polynesian tundra	wildland	NA	-12.0	11.0	72.0	23.1	79.5	90.7	NA	NA	
BART	Bartlett Experimental forest	Temperate seasonal forest	Mixed forest	wildland	0.753	7.0	122.3	545.0	5.8	88.6	143.4	residuum derived from limestone, calcareous shale, siltstone, and/or sandstone	Coarse-bony - isotic - frigid Aquic Haploblebbs	
BLAN	Bladly Experimental Farm	Woodland/shrubland	Fallow scrubland	fallow scrubland	0.669	12.0	99.1	-112.0	10.3	34.5	56.7	mexicous loess over weathered schist bedrock	Fine - mixed - subactive - mesic Udic Haploblebbs	
BONA	Caribou Pelter	Boreal forest	Spice forest	unburned wildland	NA	-3.0	26.0	15.0	26.9	97.4	155.7	NA	NA	
CLBJ	Lynan B. Johnson Natural Grassland	Woodland/shrubland	Oak savannah	prescribed fire	0.315	18.0	86.0	-524.0	19.2	67.8	98.3	Sediments and residuum from Cretaceous sedimentary deposits	NA	
CFER	Central Plains Experimental Station	Temperate grassland/shrubland	Shortgrass prairie	grazing	0.218	9.0	36.7	-626.0	10.2	52.1	89.8	alkaline to neutral alluvium, colluvium, and residuum	Fine-loamy - mixed - supereactive - mesic Ariclic Haploblebbs	
DCJS	Dakota-Coteau	Woodland/shrubland	Poplar park	low intensity grazing	0.463	4.0	43.8	-303.0	12.5	122.8	140.9	alkaline glacial till and alluvium	Fine-loamy - mixed - supereactive - frigid Typic Haploblebbs	
DEJU	Delta Junction	Boreal forest	Spice forest	wildland	NA	-3.0	31.0	69.0	5.8	165.9	184.1	mexicous loess over acid glacio-fluvial materials or till	NA	
DELA	Deer Lake	Temperate seasonal forest	Woods/Wetlands	wildland	0.496	18.0	140.0	25.0	11.7	53.8	84.0	mexicous loess over acid glacio-fluvial materials or till	Fine - mixed - semiactive - thermic Aquic Blebduhls	
DSNY	Dixey	Tropical seasonal forest/savanna	Regenerating long leaf pine	prescribed fire	0.602	22.0	122.0	-269.0	8.0	79.4	103.6	acid to slightly alkaline marine sediments	Stuhy - siltstone - hyperthermic Aricic Aksoquos	
GRSM	Great Smoky Mountains National Park	Temperate seasonal forest	Eastern deciduous forest	wildland	0.576	13.0	138.8	307.0	6.0	37.6	93.2	colluvium and residuum from mesosedimentary sandstone, siltstone, and shale	Loamy-skeletal - isotic - mesic Typic Humudults	
HARV	Harvard Forest	Temperate seasonal forest	Regenerating forest	wildland	0.731	8.0	100.2	330.0	12.8	70.3	150.7	isotic glacial till	Loamy-skeletal - isotic - mesic Typic Humudults semiactive - frigid Oxyaquic Dystrudults	
HEAL	Healy	Boreal forest	Tussock tundra	wildland	NA	-1.0	37.0	NA	13.0	46.4	59.2	Neuman gravel, poorly consolidated gravels and conglomerate	NA	
JORN	Jornada	Temperate grassland/shrubland	Desert shrubland	wildland	0.117	18.0	27.3	-1230.0	23.8	66.0	93.0	Coarse-bony - mixed - supereactive - thermic Typic Kermudults	Coarse-bony - mixed - supereactive - thermic Typic Kermudults	
KONA	Kona Agriculture	Woodland/shrubland	Cultivated tallgrass prairie	farming	0.363	13.0	88.7	-181.0	14.9	36.5	90.4	residuum derived from limestone or alkaline shale	Fine - smectitic - mesic Pacific Vertic Argiudolls	
KONZ	Kona Core	Woodland/shrubland	submontane tallgrass prairie	wildland	0.372	13.0	89.1	-157.0	14.3	55.8	89.4	moderately acid to slightly alkaline iron-oxalate rich alluvium	Fine - smectitic - mesic Pacific Udic Argiudolls	
LENO	Lenox Landing	Temperate seasonal forest	Pine oak mixed forest	wildland	0.378	18.0	151.2	-41.0	7.9	134.3	144.7	aluvial, coastal, and terrace deposits, Holocene	Fine - mixed - active - acid - thermic Vertic Epiaquops	
MHIS	Mountain Lake	Temperate seasonal forest	Eastern deciduous forest	wildland	0.836	8.0	104.2	309.0	5.7	200.7	232.6	residuum or alluvium derived from sandstone, siltstone, and shale	Coarse-bony - mixed - active - mesic Aquic Haploblebbs	
MOAB	Moab	Temperate grassland/shrubland	Desert shrubland	wildland	0.142	10.0	31.4	-2550.0	18.1	49.7	76.1	alkaline alluvium and aeolian deposits over sandstone	Coarse-bony - mixed - supereactive - mesic Udic Haploblebbs	
NGPR	Northern Great Plains Research Laboratory	Woodland/shrubland	Grassland Prairie	wildland	0.407	5.0	42.9	-341.0	20.4	54.7	77.5	neutral to alkaline loess over glacial till	Fine-loamy - mixed - supereactive - frigid Typic Haploblebbs	
NWJO	Noroot Ridge	Boreal forest	Alpine tundra	wildland	0.333	-4.0	68.0	339.0	15.8	94.6	102.7	alluvium, colluvium, and glacial till derived from acid igneous rocks	Fine-loamy - mixed - supereactive Typic Haploblebbs	
OAES	Oakes (OALS)	Woodland/shrubland	Grassland pasture	grazing	0.296	14.0	70.1	103.0	10.3	139.0	157.1	Loamy, mixed, active, thermic, Udic Haploblebbs	Loamy, mixed, active, thermic, Udic Haploblebbs	
ONAO	Onaga-Auk Skappe	Temperate grassland/shrubland	Sage shrubland	grazing	0.170	9.0	29.4	-727.0	16.8	50.9	102.2	alluvium and colluvium derived from basic igneous and sedimentary rocks	Fine-loamy - mixed - supereactive - mesic Xeric Haploblebbs	
ORNL	Oak Ridge	Temperate seasonal forest	Eastern deciduous forest	wildland	0.617	15.0	123.3	190.0	4.5	165.8	196.4	alluvium, colluvium, and glacial till derived from limestone and shale	Fine - loessitic - thermic Typic Pakudolls	
OSHS	Odyssey-Swabber	Temperate seasonal forest/savanna	Long-leaf pine forest	prescribed fire	0.761	20.0	129.8	-192.0	13.3	37.2	73.5	acid, iron-containing, alluvial, aeolian, and marine deposits	Hyperthermic - uncolored Typic Quartzipsumms	
RMNP	Rocky Mtn National Park	Temperate seasonal forest	Pine forest	wildland	0.475	7.0	49.2	55.0	10.7	31.5	72.3	Granite and gneiss. Mesogeotomic	NA	
SCBI	Sierra Nevada Bishop Institute	Temperate seasonal forest	High Poplar forest	wildland	0.719	13.0	104.1	-29.0	14.1	55.2	89.9	residuum and colluvium of basic igneous rocks	Fine-loamy - mixed - active - mesic Aquic Haploblebbs	
SERC	Savannah Environmental Research Center	Temperate seasonal forest	Coastal tulip poplar and ash	wildland	0.697	13.0	110.1	34.0	7.5	50.4	109.1	acid alluvial, fluvial, marine deposits	Fine-loamy - mixed - active - mesic Aquic Haploblebbs	
SOAP	Sagepost-Saddle	Woodland/shrubland	Poplar mesquite-grass prairie forest	prescribed fire	0.453	13.0	96.0	-408.0	27.1	45.2	54.1	granite-derived residuum	NA	
SRES	Santa Rita	Subtropical desert	Desert shrubland	wildland	0.126	22.0	39.4	-1221.0	17.1	105.3	150.2	slightly acid to strongly alkaline alluvium	Coarse-bony - mixed - calcareous - thermic Typic Torrifluvents	
STEI	Steigenthal	Temperate seasonal forest	concrete	forest harvesting	0.671	5.0	88.7	NA	25.6	91.1	196.9	acidic glacial till	Loamy-silty - mixed - supereactive - frigid Udic Haploblebbs	
STER	Stirling	Woodland/shrubland	Pasture	agriculture - dryland farming	0.230	10.0	42.5	-551.0	10.6	39.2		neutral to alkaline alluvial, aeolian, and glacio-fluvial deposits	Fine-silty - mixed - supereactive - mesic Pacific Argiudolls	
TALL	Taliskaga	Temperate seasonal forest	Longleaf pine forest	prescribed fire	0.367	15.0	145.3	70.0	6.8	35.2	99.2	acidic, iron-containing alluvial, fluvial, and glacio-fluvial deposits	Fine-loamy - siltstone - subactive - thermic Typic Argiudolls	
TOOL	Toolik	Tundra	Tussock tundra	wildland	NA	-9.0	32.0	NA	26.2	51.7	78.0	mexicous loess over weathered schist bedrock	Coarse loamy, mixed, supereactive, frigid Alfic Epiaquops	
TRIE	Trethewey	Temperate seasonal forest	N. hardwood forest	selective logging	0.667	5.0	81.0	NA	25.1	79.4	113.4	NA	NA	
UNDE	University of Notre Dame Ecosystem Research Center	Temperate seasonal forest	Northern hardwood forest	wildland	0.647	5.0	84.7	130.0	6.2	32.8	48.2	isotic glacial till and acid acidium deposits	Coarse-bony - mixed - supereactive - frigid Argic Epiaquops	
WOOD	Woodworth	Woodland/shrubland	Regenerating post oak prairie	re-seeding	0.430	4.0	42.0	-312.0	11.6	31.7	47.9	neutral to alkaline glacial till and glacio-fluvial deposits	Coarse-bony over sandy or sandy-skeletal - mixed - supereactive - frigid Typic Haploblebbs	
WREF	Wald River Experimental Research Station	Temperate rain forest	Wald-growth Douglas fir	wildland	0.773	9.0	222.0	NA	28.7	56.6	79.1	acidic-skeletal mesic Pacific Mollinamentum, Loamy-skeletal mixed Pacific Haploblebbs	Acidic-skeletal mesic Pacific Mollinamentum, Loamy-skeletal mixed Pacific Haploblebbs	

Table 4.5: Site information for a subset (n=39) of the National Ecological Observatory Network (NEON). Soil horizon depths were calculated from cores collected at the five soil plots within the flux tower footprint, and represent three distinct pedogenic horizons.

## 4.8 References

Amundson, R., H. Buck, and K. Lajtha. 2022. Soil science in the time of climate mitigation. *Biogeochemistry* (February). Available at <https://doi.org/10.1007/s10533-022-00952-6>.

Angst, G., K.E. Mueller, K.G.J. Nierop, and M.J. Simpson. 2021. Plant- or microbial-derived? A review on the molecular composition of stabilized soil organic matter. *Soil Biol. Biochem.*: 135907. Available at <https://doi.org/10.1016/j.soilbio.2021.108189>.

Bates, D.M. 2005. Fitting linear mixed models in R. *R News* 5(May): 27–30.

Batjes, N.H. 1994. Landmark papers. *Eur. J. Soil Sci.*

Batjes, N.H. 2014. Total carbon and nitrogen in the soils of the world. *Eur. J. Soil Sci.* 65(1): 10–21.

Berg, M.P., and J. Bengtsson. 2007. Temporal and spatial variability in soil food web structure. *Oikos* 116(11): 1789–1804.

Bünemann, E.K., G. Bongiorno, Z. Bai, R.E. Creamer, G. De Deyn, R. de Goede, L. Fleskens, V. Geissen, T.W. Kuyper, P. Mäder, M. Pulleman, W. Sukkel, J.W. van Groenigen, and L. Brussaard. 2018. Soil quality – A critical review. *Soil Biol. Biochem.* 120(September 2017): 105–125. Available at <https://doi.org/10.1016/j.soilbio.2018.01.030>.

Button, E.S., J. Pett-Ridge, D. V. Murphy, Y. Kuzyakov, D.R. Chadwick, and D.L. Jones. 2022. Deep-C storage: Biological, chemical and physical strategies to enhance carbon stocks in agricultural subsoils. *Soil Biol. Biochem.* 170(February): 108697. Available at <https://doi.org/10.1016/j.soilbio.2022.108697>.

Crow, S.E., T.R. Filley, M. McCormick, K. Szlávecz, D.E. Stott, D. Gamblin, and G. Conyers. 2009. Earthworms, stand age, and species composition interact to influ-

ence particulate organic matter chemistry during forest succession. *Biogeochemistry* 92(1–2): 61–82.

Drake, T.W., K. Van Oost, M. Barthel, M. Bauters, A.M. Hoyt, D.C. Podgorski, J. Six, P. Boeckx, S.E. Trumbore, L. Cizungu Ntaboba, and R.G.M. Spencer. 2019. Mobilization of aged and biolabile soil carbon by tropical deforestation. *Nat. Geosci.* 12(7): 541–546. Available at <http://dx.doi.org/10.1038/s41561-019-0384-9>.

Dungait, J. a J., D.W. Hopkins, A.S. Gregory, and A.P. Whitmore. 2012. Soil organic matter turnover is governed by accessibility not recalcitrance. *Glob. Chang. Biol.* 18(6): 1781–1796.

Eilers, K.G., S. Debenport, S. Anderson, and N. Fierer. 2012. Digging deeper to find unique microbial communities: The strong effect of depth on the structure of bacterial and archaeal communities in soil. *Soil Biol. Biochem.* 50: 58–65. Available at <http://dx.doi.org/10.1016/j.soilbio.2012.03.011>.

Filley, T.R., G.D. Cody, B. Goodell, J. Jellison, C. Noser, and A. Ostrofsky. 2002. Lignin Demethylation and Polysaccharide Decomposition in Spruce Sapwood. *Org. Geochem.* 33: 111–124.

Fleischman, F., S. Basant, A. Chhatre, E.A. Coleman, H.W. Fischer, D. Gupta, B. Güneralp, P. Kashwan, D. Khatri, R. Muscarella, J.S. Powers, V. Ramprasad, P. Rana, C.R. Solorzano, and J.W. Veldman. 2020. Pitfalls of Tree Planting Show Why We Need People-Centered Natural Climate Solutions. *Bioscience* 70(11): 947–950.

Fleischman, F., S. Basant, H. Fischer, D. Gupta, G. Garcia Lopez, P. Kashwan, J.S. Powers, V. Ramprasad, P. Rana, A. Rastogi, C. Rodriguez Solorzano, and M. Schmitz. 2021. How politics shapes the outcomes of forest carbon finance. *Curr.*

Opin. Environ. Sustain. 51: 7–14. Available at <https://doi.org/10.1016/j.cosust.2021.01.007>.

Goñi, M.A., and J.I. Hedges. 1990. Cutin-derived CuO reaction products from purified cuticles and tree leaves. *Geochim. Cosmochim. Acta* 54: 3065–3072.

Goñi, M.A., and J.I. Hedges. 1992. Lignin dimers: Structures, distribution, and potential geochemical applications. *Geochim. Cosmochim. Acta* 56(11): 4025–4043.

Goñi, M.A., N. Monacci, R. Gisewhite, J. Crockett, C. Nittrouer, A. Ogston, S.R. Alin, and R. Aalto. 2008. Terrigenous organic matter in sediments from the Fly River delta-clinoform system (Papua New Guinea). *J. Geophys. Res. Earth Surf.* 113(1). Available at <https://agupubs.onlinelibrary.wiley.com/doi/pdf/10.1029/2006JF000653>.

Goñi, M.A., and S. Montgomery. 2000. Alkaline CuO oxidation with a microwave digestion system: Lignin analyses of geochemical samples. *Anal. Chem.* 72(14): 3116–3121.

Goñi, M.A., and K.A. Thomas. 2000. Sources and transformations of organic matter in surface soils and sediments from a tidal estuary (North Inlet, South Carolina, USA). *Estuaries* 23(4): 548–564.

Greenacre, M. 2018. Chapter 5 Measures of distance between samples. *Corresp. Anal. Relat. Methods*: 1–10. Available at <http://www.econ.upf.edu/michael/stanford/maeb5.pdf%0A>

Gregory, A.S., G.J.D. Kirk, C.A. Key, B.G. Rawlins, P. Wallace, and A.P. Whitmore. 2014. An assessment of subsoil organic carbon stocks in England and Wales. *Soil Use Manag.* 30(1): 10–22.

Van Groenigen, J.W. 2018. The “4 per 1000” initiative: A credibility issue for the soil science community? *Geoderma* 309(April 2017): 118–123.

Van Groenigen, J.W., C. Van Kessel, B.A. Hungate, O. Oenema, D.S. Powlson,

and K.J. Van Groenigen. 2017. Sequestering Soil Organic Carbon: A Nitrogen Dilemma. *Environ. Sci. Technol.* 51(9): 4738–4739.

Van Groenigen, K.J., J. Six, B.A. Hungate, M.A. De Graaff, N. Van Breemen, and C. Van Kessel. 2006. Element interactions limit soil carbon storage. *Proc. Natl. Acad. Sci. U. S. A.* 103(17): 6571–6574.

Gross, C.D., and R.B. Harrison. 2019. The Case for Digging Deeper: Soil Organic Carbon Storage, Dynamics, and Controls in Our Changing World. *Soil Syst.* 3(2): 28.

Hatten, J., M. a. Goñi, and R. a. Wheatcroft. 2012. Chemical characteristics of particulate organic matter from a small, mountainous river system in the Oregon Coast Range, USA. *Biogeochemistry* 107: 43–66. Available at <http://link.springer.com/10.1007/s10533-010-9529-z>.

Hedges, J.I., R.A. Blanchette, K. Weliky, and A.H. Devol. 1988. Effects of fungal degradation on the CuO oxidation products of lignin: A controlled laboratory study. *Geochim. Cosmochim. Acta* 52(11): 2717–2726.

Hedges, J.I., and J.R. Ertel. 1982. Characterization of Lignin by Gas Capillary Chromatography of Cupric Oxide Oxidation Products. *Anal. Chem.* 54(2): 174–178.

Hedges, J.I., and D.C. Mann. 1979. The characterization of plant tissues by their lignin oxidation products. *Geochemica Cosmochim.* 43(2): 1803–1807.

J. Roger Bray, and J.T. Curtis. 1957. An Ordination of the Upland Forest Communities of Southern Wisconsin. *Ecol. Monogr.* 27(Oct): 325–349. Available at <https://www.jstor.org/stable/1942268>.

Jackson, R.B., K. Lajtha, S.E. Crow, G. Hugelius, M.G. Kramer, and G. Piñeiro.

2017. The Ecology of Soil Carbon: Pools, Vulnerabilities, and Biotic and Abiotic Controls. *Annu. Rev. Ecol. Evol. Syst.* 48: 419–445.

James, J., and R. Harrison. 2016. The effect of harvest on forest soil carbon: A meta-analysis. *Forests* 7(12).

Jenny, H. 1941. *Factors of soil formation: A system of quantitative pedology.* Dover Publications Inc., New York.

Kogel-Knabner, I. 2002. The macromolecular organic composition of plant and microbial residues as inputs to soil organic matter. *Soil Biol. Biochem.* 34: 139–162.

Kögel, I. 1986. Estimation and decomposition pattern of the lignin component in forest humus layers. *Soil Biol. Biochem.* 18(6): 589–594.

Lal, R. 2018. Digging deeper: A holistic perspective of factors affecting soil organic carbon sequestration in agroecosystems. *Glob. Chang. Biol.* 24(8): 3285–3301.

Lal, R., P. Smith, H.F. Jungkunst, W.J. Mitsch, J. Lehmann, P.K. Ramachandran Nair, A.B. McBratney, J.C. De Moraes Sá, J. Schneider, Y.L. Zinn, A.L.A. Skorupa, H.L. Zhang, B. Minasny, C. Srinivasrao, and N.H. Ravindranath. 2018. The carbon sequestration potential of terrestrial ecosystems. *J. Soil Water Conserv.* 73(6): 145A-152A.

Lambin, E.F., and P. Meyfroidt. 2011. Global land use change, economic globalization, and the looming land scarcity. *Proc. Natl. Acad. Sci. U. S. A.* 108(9): 3465–3472.

Liang, C., W. Amelung, J. Lehmann, and M. Kästner. 2019. Quantitative assessment of microbial necromass contribution to soil organic matter. *Glob. Chang. Biol.* 25(11): 3578–3590.

Liang, C., and T.C. Balser. 2011. Microbial production of recalcitrant organic matter in global soils: Implications for productivity and climate policy. *Nat. Rev. Microbiol.* 9(1): 75.

Ma, Y., B. Minasny, B.P. Malone, and A.B. Mcbratney. 2019. Pedology and digital soil mapping (DSM). *Eur. J. Soil Sci.* 70(2): 216–235.

Mayer, M., C.E. Prescott, W.E.A. Abaker, L. Augusto, L. Cécillon, G.W.D. Ferreira, J. James, R. Jandl, K. Katzensteiner, J.-P. Laclau, J. Laganière, Y. Nouvellon, D. Paré, J.A. Stanturf, E.I. Vanguelova, and L. Vesterdal. 2020. Influence of forest management activities on soil organic carbon stocks: A knowledge synthesis. *For. Ecol. Manage.* 466(January): 118127. Available at <https://linkinghub.elsevier.com/retrieve/pii/S0378>

Minasny, B., B.P. Malone, A.B. McBratney, D.A. Angers, D. Arrouays, A. Chambers, V. Chaplot, Z.S. Chen, K. Cheng, B.S. Das, D.J. Field, A. Gimona, C.B. Hedley, S.Y. Hong, B. Mandal, B.P. Marchant, M. Martin, B.G. McConkey, V.L. Mulder, S. O'Rourke, A.C. Richer-de-Forges, I. Odeh, J. Padarian, K. Paustian, G. Pan, L. Poggio, I. Savin, V. Stolbovoy, U. Stockmann, Y. Sulaeman, C.C. Tsui, T.G. Vågen, B. van Wesemael, and L. Winowiecki. 2017. Soil carbon 4 per mille. *Geoderma* 292: 59–86. Available at <http://dx.doi.org/10.1016/j.geoderma.2017.01.002>.

Nave, L.E., G.M. Domke, K.L. Hofmeister, U. Mishra, C.H. Perry, B.F. Walters, and C.W. Swanston. 2018. Reforestation can sequester two petagrams of carbon in US topsoils in a century. *Proc. Natl. Acad. Sci. U. S. A.* 115(11): 2776–2781.

Nave, L.E., C.W. Swanston, U. Mishra, and K.J. Nadelhoffer. 2013. Afforestation Effects on Soil Carbon Storage in the United States: A Synthesis. *Soil Sci. Soc. Am. J.* 77(3): 1035. Available at <https://www.soils.org/publications/sssaj/abstracts/77/3/1035>.

Nave, L.E., E.D. Vance, C.W. Swanston, and P.S. Curtis. 2011. Fire effects on temperate forest soil C and N storage. *Ecol. Appl.* 21(4): 1189–1201.

Oksanen, J., F.G. Blanchet, M. Friendly, R. Kindt, P. Legendre, D. McGlinn, P.R. Minchin, R.B. O’Hara, G.S. L., P. Solymos, M. Henry, H. Stevens, E. Szoecs, and W. Helene. 2020. Package “vegan” Title Community Ecology Package. *vegan Community Ecol. Packag. R Packag.* version 2.5-7.

Pinheiro J, B. D, D. S, S. D, and R Core Team. 2014. *nlme: Linear and Nonlinear Mixed Effects Models.* R package(2015).

Poulton, P., J. Johnston, A. Macdonald, R. White, and D. Powlson. 2018. Major limitations to achieving “4 per 1000” increases in soil organic carbon stock in temperate regions: Evidence from long-term experiments at Rothamsted Research, United Kingdom. *Glob. Chang. Biol.* 24(6): 2563–2584.

R Core Team. 2022. R Core Team 2021 R: A language and environment for statistical computing. R foundation for statistical computing. <https://www.R-project.org/>. *R Found. Stat. Comput.* 2: 2019.

Sanderman, J., T. Hengl, and G.J. Fiske. 2017. Soil carbon debt of 12,000 years of human land use. *Proc. Natl. Acad. Sci.* 2017: 201706103. Available at <http://www.pnas.org/content/early/2017/08/15/1706103114.abstract>.

Scharlemann, J.P.W., E.V.J. Tanner, R. Hiederer, and V. Kapos. 2014. Global soil carbon: Understanding and managing the largest terrestrial carbon pool. *Carbon Manag.* 5(1): 81–91.

Schlesinger, W.H. 2022. Biogeochemical constraints on climate change mitigation through regenerative farming. *Biogeochemistry.* Available at <https://doi.org/10.1007/s10533->

022-00942-8.

Schlesinger, W.H., and R. Amundson. 2019. Managing for soil carbon sequestration: Let's get realistic. *Glob. Chang. Biol.* 25(2): 386–389.

Schoeneberger, P.J., D.A. Wysocki, and E.C. Benham. 2012. *Field Book for Describing and Sampling Soils*. Natl. Soil Surv. Cent. 3.0.

Sultana, F., and A. Loftus. 2020. *The Right to Water in a Global Context: Challenges and Transformations in Water Politics*. EarthScan - Routledge, New York.

Wang, T., A. Hamann, D.L. Spittlehouse, and T.Q. Murdock. 2012. ClimateWNA-high-resolution spatial climate data for western North America. *J. Appl. Meteorol. Climatol.* 51(1): 16–29.

Weiglein, T.L., B.D. Strahm, M.M. Bowman, A.C. Gallo, J.A. Hatten, K.A. Heckman, L.M. Matosziuk, L.E. Nave, A.R. Possinger, M.D. SanClements, and C.W. Swanston. 2021. Key predictors of soil organic matter vulnerability to mineralization differ with depth at a continental scale. *Biogeochemistry* 0123456789. Available at <https://doi.org/10.1007/s10533-021-00856-x>.

Whalen, E.D., A.S. Grandy, N.W. Sokol, M. Keiluweit, J. Ernakovich, R.G. Smith, and S.D. Frey. 2022. Clarifying the evidence for microbial- and plant-derived soil organic matter, and the path towards a more quantitative understanding. *Glob. Chang. Biol.*: 0–2.

Yost, J.L., and A.E. Hartemink. 2020. How deep is the soil studied – an analysis of four soil science journals. *Plant Soil* 452(1–2): 5–18.

Zhu, X., R.D. Jackson, E.H. DeLucia, J.M. Tiedje, and C. Liang. 2020. The soil

microbial carbon pump: From conceptual insights to empirical assessments. *Glob. Chang. Biol.* 26(11): 6032–6039.

Zurr, A., E. Ieno, N. Walker, A. Saveliev, and G. Smith. 2008. *Mixed Effects Models and Extensions in ecology with R* (M Gail, K Krickeberg, J Samet, A Tsaitis, and W Wong, Eds.). 1st ed. Springer, New York.

## Chapter 5: Conclusion

Soils are increasingly viewed as a tool to combat climate change, but we lack an understanding of why soils can be highly resilient and what types of plant-derived carbon are present across ecosystems and down soil profiles. The focus of this dissertation was to fill those two essential knowledge gaps.

The first manuscript revealed the inherent resilience in forest soils to biomass removals is from the long-term accumulation of belowground root-biomass and we identified a dynamism in soil carbon transfers. Six-months following treatments surface soil carbon stores increased between 8-42%, but two-years later they returned to pre-treatment values. This rapid carbon input, and loss, within two years caused a replacement of native soil carbon that had a strong root-derived signature. We identified losses in both light fraction and intermediate fraction that were not apparent in bulk soil samples. Although the heavy fraction appeared not to change, stable isotope analysis revealed heavy fractions from all treatments and depths became enriched suggesting this ‘stable’ carbon pool is not universally stable. The light fraction nitrogen became depleted, mimicking a root-derived signal more so than a needle derived signal. Together this shows that across all operationally defined pools of soil organic matter (SOM), roots are universally buffering soil carbon losses from extreme biomass removals. However, this legacy root carbon pool developed over the last two rotations with the most recent being a 55-year old harvest, and prior to

that was presumably a mature old growth forest. If rotation length decreases before the root carbon pool is allowed to recover, soils' resilience may become more limited.

In my second and third manuscript I lean more heavily on the copper oxidation (CuO) method chronicling soils from 40 sites across the National Ecological Observatory Network. To the author's knowledge, this is the most broad and systematic CuO organic matter inventory and deepest soil horizon assessment that have ever been investigated. Despite a wide range in climates, plant communities, soil horizon pedogenesis and geologic substrate, lignin contributions to the total SOM pool were almost exclusively within a narrow range of 0.5-1.0 mg lignin/100 mg OC. We do find a general trend of decreasing lignin contributions as soil depth increases, but substituted fatty acids (leaf and root waxy coatings) contributions increased slightly at deeper soil depths. A-horizons across ecosystems had significantly different SOM compositions compared to their associated subsoils. However, within sites, neither upper or lower B-horizon SOM components were significantly different from each other. Using the Bray-Curtis dissimilarity index that incorporates more than 70 unique CuO extracted compounds, rather than broad compounds classes, we still find that CuO extracted SOM across all three soil horizons have SOM compositional abundances that are far more similar to each other, than they are dissimilar. It is well established that fresh dissolved organic matter (DOM) from litter has a unique and characteristic organic matter signal, but once it reaches mineral soil the pore water DOM composition also appears generally homogenized. Given the remarkable range of ecosystems and the diversity of plant-derived organic matter inputs, we find similar results in SOM as in DOM studies.

Overall, my research shows that soils are incredibly resilient to perturbations, but their resilience is not infinite. The mechanisms of resilience are primarily in the form of root-derived organic matter. But over time, some ecosystem inertia will likely push all soils to a narrow range of lignin and plant wax contributions to the total SOM pool such that aboveground organic matter still plays a crucial role in SOM as an ecosystem property. This also suggests we should consider SOM in a more stochastic nature. We may never be able to accurately predict how soils will respond to some perturbation, or tillage, or wildfire, or compaction, but we can generally constrain which locations are more sensitive to damage because their water and nutrient holding capacity are inherently diminished (e.g., shallow soils, thin A-horizons, low silt+clay content, high rock content, steep slopes susceptible to erosion). These locations with high sensitivity to damage are also potentially areas with the greatest potential to accumulate more soil carbon over longer periods of time. Unfortunately, what makes these sites ideal for targeted carbon farming policies are the same site-factors that make them undesirable and impractical to own and manage. It appears that soils can *technically* be a climate mitigation tool. But our inability to accurately predict responses over the long-term due to their inherent stochastic nature, and the uncertainty of a changing mother nature, limits our dependence on soils to only the basics: clothes, food, and clean water.

## 5.1 Bibliography For Preface, Introduction, and Conclusion

Amundson, R., H. Buck, and K. Lajtha. 2022. Soil science in the time of climate mitigation. *Biogeochemistry* (February). Available at <https://doi.org/10.1007/s10533-022-00952-6>.

Badgley, G., F. Chay, O.S. Chegwidan, J.J. Hamman, J. Freeman, and D. Cullenward. 2022. California's forest carbon offsets buffer pool is severely undercapitalized. *Front. For. Glob. Chang.* 5(August): 1–15.

Bailey, V., C. Pries, and K. Lajtha. 2019. What do we know about soil carbon destabilization? *Environ. Res. Lett.* 14(8). Available at <http://dx.doi.org/10.1088/1748-9326/ab2c11>.

Batjes, N.H. 1994. Landmark papers. *Eur. J. Soil Sci.*

Batjes, N.H. 2014. Total carbon and nitrogen in the soils of h. *Eur. J. Soil Sci.* 65(1): 10–21.

Bernhardt, E., and W.H. Schlesinger. 2013. *Biogeochemistry: An analysis of global change*. 3rd ed. Academic Press.

Button, E.S., J. Pett-Ridge, D. V. Murphy, Y. Kuzyakov, D.R. Chadwick, and D.L. Jones. 2022. Deep-C storage: Biological, chemical and physical strategies to enhance carbon stocks in agricultural subsoils. *Soil Biol. Biochem.* 170(February): 108697. Available at <https://doi.org/10.1016/j.soilbio.2022.108697>.

Cha, J.M., and M. Pastor. 2022. Just transition: Framing , organizing , and power-building for decarbonization. *Energy Res. Soc. Sci.* 90(October 2021): 102588. Available at <https://doi.org/10.1016/j.erss.2022.102588>.

Coleman, E.A., B. Schultz, V. Ramprasad, H. Fischer, P. Rana, A.M. Filippi, B.

Güneralp, A. Ma, C. Rodriguez Solorzano, V. Guleria, R. Rana, and F. Fleischman. 2021. Limited effects of tree planting on forest canopy cover and rural livelihoods in Northern India. *Nat. Sustain.*. Available at <https://www.nature.com/articles/s41893-021-00761-z>.

Cotrufo, M.F., M.D. Wallenstein, C.M. Boot, K. Denef, and E. Paul. 2013. The Microbial Efficiency-Matrix Stabilization (MEMS) framework integrates plant litter decomposition with soil organic matter stabilization: do labile plant inputs form stable soil organic matter? *Glob. Chang. Biol.* 19(4): 988–995. Available at <http://doi.wiley.com/10.1111/gcb.12113>.

EPA. 1983. Can we delay a greenhouse warming? Washington D.C.

Fleischman, F., S. Basant, A. Chhatre, E.A. Coleman, H.W. Fischer, D. Gupta, B. Güneralp, P. Kashwan, D. Khatri, R. Muscarella, J.S. Powers, V. Ramprasad, P. Rana, C.R. Solorzano, and J.W. Veldman. 2020. Pitfalls of Tree Planting Show Why We Need People-Centered Natural Climate Solutions. *Bioscience* 70(11): 947–950.

Fleischman, F., S. Basant, H. Fischer, D. Gupta, G. Garcia Lopez, P. Kashwan, J.S. Powers, V. Ramprasad, P. Rana, A. Rastogi, C. Rodriguez Solorzano, and M. Schmitz. 2021. How politics shapes the outcomes of forest carbon finance. *Curr. Opin. Environ. Sustain.* 51: 7–14. Available at <https://doi.org/10.1016/j.cosust.2021.01.007>.

Fleischman, F., E. Coleman, H. Fischer, P. Kashwan, M. Pfeifer, V. Ramprasad, C.R. Solorzano, J.W. Veldman, and B.B.N. Strassburg. 2022. Restoration prioritization must be informed by marginalized people. *607*(October 2020): 5–9.

Van Groenigen, J.W. 2018. The “4 per 1000” initiative: A credibility issue for the soil science community? *Geoderma* 309(April 2017): 118–123.

Van Groenigen, J.W., C. Van Kessel, B.A. Hungate, O. Oenema, D.S. Powlson, and K.J. Van Groenigen. 2017. Sequestering Soil Organic Carbon: A Nitrogen Dilemma. *Environ. Sci. Technol.* 51(9): 4738–4739.

Van Groenigen, K.J., J. Six, B.A. Hungate, M.A. De Graaff, N. Van Breemen, and C. Van Kessel. 2006. Element interactions limit soil carbon storage. *Proc. Natl. Acad. Sci. U. S. A.* 103(17): 6571–6574.

Gross, C.D., and R.B. Harrison. 2019. The Case for Digging Deeper: Soil Organic Carbon Storage, Dynamics, and Controls in Our Changing World. *Soil Syst.* 3(2): 28.

Hall, S. 2015. Exxon Knew about Climate Change Almost 40 Years Ago News and Research. *Sci. Am.*: 1–5. Available at <https://www.scientificamerican.com/article/exxon-knew-about-climate-change-almost-40-years-ago/>.

House Committee on Oversight and Reform. 2021. Fueling the Climate Crisis: Exposing Big Oil’s Disinformation Campaign to Prevent Climate Action. 117th Congr.. Available at <https://oversight.house.gov/legislation/hearings/fueling-the-climate-crisis-exposing-big-oil-s-disinformation-campaign-to>.

IPCC. 2013. *Climate Change 2013: The Physical Science Basis. Contribution of Working Group I to the Fifth Assessment Report of the Intergovernmental Panel on Climate Change* (TF Stocker, D Qin, G-K Plattner, M Tignor, SK Allen, J Boschung, A Nauels, Y Xia, V Bex, and PM Midgley, Eds.). Cambridge University Press, Cambridge, United Kingdom and New York, NY, USA.

IPCC - Intergovernmental Panel on Climate Change. 1990. *IPCC First Assessment Report - Working Group I: Scientific Assessment of Climate Change*. IPCC:

414. Available at <https://www.ipcc.ch/report/ar1/wg1/>.

IPCC - Intergovernmental Panel on Climate Change. 2021. Summary for Policy Makers - IPCC 6th Assessment - The Physical Science Basis. Intergov. Panel Clim. Chang.: 3949. Available at <https://www.ipcc.ch/report/ar6/wg1/downloads/report/IPCC-AR6-WGI-Full-Report.pdf>.

Janzen, H.H., K.J. van Groenigen, D.S. Powlson, T. Schwinghamer, and J.W. van Groenigen. 2022. Photosynthetic limits on carbon sequestration in croplands. *Geoderma* 416(March): 115810. Available at <https://doi.org/10.1016/j.geoderma.2022.115810>.

Jenny, H. 1941. Factors of soil formation: A system of quantitative pedology. Dover Publications Inc., New York.

Kögel-Knabner, I., G. Guggenberger, M. Kleber, E. Kandeler, K. Kalbitz, S. Scheu, K. Eusterhues, and P. Leinweber. 2008. Organo-mineral associations in temperate soils: Integrating biology, mineralogy, and organic matter chemistry. *J. Plant Nutr. Soil Sci.* 171(1): 61–82. Available at <http://doi.wiley.com/10.1002/jpln.200700048> (verified 10 July 2014).

Kopittke, P.M., R.C. Dalal, C. Hoeschen, C. Li, N.W. Menzies, and C.W. Mueller. 2020. Soil organic matter is stabilized by organo-mineral associations through two key processes: The role of the carbon to nitrogen ratio. *Geoderma* 357(August 2019): 113974. Available at <https://doi.org/10.1016/j.geoderma.2019.113974>.

Lajtha, K. 2017. Brave new world. *Biogeochemistry* 133(1): 3–5.

Lal, R. 2018. Digging deeper: A holistic perspective of factors affecting soil organic carbon sequestration in agroecosystems. *Glob. Chang. Biol.* 24(8): 3285–3301.

Lambin, E.F., and P. Meyfroidt. 2011. Global land use change, economic glob-

alization, and the looming land scarcity. *Proc. Natl. Acad. Sci. U. S. A.* 108(9): 3465–3472.

Lehmann, J., and M. Kleber. 2015. The contentious nature of soil organic matter. *Nature* 528: 60–68.

Liang, C., J.P. Schimel, and J.D. Jastrow. 2017. The importance of anabolism in microbial control over soil carbon storage. *Nat. Microbiol.* 2(8).

Masoom, H., D. Courtier-Murias, H. Farooq, R. Soong, B.P. Kelleher, C. Zhang, W.E. Maas, M. Fey, R. Kumar, M. Monette, H.J. Stronks, M.J. Simpson, and A.J. Simpson. 2016. Soil Organic Matter in Its Native State: Unravelling the Most Complex Biomaterial on Earth. *Environ. Sci. Technol.* 50(4): 1670–1680. Available at <http://pubs.acs.org/doi/abs/10.1021/acs.est.5b03410>.

McCool, K., S. Holub, S. Gao, B. Morrisette, J. Blunn, A.C. Gallo, and J. Hatten. In Review - Quantifying impacts of forest fire on soil carbon in a young, intensively managed tree farm in the western Oregon Cascades. *Soil Sci. Soc. Am. J.*: 1–23.

McGill, B.M., S.K. Hamilton, N. Millar, and G.P. Robertson. 2018. The greenhouse gas cost of agricultural intensification with groundwater irrigation in a Midwest U.S. row cropping system. *Glob. Chang. Biol.* 24(12): 5948–5960.

Minasny, B., B.P. Malone, A.B. McBratney, D.A. Angers, D. Arrouays, A. Chambers, V. Chaplot, Z.S. Chen, K. Cheng, B.S. Das, D.J. Field, A. Gimona, C.B. Hedley, S.Y. Hong, B. Mandal, B.P. Marchant, M. Martin, B.G. McConkey, V.L. Mulder, S. O'Rourke, A.C. Richer-de-Forges, I. Odeh, J. Padarian, K. Paustian, G. Pan, L. Poggio, I. Savin, V. Stolbovoy, U. Stockmann, Y. Sulaeman, C.C. Tsui, T.G. Vågen,

B. van Wesemael, and L. Winowiecki. 2017. Soil carbon 4 per mille. *Geoderma* 292: 59–86. Available at <http://dx.doi.org/10.1016/j.geoderma.2017.01.002>.

Mufson, S., C. Mooney, J. Eilperin, J. Muyskens, and S. Georges. 2019. 2° C: BEYOND THE LIMIT: Extreme Climate Change has Arrived in America. Washington Post: 1–37. Available at <https://www.washingtonpost.com/graphics/2019/national/climate-environment/climate-change-america/>.

Mulvey, K., and S. Shulman. 2015. The Climate Deception Dossiers: Internal Fossil Fuel Industry Memos Reveal Decades of Corporate Disinformation.

Nave, L.E., G.M. Domke, K.L. Hofmeister, U. Mishra, C.H. Perry, B.F. Walters, and C.W. Swanston. 2018. Reforestation can sequester two petagrams of carbon in US topsoils in a century. *Proc. Natl. Acad. Sci. U. S. A.* 115(11): 2776–2781.

Possinger, A.R., M.J. Zachman, A. Enders, B.D.A. Levin, D.A. Muller, L.F. Kourkoutis, and J. Lehmann. 2020. Organo–organic and organo–mineral interfaces in soil at the nanometer scale. *Nat. Commun.* 11(1): 1–11.

Poulton, P., J. Johnston, A. Macdonald, R. White, and D. Powlson. 2018. Major limitations to achieving “4 per 1000” increases in soil organic carbon stock in temperate regions: Evidence from long-term experiments at Rothamsted Research, United Kingdom. *Glob. Chang. Biol.* 24(6): 2563–2584.

Powlson, D.S., A.P. Whitmore, and K.W.T. Goulding. 2011. Soil carbon sequestration to mitigate climate change: A critical re-examination to identify the true and the false. *Eur. J. Soil Sci.* 62(1): 42–55.

Rabalais, N.N., R.E. Turner, and W.J. Wiseman. 2002. Gulf of Mexico hypoxia, a.k.a. “The dead zone.” *Annu. Rev. Ecol. Syst.* 33: 235–263.

Reilly, M.J., A. Zuspan, J.S. Halofsky, C. Raymond, A. McEvoy, A.W. Dye, D.C. Donato, J.B. Kim, B.E. Potter, N. Walker, R.J. Davis, C.J. Dunn, D.M. Bell, M.J. Gregory, J.D. Johnston, B.J. Harvey, J.E. Halofsky, and B.K. Kerns. 2022. Cascadia Burning: The historic, but not historically unprecedented, 2020 wildfires in the Pacific Northwest, USA. *Ecosphere* 13(6): 1–20.

Rhymes, J., I. Cordero, M. Chomel, J. Lavallee, A. Straathof, D. Ashworth, H. Langridge, M. Semchenko, F. de Vries, D. Johnson, and R. Bardgett. 2020. Are researchers following best storage practices for measuring soil biochemical properties? *SOIL Discuss.* (3): 1–15.

Sanderman, J., T. Hengl, and G.J. Fiske. 2017. Soil carbon debt of 12,000 years of human land use. *Proc. Natl. Acad. Sci.* 2017: 201706103. Available at <http://www.pnas.org/content/early/2017/08/15/1706103114.abstract>.

Scharlemann, J.P.W., E.V.J. Tanner, R. Hiederer, and V. Kapos. 2014. Global soil carbon: Understanding and managing the largest terrestrial carbon pool. *Carbon Manag.* 5(1): 81–91.

Schlesinger, W.H. 2022. Biogeochemical constraints on climate change mitigation through regenerative farming. *Biogeochemistry*. Available at <https://doi.org/10.1007/s10533-022-00942-8>.

Schlesinger, W.H., and R. Amundson. 2019. Managing for soil carbon sequestration: Let's get realistic. *Glob. Chang. Biol.* 25(2): 386–389.

Setzer, J., and L.C. Vanhala. 2019. Climate change litigation: A review of research on courts and litigants in climate governance. *Wiley Interdiscip. Rev. Clim. Chang.* 10(3): 1–19.

Six, J., R.T. Conant, E. a Paul, and K. Paustian. 2002. Stabilization mechanisms of soil organic matter: Implications for C-saturation of soils. *Plant Soil* 241: 155–176.

Sparks, D.L. 2003. *Environmental soil chemistry*. 2nd ed. Academic Press, San Diego, CA.

Stockmann, U., M.A. Adams, J.W. Crawford, D.J. Field, N. Henakaarchchi, M. Jenkins, B. Minasny, A.B. McBratney, V. de R. de Courcelles, K. Singh, I. Wheeler, L. Abbott, D.A. Angers, J. Baldock, M. Bird, P.C. Brookes, C. Chenu, J.D. Jastrow, R. Lal, J. Lehmann, A.G. O'Donnell, W.J. Parton, D. Whitehead, and M. Zimmermann. 2013. The knowns, known unknowns and unknowns of sequestration of soil organic carbon. *Agric. Ecosyst. Environ.* 164(2013): 80–99. Available at <http://dx.doi.org/10.1016/j.agee.2012.10.001>.

Sultana, F., and A. Loftus. 2020. *The Right to Water in a Global Context: Challenges and Transformations in Water Politics*. EarthScan - Routledge, New York.

Wendt, J.W., and S. Hauser. 2013. An equivalent soil mass procedure for monitoring soil organic carbon in multiple soil layers. *Eur. J. Soil Sci.* 64(1): 58–65.

Wozniacka, G. 2020. Are Carbon Markets for Farmers Worth the Hype? *Civil Eats*: 1–9. Available at <https://civileats.com/2020/09/24/are-carbon-markets-for-farmers-worth-the-hype/>.

Yarmuth, J. 2022. *Inflation Reduction Act of 2022*. House of Representatives, Washington D.C.

Yost, J.L., and A.E. Hartemink. 2020. How deep is the soil studied – an analysis of four soil science journals. *Plant Soil* 452(1–2): 5–18.